

Dissertation zur Erlangung des Doktorgrades der Fakultät für Chemie und
Pharmazie der Ludwig-Maximilians-Universität München

Molecular Basis of Rrn3-regulated RNA Polymerase I Initiation



Claudia Blattner

aus

Lörrach

2011

Erklärung

Diese Dissertation wurde im Sinne von §13 Abs. 3 bzw. 4 der Promotionsordnung vom 29. Januar 1998 (in der Fassung der sechsten Änderungssatzung vom 16. August 2010) von Herrn Prof. Dr. Patrick Cramer betreut.

Ehrenwörtliche Versicherung

Diese Dissertation wurde selbstständig, ohne unerlaubte Hilfe erarbeitet.
München, am 14.10.2011

Claudia Blattner

Dissertation eingereicht am	21.10.2011
1. Gutachter	Prof. Patrick Cramer
2. Gutachter	Prof. Roland Beckmann
Mündliche Prüfung am	05.12.2011

Acknowledgements

First of all, I would like to thank Patrick who has been a great supervisor and mentor over the last years. Thank you for your constant support and advice, and for sharing your enthusiasm about science. I am very grateful for the opportunity, to do my PhD in this fantastic lab, and to experience this very productive setting but also social atmosphere.

I want to extend this acknowledgement not only to the lab, but also to the whole scientific environment I had the chance to work in. This includes the entire Gene Center, with its great and collaborative atmosphere, and extends to the MPI, Martinsried, and the research groups and people involved in the IMPRS-Is program, which provided a great framework for doing research but also getting insight into a broader spectrum of life sciences and to stay in contact with other researchers. In this context, many thanks to Maxi and Hans-Jörg, who coordinated all the workshops and other IMPRS activities I could participate in.

I also got a lot of advice and help from people in the lab. I want to thank Alan for the help and training in crystallography, for spending countless hours at the synchrotron with me, explaining, but also having great conversations and drinking whiskey.

Many thanks to Rieke for exchanging our experiences and thoughts throughout our PhD time, for being a great and fun roommate at all the retreats, and conferences. Thanks to Elmar for interesting conversations and your enthusiasm about science, Tobi, for explaining and helping most patiently with so many bioinformatic programs.

Thank you Jenne, for a lot of help in the lab right from the start until today with various issues, and for your friendship. Many thanks to Jasmin, for endless conversations, for your general advice on labwork and especially for being a great friend.

Thanks to Kerstin, Sarah and Fuensanta for enjoyable hikes together, parties, and christmas-cookie sessions.

I also would like to thank Claudia for keeping the lab running and being the source of the good atmosphere. Thanks to Stefan Benkert, not only for the yeast fermentation, but also for help with a lot of technical issues.

Many thanks to all the others in the lab, who contributed to the great working atmosphere, for a great time not only in the lab, but also apart from working hours, during retreats, beer garden visits and our annual "lab-wiesn". Also many thanks to my student

Sandra, who was a great help in starting the core factor project, I really appreciate your interest and excitement about this work.

I thank Thomas Fröhlich for frequent and very helpful masspec protein identification. Further, I would like to acknowledge all the people contributing to the experiments, that made this work successful. This includes my collaboration partners Kristina Lorenzen from the lab of Albert Heck at the University of Utrecht, Franz Herzog from the lab of Ruedi Aebersold at the ETH, Zürich, Gregor Witte from Karl-Peter Hopfner's lab at the Gene Center, and Andreas Mayer from our lab.

Many thanks also to the people from the Beckmann lab, Otto Berninghausen, Charlotte Ungewickell and Thomas Becker who helped me with EM data collection and processing, and patiently answered all my questions, and, of course, Anselm for his help.

Finally, I want to thank my parents, who aroused my interest in science and supported and motivated me to make my way, also when things were not easy. And thank you Niklas, for your patience, your support and understanding.

Summary

Eukaryotic nuclear transcription is carried out by three different Polymerases (Pol), Pol I, Pol II and Pol III. Among these, Pol I is dedicated to transcription of the rRNA, which is the first step of ribosome biogenesis, and cell growth is regulated during Pol I transcription initiation by the conserved factor Rrn3/TIF-IA in yeast/human. A wealth of structural information is available on Pol II and its general transcription factors (GTFs). Recently, also the architectures of Pol I and Pol III have been described by electron microscopy and the additional subunits that are specific to Pol I and Pol III have been identified as orthologs of the Pol II transcription factors TFIIF and TFIIE. Nevertheless, we still lack information about the architecture of the Pol I initiation complex and structural data is missing explaining the regulation of Pol I initiation mediated by its central transcription initiation factor Rrn3.

The Rrn3 structure solved in this study reveals a unique HEAT repeat fold and indicates dimerization of Rrn3 in solution. However, the Rrn3-dimer is disrupted upon Pol I binding. The Rrn3 structure further displays a surface serine patch. Phosphorylation of this patch represses human Pol I transcription (Mayer *et al*, 2005; Mayer *et al*, 2004), and a phospho-mimetic patch mutation prevents Rrn3 binding to Pol I *in vitro*, and reduces *S. cerevisiae* cell growth and Pol I gene occupancy *in vivo*. This demonstrates a conserved regulation mechanism of the Pol I-Rrn3 interaction. Crosslinking indicates that Rrn3 does not only interact with Pol I subunits A43/14, but the interface further extends past the RNA exit tunnel and dock domain to AC40/19. The corresponding region of Pol II binds the Mediator head (Soutourina *et al.*, 2011) that co-operates with TFIIB (Baek *et al*, 2006). Consistent with this, the Rrn3 binding partner, core factor subunit Rrn7, is predicted to be a TFIIB homologue.

Taken together, our results provide the molecular basis of Rrn3-regulated Pol I initiation and cell growth and indicate a universally conserved architecture of eukaryotic transcription initiation complexes.

Publication

Blattner C, Jennebach S, Herzog F, Mayer A, Cheung AC, Witte G, Lorenzen K, Hopfner K-P, Heck AJR, Aebersold R, Cramer P (2011). Molecular basis of Rrn3-regulated RNA polymerase I initiation and cell growth. *Genes Dev* **25**(19): 2093-2105.

Contributions

The many experiments performed and results presented in this study were achieved with the help, advice and collaboration of several specialized researchers, whose contributions are listed below in detail.

Claudia Blattner carried out all experiments apart from the ones listed below and determined the X-ray structure of Rrn3 with help and advice from Alan Cheung.

SAXS analysis of the Rrn3 dimer was carried out by Gregor Witte.

Native MS was carried out by Kristina Lorenzen.

Protein crosslinking-MS analysis was carried out by Stefan Jennebach and Franz Herzog.

ChIP analysis was done by Andreas Mayer.

Contents

Erklärung.....	1
Ehrenwörtliche Versicherung.....	1
Acknowledgements.....	2
Summary.....	4
Publication.....	5
Contributions.....	5
Contents.....	6
1 Introduction.....	9
1.1 Eukaryotic Transcription Systems.....	9
1.1.1 General Transcription Factors (GTFs).....	11
1.1.2 Structural studies on eukaryotic polymerase systems.....	12
1.2 rDNA transcription in the context of ribosome biogenesis and function.....	14
1.2.1 Ribosome composition and biogenesis.....	14
1.2.2 rRNA production.....	16
1.3 RNA Polymerase I transcription initiation complex.....	17
1.3.1 Organization of the rRNA genes.....	17
1.3.2 Initiation complex formation in mammals.....	17
1.3.3 Initiation complex formation in yeast.....	18
1.4 Regulation of RNA Polymerase I transcription.....	19
1.4.1 General mechanisms that control rRNA transcription.....	19
1.4.2 Rrn3 interaction with RNA Polymerase I.....	20
1.4.3 Regulation of the Rrn3-Pol I interaction in mammals.....	21
1.4.4 Regulation of the Rrn3-Pol I interaction in yeast.....	21
1.5 Aims and scope of this study.....	23
2 Materials and Methods.....	24
2.1 Materials.....	24
2.1.1 Bacterial strains.....	24
2.1.2 Yeast strains.....	24
2.1.3 Oligonucleotides.....	25
2.1.4 Plasmids.....	28
2.1.5 Chemicals.....	30
2.1.6 Media and additives.....	31
2.1.7 Buffers and solutions.....	32
2.2 General Methods.....	35

2.2.1 Preparation and transformation of competent <i>E.coli</i> cells.....	35
2.2.2 Preparation and transformation of competent <i>S. cerevisiae</i> cells.....	36
2.2.3 Cloning and mutagenesis	36
2.2.4 Protein expression in <i>E. coli</i>	38
2.2.5 purification of recombinant Rrn3.....	38
2.2.6 Protein analysis	39
2.3 Rrn3 Crystallization and characterization	41
2.3.1 Crystallization screening.....	41
2.3.2 Crystal structure determination.....	41
2.3.3 Small angle X-ray scattering	41
2.3.4 Static light scattering analysis	42
2.4 RNA Polymerase I-Rrn3 complex preparation and characterization	43
2.4.1 Purification of endogenous RNA Polymerase I	43
2.4.2 Assembly of the RNA Polymerase I-Rrn3 complex.....	44
2.4.3 Native Mass-Spectrometry analysis	44
2.4.4 Protein crosslinking and Mass Spectrometry.....	44
2.4.5 Purification of recombinant A43/14	45
2.4.6 Protein interaction analysis.....	45
2.4.7 Cryo-EM data collection and processing.....	46
2.5 Yeast genetics and assays.....	47
2.5.1 Sporulation and Tetrad dissection	47
2.5.2 long-term storage of yeast strains	47
2.5.3 Mating type determination	47
2.5.4 Gene disruption and epitope tagging.....	48
2.5.5 quantitative western blot analysis	48
2.5.6 Complementation and phenotyping assays.....	49
2.5.7 Chromatin Immunoprecipitation (ChIP) analysis	49
2.6 Bioinformatic tools	51
3 Results	52
3.1 Structural characterization of the RNA Polymerase I transcription initiation factor Rrn3	52
3.1.1 Rrn3 crystallization	52
3.1.2 Rrn3 has a unique HEAT repeat structure.....	55
3.1.3 Rrn3 forms dimers in solution.....	57
3.1.4 The Rrn3 structure exhibits characteristic surface properties.....	59
3.2 Structural and functional characterization of the RNA Polymerase I-Rrn3 complex. 60	

3.2.1 Rrn3 binds Pol I as a monomer	60
3.2.2 Rrn3 does not bind subunits A43/14 alone.....	62
3.2.3 The Rrn3 structure exhibits a serine patch that is important for cell growth	63
3.2.4 The serine patch is involved in Pol I binding <i>in vitro</i>	64
3.2.5 The Rrn3 serine patch is required for cell growth and promoter recruitment <i>in vivo</i>	65
3.2.6 Rrn3 binds Pol I near subcomplex AC40/19	67
3.3 Model of a minimal RNA Polymerase I initiation Complex	68
3.3.1 Model of the Pol I-Rrn3 complex	68
3.3.2 Rrn7 is the TFIIB-related factor in the RNA Polymerase I initiation apparatus.....	69
3.3.3 Architecture of the Pol I initiation complex	70
4 Discussion	72
5 Conclusions and Outlook.....	75
6 Appendix (unpublished results)	77
6.1 EM studies on the Pol I-Rrn3 complex	77
6.2 Pol I Phosphopeptide mapping	79
6.3 Rrn7 structure prediction and modeling.....	81
6.4 Core Factor purification.....	82
7 Abbreviations	84
8 References.....	86
Curriculum Vitae.....	99

1 Introduction

1.1 Eukaryotic Transcription Systems

The central dogma of biology describes the transfer of information from DNA to RNA to the synthesis of Proteins. The first step of this process is carried out by RNA Polymerases. While in archaea and bacteria one polymerase is sufficient to produce all transcripts, in eukaryotic systems this process is more elaborate and thus carried out by three distinctly specialized polymerase systems that share a partly identical core structure but differ in the composition of their additional subunits and their transcription factors (Table 1).

Table 1. Subunits of RNA Polymerases

	Pol I subunit	Corresponding subunit in Pol II	Corresponding subunit in Pol III		
10 subunit core	A190	Rpb1	C160	homolog	
	A135	Rpb2	C128	homolog	
	AC40	Rpb3	AC40	homolog	
	AC19	Rpb11	AC19	homolog	
	A12.2	Rpb9	C11	homolog	
	Rpb5(ABC27)	Rpb5	Rpb5	common	
	Rpb6(ABC23)	Rpb6	Rpb6	common	
	Rpb8(ABC14.5)	Rpb8	Rpb8	common	
	Rpb10(ABC10a)	Rpb10	Rpb10	common	
	Rpb12(ABC10b)	Rpb12	Rpb12	common	
Subcomplex A14/43	A43	Rpb7	C25	counterpart	
	A14	Rpb4	C17	counterpart	
Subcomplex A49/34.5	A34.5	TFIIF- β (Rap30/Tfg2)	C53	Pol I/III specific	
	A49 N-term	TFIIF- α (Rap74/Tfg1)	C37	Pol I/III specific	
	A49 C-term		TFIIE- β	C34	Pol I/III specific
			TFIIE- α	C82	Pol III specific
				C31	Pol III specific
Total	14 subunits	12 subunits	17 subunits		

Pol I is located in the nucleolus and produces the 35S rRNA precursor which is cotranscriptionally processed into the 18S, 25S and 5.8S rRNA (Kos and Tollervey, 2010). Pol II, residing in the nucleoplasm, synthesizes mainly mRNAs, while Pol III generates small non-coding RNAs such as tRNAs, snRNAs and the 5S rRNA, also in the nucleoplasm (Paule and White, 2000). Five subunits, Rpb5, Rpb6, Rpb8, Rpb10 and Rpb12 are shared between Pol I, Pol II and Pol III, and another five Pol II specific subunits (Rpb1, Rpb2, Rpb3, Rpb11 and Rpb9) have counterparts in Pol I and Pol III that contain regions of sequence and structural similarity. Two additional subunits, the heterodimer Rpb4/7, which are not included in the Pol II core complex show homology to the Pol I subunits A43/14.5 (Kuhn *et al*, 2007) and Pol III subunits C17/25 (Jasiak *et al*, 2006). Pol I additionally comprises the heterodimer A49/34.5 which mediates RNA cleavage and stimulates Pol I processivity (Geiger *et al*, 2010) and has a counterpart in the Pol III subunits C37/53 (Kassavetis *et al*, 2010; Landrieux *et al*, 2006). Parts of these subunits have recently been shown to have a distant homology to the Pol II transcription factors TFIIF and TFIIE as indicated in Table 1 (Geiger *et al*, 2010; Wu *et al*, 2011). Further, Pol I subunits A49/34.5 are essential for the high Pol I loading rates on the rDNA gene through mediating contacts between adjacent enzymes and deletions of A34.5 and especially A49 cause dramatical changes in nucleolar morphology (Albert *et al*, 2011). A49/34.5 also seem to play a role in Pol I-Rrn3 complex formation and the subsequent release of Rrn3 from the elongating polymerase (Albert *et al*, 2011; Beckouet *et al*, 2008), although the mechanism of this effect is not yet understood.

Pol III is the largest of the three enzymes and encompasses three further subunits C31, C34 and C82 (Wang and Roeder, 1997). Recently it has been postulated that the C82/34 heterodimer (Lorenzen *et al*, 2007) is distantly related to TFIIE (Geiger *et al*, 2010; Lefevre *et al*, 2011).

1.1.1 General Transcription Factors (GTFs)

For efficient initiation Pol II requires the general transcription initiation factors TFIIB, -D, -E, -F and -H. The multifunctional factor TFIIB comprises four structural segments: the core domain, B-linker, B-reader and an N-terminal Zn-ribbon. The Zn-ribbon stably binds the Pol II dock domain, whereas the TFIIB core domain, comprising two cyclin folds, binds TBP and DNA. This interaction helps to recruit Pol II to the promoter DNA (Chen and Hahn, 2003; Nikolov *et al*, 1995). The B-linker is involved in promoter opening, while the B-reader assists in open complex formation and recognizes the initiator sequence (Inr), thereby enabling correct start site selection (Kostrewa *et al*, 2009). TFIIB further interacts with TFIID, a 15-subunit complex containing TATA box-binding protein (TBP) (Burley and Roeder, 1996; Lee and Young, 2000; Yamashita *et al*, 1993). The essential transcription factors TFIIIE and TFIIF are located on opposite sides of the Pol II central cleft (Chen *et al*, 2007; Eichner *et al*, 2010) where they affect post-recruitment steps and the transition from transcription initiation to elongation (Flores *et al*, 1991; Yan *et al*, 1999). TFIIH binds promoter DNA downstream of the transcription-bubble and displays a helicase activity that assists promoter melting. Further, TFIIH is involved in phosphorylation of the Rpb1 CTD and finally also enhances promoter clearance by stimulating stalled elongation complexes (Coulombe and Burton, 1999; Kim *et al*, 2000).

TBP is common to all three polymerases, and TFIIH is not only a Pol II GTF, but also plays an essential role in Pol I transcription (Iben *et al*, 2002). Further, homologies to TFIIF- β (Rap30) have been described for the Pol I subunit A34.5 (Geiger *et al*, 2010) and for the Pol III specific subunit C53 (Wu *et al*, 2011). The N-terminal domain of Pol I subunit A49 is homologous to the Pol II initiation factor TFIIF- α (Rap74) and to the Pol III-specific subunit C37, while the C-terminal domain of A49 is homologous to the Pol II initiation factor TFIIIE- β and to the Pol III-specific subunit C34 (Geiger *et al*, 2010). The Pol I subunit A12.2 seems to be the source of an intrinsic cleavage activity and additionally shows sequence homology to TFIIS (Kuhn *et al*, 2007). The Pol III specific initiation factor Brf1 has been identified as the homolog of TFIIB (Colbert and Hahn, 1992; Teichmann *et al*, 2000; Wang and Roeder, 1995), while no TFIIB homolog has been reported in the Pol I system to date.

Table 2. Pol II general transcription factors. Function and homologies to other transcription systems (Geiger *et al*, 2010; Hahn, 2004; Kuhn *et al*, 2007; Thomas and Chiang, 2006; Wang and Roeder, 1995).

GTF Pol II	Sub- units	Pol I homolog	Pol III homolog	Function
TFIIA	2			Stabilizes TBP and TFIID-DNA binding. Blocks transcription inhibitors. Positive and negative gene regulation.
TFIIB	1		Brf1	Binds TBP, Pol II, and promoter DNA. Helps to fix transcription start site.
TFIID/ TBP	15	TBP	TBP	Binds TATA element and deforms promoter DNA. Assembly platform for TFIIB, TFIIA and TAFs
TFIIE	2	A49-C-term	C34	Binds promoter near transcription start site. May help to open or stabilize transcription bubble in open complex
TFIIF	3	A49-N-term A34.5	C37 C53	Binds Pol II and is involved in Pol II recruitment to PIC and in Open Complex formation
TFIIS	1	A12.3		Stimulates intrinsic transcript cleavage activity of RNA Pol II allowing backtracking to resume RNA synthesis after transcription arrest; stimulates PIC assembly at some promoters
TFIIH	10			ATPase/helicase necessary for promoter opening and promoter clearance; helicase activity for transcription coupled DNA repair; kinase activity required for phosphorylation of RNA Pol II CTD; facilitates transition from initiation to elongation

1.1.2 Structural studies on eukaryotic polymerase systems

Today a wealth of detailed structural information is available on Pol II and associated factors. Several years ago the core and finally the complete Pol II structure have been solved (Armache *et al*, 2005; Cramer *et al*, 2001) (Figure 1). Structures for TFIIE α/β have been solved and an evolutionary conservation to archaeal TFE has been demonstrated (Meinhart *et al*, 2003; Okuda *et al*, 2000), as well as structures of the TFIIF subunits Rap30/TFIIF β and Rap74/TFIIF α (Gaiser *et al*, 2000; Groft *et al*, 1998; Kamada *et al*, 2001). The location of TFIIF on the Pol II structure was determined by crosslinking (Chen *et al*, 2010). The structure of a Pol II-TFIIS complex was elucidated (Kettenberger *et al*, 2003), and finally, also a Pol II-TFIIB complex was structurally described (Kostrewa *et al*, 2009; Liu *et al*, 2010).

There are electron microscopy structures available describing Pol I and Pol III indicating the locations of the specific subunits A43/14 and A49/34.5 for Pol I (De Carlo *et al*, 2003; Kuhn *et al*, 2007) (Figure 1) and C17/25 and C53/37 as well as C82/34/31 for Pol III (Fernandez-Tornero *et al*, 2010). The latter complex was described in detail together with

the X-ray structure of Maf1, a negative regulator of Pol III transcription (Vannini *et al*, 2010) (Figure 1).

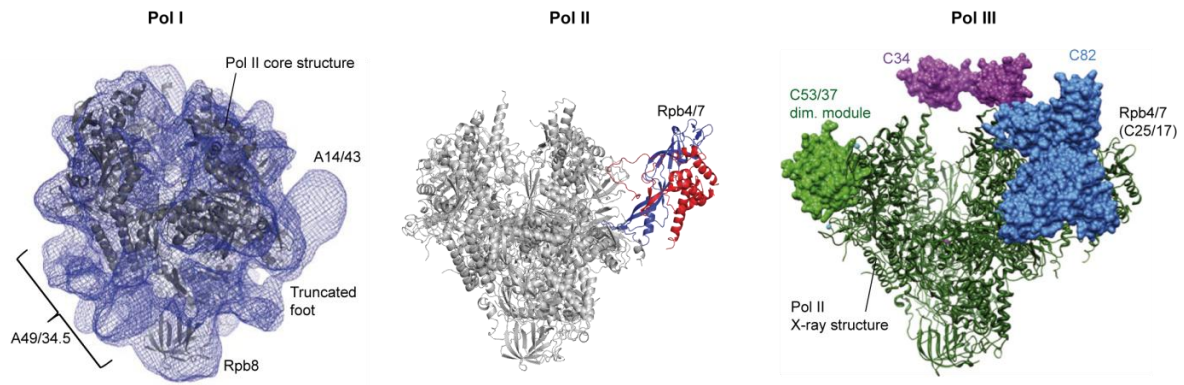


Figure 1. Current structural models of the three eukaryotic polymerases, front view.

Further, the Pol III transcription factor Brf1 has been identified as the homolog of TFIIB (Colbert and Hahn, 1992; Teichmann *et al*, 2000), and structural information is available for both, Brf1 (Juo *et al*, 2003) and TFIIB (Kosa *et al*, 1997; Kostrewa *et al*, 2009; Liu *et al*, 2010). Structures of the specific Pol III subunits C17/25 (Jasiak *et al*, 2006) and C82 (human hRPC62) (Lefevre *et al*, 2010) are available, as well as for the Pol I specific subunits A43/14 (Geiger *et al*, 2008; Kuhn *et al*, 2007) and A49/34.5 (Geiger *et al*, 2010).

Besides the GTFs Pol II further requires additional coactivator complexes to enable activated transcription, especially the mediator, a 25 polypeptide assembly (Kim *et al*, 1994). Several efforts have been made to understand and structurally characterize this complex, which is segmented into four different modules: the head, middle, tail and kinase module (Kang *et al*, 2001). The topology of the mediator middle module has been described (Koschubs *et al*, 2010) and structures have been solved for subunits of the mediator middle module (Baumli *et al*, 2005; Koschubs *et al*, 2009) and head module (Imasaki *et al*, 2011; Lariviere *et al*, 2006; Lariviere *et al*, 2008; Seizl *et al*, 2011). Recently the interaction interface between the mediator head module subunit Med17 and Pol II has been identified through crosslinking and mutational analysis (Soutourina *et al*, 2011). Despite this wealth of structural data and the many established homologies between the systems, we are still lacking a lot of structural information on Pol I. For example, no homologous factor to TFIIB has been described in the Pol I system. Structural data is also missing for the essential Pol I core factor subunits and the specific initiation factor Rrn3.

1.2 rDNA transcription in the context of ribosome biogenesis and function

1.2.1 Ribosome composition and biogenesis

Ribosomes are the earliest and most complex molecular machines in an organism, providing the basis for protein biosynthesis and thereby sustaining cell growth. Today's ribosomes most likely evolved from protoribosomes that were only made up by RNA (Poole *et al*, 1998). Eukaryotic ribosomes still comprise up to two thirds of RNA and one third of ribosomal Proteins, and the formation of peptide bonds is predominantly catalysed by ribosomal RNAs that constitute the major architectural and catalytic components of the ribosome.

Ribosome biogenesis occupies a major part of all cellular energy and metabolic effort and therefore is tightly regulated in connection to cell growth and proliferation.

Thus the production of the 25S, 18S and 5.8S rRNAs, which form one single gene transcribed by Pol I, and the 5S rRNA encoded on the same locus, but transcribed by Pol III, needs to be tightly coregulated.

All three eukaryotic polymerases are required simultaneously to produce the four ribosomal RNAs and more than 70 ribosomal proteins. Thus, 60 % of total transcription in rapidly growing cells is devoted to the production of ribosomal RNA (Warner, 1999). One yeast rDNA repeat is a 9.1 kb unit, comprising the sequence encoding the 35S rRNA and two nontranscribed spacers (NTS) at both ends, separating the 35S rDNA from the 5S rRNA gene, which is transcribed by Pol III (Venema and Tollervey, 1999). The 35S operon comprises the DNA sequences for the 18S, 5.8S, and 25S rRNAs which are separated by the two internal transcribed spacers (ITS), and flanked at either end by two external transcribed spacers (ETS) (Figure 2).

Pre-rRNA processing has been broadly studied in *S. cerevisiae* and the initial cleavage sites of the 35S rRNA, the earliest detectable pre-rRNA, have been described precisely. Splicing of the 3'-ETS occurs cotranscriptionally and is followed by cleavage of the 5'-ETS and the ITS1. The ITS2, separating the 5.8S and the 25S rRNA gene, is cleaved several steps later. Subsequent chemical modifications and further processing steps of the pre-rRNA are accompanied and preceded by the assembly of r-proteins (Venema and Tollervey, 1999).

Small nucleolar RNAs (snoRNAs) facilitate and assist many chemical modification steps in the pre-rRNA by correctly positioning the RNA modifying enzymes on the pre-rRNA

through base-pairing with the target sequence. SnoRNAs form small ribonucleoprotein particles (snoRNPs) in the cell (Kiss, 2001). Most of the chemical modifications during rRNA processing involve 2'-O-methylation of the sugar moiety and pseudouridylation of uridine residues (Granneman and Baserga, 2004).

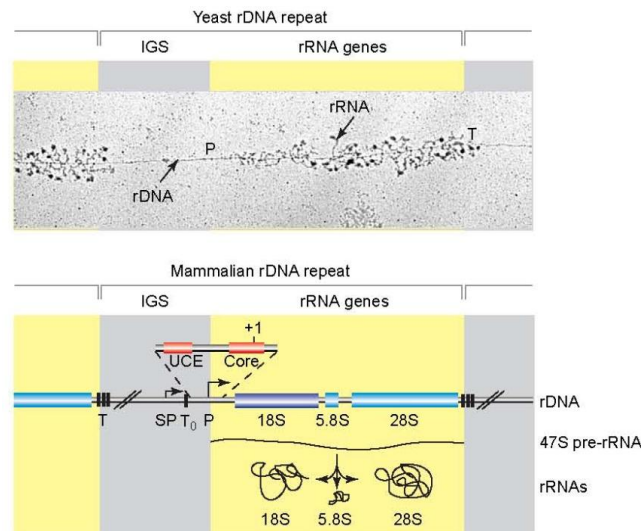


Figure 2. upper panel: electron microscopic image of a yeast nuclear chromatin spread ('Miller Spread') Proteins associated with growing rRNA strands are stained. Promoter (P) terminator (T), intergenic spacer (IGS). lower panel: representative eukaryotic rDNA repeat. The rRNA genes form a single transcription unit that yields the 35S precursor rRNA which is in part cotranscriptionally processed into the 18S, 5.8S and 28S rRNA (28S rRNA = 25S in yeast)(Russell and Zomerdijk, 2005). The 5S rRNA is also encoded on the same locus, but transcribed by Pol III, and thus not depicted in this figure.

Ribosome assembly, which also starts cotranscriptionally, is mediated by several additional proteins and is important to establish the complex folding of the mature rRNAs (Granneman and Baserga, 2004). Yeast cells package the primary pre-rRNA transcript into large 90S complexes, which can be observed as a terminal knob in Miller chromatin spreads (Miller and Beatty, 1969; Russell and Zomerdijk, 2005) (Figure 2). The 90S pre-ribosomes are then further processed to develop into 43S and 66S particles, precursors of the final 40S and 60S ribosomal subunits. The 43S pre-ribosomes are further processed to the final 40S subunit in the cytoplasm, whereas the 66S preribosomes are subjected to several maturation steps directly in the nucleus before their export to the cytoplasm (Granneman and Baserga, 2004; Tschochner and Hurt, 2003).

Although the precursor of the 18S, 28S and 5.8S rRNA is synthesized by Pol I and the precursor of the 5S rRNA is independently synthesized by Pol III, the 28S, 5.8S and 5S rRNA finally assemble together with 46 r-proteins to the large ribosomal subunit, while the 18S

rRNA forms the small ribosomal subunit together with 32 r-proteins (Ferreira-Cerca *et al*, 2007).

As a consequence of the exceptionally high synthetic effort made by the Pol I transcription machinery, this is a central point for the control of cell growth and proliferation and was identified and investigated as a target for the treatment of cancer, with several tumor suppressors and oncogenes targeting this process (Drygin *et al*, 2010; White, 2005).

1.2.2 rRNA production

Synthesis of the precursors of the 18S, 25S, 5.8S and 5S rRNAs, that are transcribed by Polymerases I and III, is under control of extracellular signaling cascades triggered by nutrient deprivation or other cellular stress, in order to keep the balance between the growth state of the cell and accumulation of rRNAs. Regulation of the transcription machineries in response to cell proliferation and growth factor signaling is essential to assure production of all four rRNAs at approximately equimolar levels. This is accomplished at different stages of transcription, on an epigenetic level (see also 1.4.1) or through control of transcription from each active gene by modification of transcription factors.

There are several kinase pathways targeting Pol I and Pol III adjunct factors. In the Pol III system, TOR-dependent regulation of transcription is achieved through phosphorylation of the repressor Maf1 which strongly binds to the polymerase only in its dephosphorylated form and thereby inhibits transcription initiation (Towpik *et al*, 2008).

The Pol I initiation system is regulated mainly through phosphorylations of UBF, CF and Rrn3. So far, this has mainly been studied in mammalian systems, which will be discussed in detail in chapter 1.3.3 and 1.4.1. Further, a certain phosphorylation pattern of the Polymerase may be required for stable interaction with Rrn3 and hence transcription initiation. Several phosphorylation sites in mammalian Rrn3 have been reported in the last years. Details on this topic are discussed in chapter 1.4.

1.3 RNA Polymerase I transcription initiation complex

1.3.1 Organization of the rRNA genes

The nucleolar organizing regions are made up by approximately 150 copies of rRNA genes, which are arranged in clusters of tandem head-to-tail repeats (Russell and Zomerdijk, 2005) (see also Figure 2). In yeast and mammals the rDNA promoter comprises approximately 150 bp upstream of the transcription start site. Usually, these promoters contain two sequence elements, the upstream element (UCE/ UE) and the core promoter element (core/ CE) (Boukhgalter *et al*, 2002; Hamada *et al*, 2001) (reviewed in (Moss *et al*, 2007)). Despite little sequence conservation in this region, all systems require TATA binding protein (TBP) and a group of TBP associated factors (TAFs) to recognize the promoter as a precondition for transcription initiation. However, besides some similarities the required TAFs can differ dramatically in composition and function between yeast and higher eukaryotes.

1.3.2 Initiation complex formation in mammals

Prior to the onset of Pol I transcription, a pre-initiation complex is assembled close to the transcription start site, comprising the upstream binding factor (UBF) and the promoter-selectivity factor (SL1). Mammalian UBF is a 97 kDa HMG-1 box protein with specific DNA binding capabilities, which is highly conserved in vertebrates. UBF helps to preserve rDNA gene activity and architecture through binding the promoter, the enhancer and the rDNA throughout the transcribed region (Denissov *et al*, 2011; Russell and Zomerdijk, 2005). SL1, an initiation factor comprising the subunits Taf_{1110/95}, TAF_{168/63}, TAF₁₄₈, TAF₁₄₁ and TBP (Comai *et al*, 1992; Gorski *et al*, 2007), is assembled at the promoter region, and provides promoter specificity by binding promoter DNA and UBF. Together these factors build up a stable complex. UBF binds and recruits SL1 via its C-terminal domain through a phosphorylation-dependent interaction, which is probably enhanced by casein kinase II phosphorylation (Kihm *et al*, 1998; Kwon and Green, 1994; Tuan *et al*, 1999; Voit *et al*, 1992). Further possible interactions between UBF and SL1 are discussed to occur either through a direct contact or through induced changes in DNA structure (Jantzen *et al*, 1992). The last step prior to transcription initiation is the recruitment of Pol I in complex

with the initiation factor TIF-IA, a phosphoprotein which is highly regulated with several signaling pathways converging on the control of this interaction (Drygin *et al*, 2010).

1.3.3 Initiation complex formation in yeast

The yeast Pol I initiation machinery differs substantially from the mammalian system although there are still some parallels. The factors that assemble at the upstream promoter element comprise two histones H3 and H4, an uncharacterized 30 kDa protein (UAF30) and the non-essential factors Rrn5, Rrn9 and Rrn10 (Keys *et al*, 1996), together they form the upstream activating factor (UAF). These subunits interact with TBP, the only factor common to all eukaryotic transcription systems, that is required for recruitment of the core factor and efficient transcription (Steffan *et al*, 1996). Subsequent to TBP binding, the core factor (CF), comprising the essential subunits Rrn6, Rrn7 and Rrn11, assembles at the core promoter element whereupon all three subunits interact with TBP (Bordi *et al*, 2001; Keener *et al*, 1998; Lalo *et al*, 1996; Moss *et al*, 2007; Steffan *et al*, 1996). The yeast core factor subunits Rrn6, Rrn7 and Rrn11 resemble the human SL1 subunits TAF₁₁₁₀, TAF₁₆₈ and TAF₁₄₈. No yeast homolog to the fourth mammalian SL1 subunit TAF₁₄₁ has been described so far.

Similar to the mammalian system, Pol I is finally recruited to the rDNA promoter together with the central transcription initiation factor Rrn3, the yeast homolog of TIF-IA (Bodem *et al*, 2000; Moorefield *et al*, 2000). The Pol I–Rrn3 interaction also appears to be phospho-regulated, but the underlying mechanisms are less understood and fewer details are known about possible phosphorylation sites.

Table 3. Pol I initiation Factors

Yeast	Mammals
Core factor (CF)	TIF-IB/ SL1
Rrn6	Taf ₁₁₁₀ /95
Rrn7	TAF ₁₆₈ /63
Rrn11	TAF ₁₄₈
Upstream activating factor (UAF)	
Rrn5, Rrn9, Rrn10, UAF30, H3, H4	UBF
TBP	TBP
Rrn3	TIF-IA

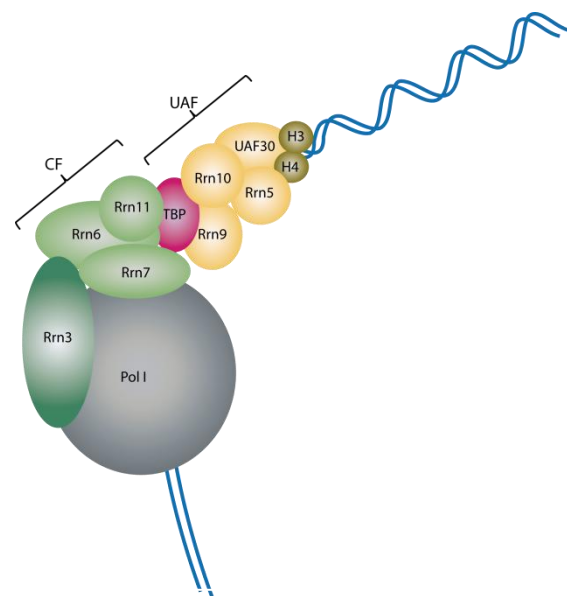


Figure 3. Assembly of the Pol I initiation complex, adapted from (Moss *et al*, 2007).

1.4 Regulation of RNA Polymerase I transcription

1.4.1 General mechanisms that control rRNA transcription

Regulation of RNA Polymerase I transcription in response to cellular signals can be achieved at two levels. On the one hand the number of active genes can be regulated on an epigenetic level, or, as a short-term response the rate of transcription from each active rRNA gene is adjusted. In growing yeast cells, only half of the rRNA genes are active, and these are randomly distributed over the rRNA gene locus (Dammann *et al*, 1995). NoRC, a nucleolar remodeling complex that consists of the ATPase SNF2h and TIP5 (TTF-1-interacting protein-5), silences rRNA genes through recruitment of a DNA methyltransferase, a histone deacetylase and a histone methyltransferase. NoRC thereby leads to changes in chromatin structure and establishment of a heterochromatic state of the rDNA promoter, by mediating methylation of the Lys9 residue of histone H3 and by causing histone hypoacetylation and DNA methylation in a certain temporal order (Guettg *et al*, 2010; Santoro *et al*, 2002) (Santoro and Grummt, 2005). Further, in response to nutrient starvation, TOR kinase regulates association of Rpd3-Sin3 histone deacetylase (HDAC) with rDNA chromatin, thereby controlling acetylation of histone H4. Hypoacetylation of H4 leads to loss of nucleolar structure and RNA Pol I delocalization (Tsang *et al*, 2003).

Control of rRNA production is also achieved through alterations in the rate of transcription from each active gene. In mammalian systems, in contrast to yeast, rDNA transcription is regulated in a cell-cycle dependent manner. SL1 subunit TAF₁₁₀ is phosphorylated by cdc2/ cyclin B, leading to SL1 inactivation, loss of interaction with UBF and mitotic repression of rRNA synthesis (Heix *et al*, 1998). Moreover, PIC assembly and stability is regulated through UBF phosphorylation levels, with kinetics slightly different from SL1 phospho-regulation (Klein and Grummt, 1999). These events together lead to a cell-cycle dependent regulation of rDNA transcription in mammals.

Another target for transcriptional regulation is the recruitment of Pol I to the rDNA promoter and the PIC. This step is mediated through formation of a stable initiation-competent Pol I-Rrn3 complex and recruitment of this complex to SL1/CF, and is repressed or enhanced through phosphorylation at several distinct positions either on the Pol I or on the Rrn3/ TIF-IA surface.

1.4.2 Rrn3 interaction with RNA Polymerase I

Yeast whole cell extracts contain a 17-fold excess of Pol I (15200 copies/cell) compared to the Pol I-specific initiation factors UAF and CF (750 and 950 copies/cell, respectively) whereas only a three-fold excess compared to Rrn3 (5300 copies/cell). This indicates that only a minor fraction of Pol I interacts with UAF and CF during transcription initiation, in agreement with the fact that UAF and CF remain bound to the promoter during several rounds of transcription which was further proved by ChIP analysis (Bier *et al*, 2004). Whereas the free forms of Rrn3 and Pol I are much more abundant in cellular extracts than the other initiation factors, levels of the Pol I-Rrn3 complex, the initiation competent form of Pol I, equal the levels of UAF and CF (Bier *et al*, 2004; Milkereit and Tschochner, 1998; Yamamoto *et al*, 1996). While clearly an excess of Pol I is needed for the high loading rate of transcribing polymerases on the gene, a reason for the abundant presence of Rrn3 remains unclear. Upon elongation, Pol I leaves UAF and CF at the promoter and at the same time or shortly thereafter Rrn3 is released as well from the elongating polymerase (Bier *et al*, 2004). The function of Rrn3 is conserved between yeast and higher eukaryotes (Bodem *et al*, 2000; Moorefield *et al*, 2000).

Upon Pol I recruitment, Rrn3 interacts with the Pol I specific subunit A43 in *S. cerevisiae* (Peyroche *et al*, 2000) and in *S. pombe* with the A43 homolog RPA21, thus this contact seems to be evolutionarily conserved (Imazawa *et al*, 2002). This crucial interaction is stabilized by the subunit A14 (Ker1p in *S. pombe*) (Imazawa *et al*, 2005). Rrn3 mediates recruitment of Pol I to the PIC through an additional interaction with the core factor subunits Rrn6/TAF₁₁₀ and Rrn7/TAF₁₆₃ (Miller *et al*, 2001; Peyroche *et al*, 2000). Release of Rrn3 from elongating Pol I is triggered by the subunits A49/34.5 possibly through contacts between adjacent polymerases which are packed tightly on the rDNA strand upon entering the elongation phase (Albert *et al*, 2011; Beckouet *et al*, 2008) but the detailed underlying mechanism remains elusive. Several signaling pathways triggered by cellular stress response and growth factors converge on regulation of the interaction between Rrn3 and Pol I. Formation of the Rrn3-Pol I complex is necessary for transcription initiation *in vivo*. Nevertheless, free Pol I can be recruited to the rDNA promoter at low levels *in vitro*, but Rrn3 binding is still required for initiation (Aprikian *et al*, 2001; Schnapp and Grummt, 1991; Schnapp *et al*, 1993). This implicates an additional role for Rrn3 in retaining an initiation-competent polymerase after the step of recruitment.

1.4.3 Regulation of the Rrn3-Pol I interaction in mammals

The interaction of Rrn3 (TIF-IA in mammals) with the Pol I complex is regulated by growth factor signaling pathways that connect nutrient availability to rRNA production (Drygin *et al*, 2010; Grummt and Voit, 2010), which can account for up to 60% of all nuclear transcription (Warner, 1999). Signaling cascades trigger phosphorylation and dephosphorylation of TIF-IA (Cavanaugh *et al*, 2002; Drygin *et al*, 2010). TIF-IA phosphorylation at several different positions has been reported to influence on the one hand TIF-IA-Pol I complex formation and stability, and on the other hand interaction of Rrn3 with SL1. While rapamycin mediated inhibition of TOR kinase causes phosphorylation of S199 in TIF-IA, which impairs Pol I-TIF-IA complex formation, dephosphorylation of the N-terminal serine S44 as a result of rapamycin treatment leads to translocation of TIF-IA to the cytoplasm (Mayer *et al*, 2004). Phosphorylation of T200 by JNK2 triggered by oxidative stress leads to loss of interaction between TIF-IA and SL1 as well as Pol I and translocation of TIF-IA from the nucleolus into the nucleoplasm and thereby reduces rRNA gene transcription rates (Mayer *et al*, 2005). Phosphorylation of S170/172 by CK2 leads to release of TIF-IA from elongating Pol I and thereby promotes efficient transcription, while dephosphorylation by FCP1 allows reassociation of the Pol I-TIF-IA complex, thereby initializing a new transcription cycle (Bierhoff *et al*, 2008; Panova *et al*, 2006). Phosphopeptide mapping further revealed two phosphoserines S633 and S649 that need to be phosphorylated by ERK and RSK to retain TIF-IA function (Zhao *et al*, 2003). In contrast to these results, phosphorylation of S635 by AMP-activated protein kinase in response to nutrient deprivation inhibits interaction of TIF-IA with SL1 and thereby prevents formation of an active transcription initiation complex (Hoppe *et al*, 2009).

1.4.4 Regulation of the Rrn3-Pol I interaction in yeast

Control of Rrn3 dependent recruitment and initiation of Pol I has been described and understood in less detail in the yeast system than in mammals. However, there is evidence, that the free form of Rrn3 is predominantly phosphorylated, whereas unphosphorylated Rrn3 is able to stably bind Pol I. In turn, Pol I phosphorylation at specific sites seems to be a prerequisite for stable association with Rrn3 and efficient transcription initiation (Fath *et al*, 2001; Gerber *et al*, 2008). The Pol I-Rrn3 interaction seems to be regulated through the TOR kinase or kinases downstream the TOR signaling pathway, as

Rapamycin treatment causes a decrease in the amount of Rrn3-Pol I complex, similar to the observations in stationary phase (Claypool *et al*, 2004).

Rrn3 has been shown to interact with the Pol I specific subunit A43 (Peyroche *et al*, 2000), which is evolutionarily conserved. In agreement, RPA21, the *S. pombe* homolog of A43, has been identified as the interaction partner of *S. pombe* Rrn3 (Imazawa *et al*, 2002). While in the mammalian system this interaction needs to be disrupted after initiation in order to maintain efficient transcription and to keep nucleolar structure (Bierhoff *et al*, 2008), in the yeast system a strain with a permanent fusion of A43 to Rrn3 is viable with the same growth rates as wild type (Laferte *et al*, 2006).

Several phosphosites have been identified on the Pol I surface (Gerber *et al*, 2008), five of which are located in subunit A43, although partly in a non-essential c-terminal region. However, two of them, S208 and S220 are situated in a flexible loop after a conserved region from P42 to D172, which has been shown to be required for Rrn3 binding (Peyroche *et al*, 2000), and thus might have a regulatory effect on Rrn3-Pol I interaction, but this remains speculative.

1.5 Aims and scope of this study

Understanding the architecture of all tree eukaryotic nuclear RNA Polymerases and their interactions with associated factors, not only provides a more comprehensive picture on how transcription processes are regulated, but also helps us to understand how different specificities have evolved. While models for the minimal initiation complexes of Pol II and Pol III have been described in the last years (Chen and Hahn, 2004; Kostrewa et al., 2009; Liu et al., 2010; Vannini et al., 2010), the architecture of the Pol I initiation complex still remains unknown. There are several reasons for this, on the one hand the lack of a known TFIIB-related factor in the Pol I system, and on the other hand, the very little knowledge on the Pol I initiation factors Rrn6, Rrn7, and Rrn11. Finally, we are also still lacking information on the structure of the central Pol I initiation factor Rrn3 and its precise position on the Pol I surface.

To understand how Pol I transcription and cell growth are regulated, structural insights into the Pol I-Rrn3 initiation complex are required.

In this study, a structural and functional approach will be taken to characterize the Rrn3 protein and its interaction with Pol I. An intermediate goal of this project is to solve the crystal structure of Rrn3, purified from an exogenous source. Based on this structure, functional studies will be designed, in order to clearly identify interaction sites of Rrn3 with Pol I. Given that a stable complex between Rrn3 and Pol I will be obtained *in vitro*, crosslinking/mass spectrometry analysis will be utilized to define the exact contact points.

Furthermore, we plan to examine the possibility of a phospho-regulation of the Rrn3-Pol I complex, based on published data for the mammalian system.

A side-goal of this study is to gain further information on the core factor subunits and to find possible homologies to Pol II transcription factors, which could finally lead to a new model for the Pol I initiation complex.

2 Materials and Methods

2.1 Materials

2.1.1 Bacterial strains

Bacterial strains used in this study are listed in Table 4. XL-1 Blue cells were used for cloning, and BL21-CodonPlus(DE3)RIL for recombinant protein expression.

Table 4. *E. coli* strains used in this work

Strain	Genotype	Source
XL-1 Blue	rec1A; endA1; gyrA96 ; thi-1 ; hsdR17; supE44 ; elA1 ; lac[F'proAB lacI ^q ZDM15 Tn10(Tet ^r)]	Stratagene
BL21-CodonPlus (DE3)RIL	B; F ⁻ ; ompT; hsdS(r _B ⁻ m _B ⁻); dcm ⁺ ; Tet ^r ; gal λ(DE3); endA; Hte [argU, ileY, leuW, Cam ^r]	Stratagene

2.1.2 Yeast strains

Yeast strains were obtained from Euroscarf and further modified in this work. All strains used are listed in Table 5.

Table 5. *S. cerevisiae* strains used in this work

Strain	Genotype	Source
Rrn3Δ (diploid)	BY4743; Mat a/a; his3D1/his3D1; leu2D0/leu2D0; lys2D0/LYS2; MET15/met15D0; ura3D0/ura3D0; YKL125w::kanMX4/YKL125w	Euroscarf Y24975
Rrn3 shuffle	BY4743; Mat a; sporulated; his3D1/his3D1; leu2D0/leu2D0; lys2D0/LYS2; MET15/met15D0; ura3D0/ura3D0; YKL125w::kanMX4/pRS316-Rrn3	this work
Rrn3 shuffle/ A190-TAP	BY4743; Mat a; sporulated; his3D1/his3D1; leu2D0/leu2D0; lys2D0/LYS2; MET15/met15D0; ura3D0/ura3D0; YKL125w::kanMX4/pRS316-Rrn3; YOR341W::YOR341W -TAP-His3MX	this work
Rrn3 shuffle/A43-TAP	BY4743; Mat a; sporulated; his3D1/his3D1; leu2D0/leu2D0; lys2D0/LYS2; MET15/met15D0; ura3D0/ura3D0; YKL125w::kanMX4/pRS316-Rrn3; YOR340C::YOR340C -TAP-His3MX	this work
Rrn3 shuffle/ A190-3xHA	BY4743; Mat a; sporulated; his3D1/his3D1; leu2D0/leu2D0; lys2D0/LYS2; MET15/met15D0; ura3D0/ura3D0; YKL125w::kanMX4/pRS316-Rrn3; YOR341W::YOR341W -3xFlag-His3MX	this work this work
Pol I purification strain/ GPY2	From YPH499/500; leu2-Δ1 ade2-101 trp1-Δ63 ura3-52 his3-Δ200; lys2-801 rpa43Δ::LEU2, pAS22 (Trp1) (A43 with HA and 6-His tag)	

2.1.3 Oligonucleotides

Oligonucleotides used in this study for cloning, mutagenesis and sequencing were ordered at Thermo Scientific at RP-HPLC quality. A list of all nucleotide sequences can be found in Table 6.

Table 6. Oligonucleotides. The name indicates the target gene, restriction sites if encoded in the primer and sites of mutations. The species of origin is *S.cerevisiae* if not indicated differently.

ID	Name	sequence
CB-P001	Fwd Rrn3Nhe1	GGAATTCGCTAGCATGATGGCTTTTGAGAATACAAGTAAACGACC
CB-P002	Rev Rrn3HindIII	ATTGCTTAAAGCTTTTAGTCATCCGACCCATCACTTTCATATTCC
CB-P003	Rrn3Strep-Nhe_fwd	GGAATTCGCTAGCTGGAGCCACCCGCAGTTCGAAAAAATGATGGCTTTTGAGAAT ACAAGTAAACGACC
CB-P004	Rrn3 delta loop 242-323_fwd	GAAAAGATTATTTTCGATTGATGGAATCAAAGAACTTTCCACC
CB-P005	Rrn3 delta loop 242-323_fwd	GGTGGAAAGTTCTTTGATTCCATCAATCGAAATAATCTTTTC
CB-P006	Rrn3 N-33 Nhe1_fwd	GGAATTCGCTAGCATGGGCCTGGTAACCCCTCAACCAGAGGAG
CB-P007	Nhe1 Rrn3 delta N 44_fwd	GGAATTCGCTAGCGATGAAGTGTTTCAGCGGCCATGTATAG
CB-P008	Rrn3 Glu394ALA_fwd	CACAACAACAATTAGCACTAATGGATTC
CB-P009	Rrn3 Glu394ALA_rev	GAATCCATTAGTGCTAATTGTTGTTGTG
CB-P010	Rrn3 Asp405ALA_fwd	GTGACTGATAGCTATTTTCGTTTGCC
CB-P011	Rrn3 Asp405ALA_rev	GGCAAACGAAATAGCTATCAGTGTCAC
CB-P012	Rrn3 Arg452GLY_fwd	CGTCCTGGTTGAATGGATACGTTATCGAAAG
CB-P013	Rrn3 Arg452GLY_rev	CTTTCGATAACGTATCCATTCAACCAGGACG
CB-P014	Rrn3 S444D_fwd	CAAATTATTTTCGTTGCAGACTATTTAACGTCCTGGTTG
CB-P015	Rrn3 S444D_rev	CAACCAGGACGTTAAATAGTCTGCAACGAAAATAATTTG
CB-P016	Rrn3 S448D_fwd	CGTTGCAAGCTATTTAACGGACTGGTTGAATAGATACG
CB-P017	Rrn3 S448D_rev	CGTATCTATTCAACCAGTCCGTTAAATAGCTTGCAACG
CB-P018	Rrn3 S444/448D_fwd	CGTTGCAGACTATTTAACGGACTGGTTGAATAGATACG
CB-P019	Rrn3 S444/448D_rev	CGTATCTATTCAACCAGTCCGTTAAATAGTCTGCAACG
CB-P020	Rrn3 S444A_fwd	CAAATTATTTTCGTTGCAGCCTATTTAACGTCCTGGTTG
CB-P021	Rrn3 S444A_rev	CAACCAGGACGTTAAATAGGCTGCAACGAAAATAATTTG
CB-P022	Rrn3 S448A_fwd	CGTTGCAAGCTATTTAACGGCCTGGTTGAATAGATACG
CB-P023	Rrn3 S448A_rev	CGTATCTATTCAACCAGGCCGTTAAATAGCTTGCAACG
CB-P024	Rrn3 Leu251^Glu320_fwd	GAATTAGATGAATTAGGAGGAGGAGAGTTGACGCAGGGAATC
CB-P025	Rrn3 Leu251^Glu320_rev	GATTCCTGCGTCAACTCTCCTCCTCAATTCATCTAATTC
CB-P026	Rrn3 ΔN_Ser48_start_fwd	GTGCAAGACAACAGCTGACAAGATGTGAGCGCCATGTATAGCAGG
CB-P027	Rrn3 ΔN_Ser48_start_rev	CCTGCTATACATGGCCGCTGACATCTTGTGAGCTGTTGTCTTGAC
CB-P028	Rrn3 DeltaC_Pro596_fwd	CAGAGTTACTTCCCATATGATCCTTAAGGTCTTTTTTCATAGGTATCTTCG
CB-P029	Rrn3 DeltaC_Pro596_rev	CGAAGATACCTATGAAAAAGACCTTAAGGATCATATGGGAAGTAACTCTG
CB-P030	Rrn3 dC617_fwd	CATAGAGTGGAGTGAAGCAAGCTAAGGTCTTTTTTCATAGGTATCTTC
CB-P031	Rrn3 dC617_rev	GAAGATACCTATGAAAAAGACCTTAGCTTGCTTCACTCCACTCTATG

ID	Name	sequence
CB-P032	Rrn3 dC596_fwd	GTTACTTCCCATATGATCCTTAAAAGCTTGCGGCCGC
CB-P033	Rrn3 dC596_rev	GCGGCCGCAAGCTTTTAAAGGATCATATGGGAAGTAAC
CB-P034	Rrn3 S101A_fwd	CTTTGGATATCTTAGCTAGTAATATCAACAGGATAG
CB-P035	Rrn3 S101A_rev	CTATCCTGTTGATATTACTAGCTAAGATATCCAAAAG
CB-P036	Rrn3 S101D_fwd	CTTTGGATATCTTAGATAGTAATATCAACAGGATAG
CB-P037	Rrn3 S101D_rev	CTATCCTGTTGATATTACTATCTAAGATATCCAAAAG
CB-P038	Rrn3 S102A_fwd	GGATATCTTATCTGCTAATATCAACAGGATAGAATCC
CB-P039	Rrn3 S102A_rev	GGATTCTATCCTGTTGATATTAGCAGATAAGATATCC
CB-P040	Rrn3 S102D_fwd	GGATATCTTATCTGATAATATCAACAGGATAGAATCC
CB-P041	Rrn3 S102D_rev	GGATTCTATCCTGTTGATATTATCAGATAAGATATCC
CB-P042	Rrn3 S109A_fwd	CAACAGGATAGAAGCCTCCAGGGGAACTTTC
CB-P043	Rrn3 S109A_rev	GAAAGTCCCCTGGAGGCTTCTATCCTGTTG
CB-P044	Rrn3 S109D_fwd	CAACAGGATAGAAGACTCCAGGGGAACTTTC
CB-P045	Rrn3 S109D_rev	GAAAGTCCCCTGGAGTCTTCTATCCTGTTG
CB-P046	Rrn3 S110A_fwd	CAACAGGATAGAATCCGCCAGGGGAACTTTC
CB-P047	Rrn3 S110A_rev	GAAAGTCCCCTGGCGGATTCTATCCTGTTG
CB-P048	Rrn3 S110D_fwd	CAACAGGATAGAATCCGACAGGGGAACTTTC
CB-P049	Rrn3 S110D_rev	GAAAGTCCCCTGTCCGATTCTATCCTGTTG
CB-P050	Rrn3 S145A_fwd	CATCAAATCCTTTGCGGAGTATACCAAATGGTG
CB-P051	Rrn3 S145A_rev	CACCATTTGGGTATACTCGCGCAAAGGATTTTGATG
CB-P052	Rrn3 S145D_fwd	CATCAAATCCTTTGCGATAGTATACCAAATGGTG
CB-P053	Rrn3 S145D_rev	CACCATTTGGGTATACTATCGCAAAGGATTTTGATG
CB-P054	Rrn3 S146A_fwd	CAAATCCTTTGCTCGGCTATACCAAATGGTGG
CB-P055	Rrn3 S146A_rev	CCACCATTTGGGTATAGCCGAGCAAAGGATTTTG
CB-P056	Rrn3 S146D_fwd	CAAATCCTTTGCTCGGATATACCAAATGGTGG
CB-P057	Rrn3 S146D_rev	CCACCATTTGGGTATATCCGAGCAAAGGATTTTG
CB-P058	Rrn3 S185A_fwd	CTTAAGGATGATTCCCGCCTCGATGGGATTCATAGATAC
CB-P059	Rrn3 S185A_rev	CTTAAGGATGATTCCCGCCTCGATGGGATTCATAGATAC
CB-P060	Rrn3 S185D_fwd	CTTAAGGATGATTCCCGACTCGATGGGATTCATAGATAC
CB-P061	Rrn3 S185D_rev	GTATCTATGAATCCCATCGAGTCGGAATCATCCTTAAG
CB-P062	Rrn3 S186A_fwd	CTTAAGGATGATTCCCTCCGATGGGATTCATAGATAC
CB-P063	Rrn3 S186A_rev	GTATCTATGAATCCCATCGCGGAGGAATCATCCTTAAG
CB-P064	Rrn3 S186D_fwd	CTTAAGGATGATTCCCTCCGATATGGGATTCATAGATACATATTTGGCC
CB-P065	Rrn3 S186D_rev	GGCAAATATGTATCTATGAATCCCATATCGGAGGAATCATCCTTAAG
CB-P066	Rrn3_Seq600	GGGATTCATAGATACATATTTGGCCAAATTTTCC
CB-P067	Rrn3_Seq1100	CACTCTAACAAATTATTTAAACGCATGTTCTAC
CB-P068	Rrn3_seqfwd	CAGCGGCCATGTATAGCA
CB-P069	Rrn3 pRS315_fwd-NotI-complementary	TACGACTCACTATAGGGCGAATTGGAGCTCCACCGGGTGGCGGCCGCCGTTAC TTACTGTGTTCAAGATGAAGCAACTGTACC
CB-P070	Rrn3 pRS315_rev-Sall-complementary	CTACTAAAGGGAACAAAAGCTGGGTACCGGGCCCCCTCGAGGTCGACCCCA CAGAACTCTTTAATAAGTAGACCTGCG

ID	Name	sequence
CB-P071	Rrn3 pRS316_fwd-NotI-complementary	TACGACTCACTATAGGGCGAATTGGAGCTCCACCGCGGTGGCGGCCGCCGTTAC TTACTGTGTTCAAGATGAAGCAACTGTACC
CB-P072	Rrn3 pRS316_rev-Sall-complementary	CTCACTAAAGGGAACAAAAGCTGGGTACCGGGCCCCCCTCGAGGTCGACCCCCA CAGAAACTCTTTAATAAGTAGACCTGCG
CB-P073	TAP genom A190 fwd	GAACAATGTTGGTACGGGTTCAATTTGATGTGTTAGCAAAGGTTCCAATGCGGCT TCCATGGAAAAGAGAAG
CB-P074	TAP genom A190 rev	TCCTTCAAATAAACTAATATTAATCGTAATAATTATGGGACCTTTTGCCTGCTTTA CGACTCACTATAGGG
CB-P075	TAP genom A43 fwd	CGTATACGAGGAAAACACCAGTGAAAGCAATGATGGTGAATCGAGTGATAGTGA TTCCATGGAAAAGAGAAG
CB-P076	TAP genom A43 rev	CCTATATCAATAACGTATATCTTTATTTGTTTTGATTTTTTCTATTTTTCCCGTCTAC GACTCACTATAGGG
CB-P077	R3_Bam/Hind cterm_fwd	GAAAGTGATGGATCCGATGACTAAGCTTTTTTTTC
CB-P078	R3_Bam/Hind cterm_rev	GAAAAAAAAGCTTAGTCATCGGATCCATCACTTTTC
CB-P079	pRS315-Rrn3-TAP_fwd	GCAAGCGGGGAATATGAAAGTGATGGGTCGGATGACTCCATGGAAAAGAGAAG
CB-P080	pRS315-Rrn3-TAP_rev	CGGGCATGTCTCGAAGATACCTATGAAAAAGACCTCAGTTGACTTCCC
CB-P081	HA genom A190 fwd	GAACAATGTTGGTACGGGTTCAATTTGATGTGTTAGCAAAGGTTCCAATGCGGCT CGTACGCTGCAGGTCGAC
CB-P082	HA genom A190 rev	TCCTTCAAATAAACTAATATTAATCGTAATAATTATGGGACCTTTTGCCTGCTTAT CGATGAATTCGAGCTCG
CB-P083	A43 S208D_fwd	GTTTGGGCAAATTTGACTTTGGAAACAGATCTTTGGG
CB-P084	A43 S208D_rev	CCCAAAGATCTGTTTCCAAGTCAAATTTGCCCAAAC
CB-P085	A43 S220D_fwd	CACTGGGTAGATGATAATGGTGAACCCATTGAC
CB-P086	A43 S208D_rev	GTCAATGGGTTACCATTATCATCTACCCAGTG
CB-P087	A43 S262/263D_fwd	GGCAATGGCTATAACGACGATCGTTCCCAAGC
CB-P088	A43 S262/263D_rev	GCTTGGGAACGATCGTCGTTATAGCCATTGCC
CB-P089	A43 S285D_fwd	GTATTTGATGACGAAGTTGACATCGAAAACAAAGAGAGCC
CB-P090	A43 S285D_rev	GGCTCTCTTTGTTTCGATGTCAACTTCGTCAATCAATAAC
CB-P091	Rrn6-NheI_fwd	GGAATTCGCTAGCATGAGTGAGGGACAAATCCAAGCTCAGATGTG
CB-P092	Rrn6-HindIII_rev	ATTGCTTAAAGCTTTTATCCAACCCCGGATCCTTTTCTTC
CB-P093	Rrn11-NdeI_fwd	GGAATTCATATGTTTGAAGTCCCTATAACTTTAACTAATAGG
CB-P094	Rrn11-NotI_rev	ATTGCTTAGCGGCCGCTCACTCACTTGAGTCTTCATCACTG
CB-P095	Rrn11-NotI-ohneStop_rev	ATTGCTTAGCGGCCGCTCACTTGAGTCTTCATCACTGTAATGC
CB-P096	Rrn6/11 2step_fwd	AATAATTTTGTTTAACTTTAAGAAGGAGATATACCATGTTTGAAGTCCCTATAACTT TAACTAATAGG
CB-P097	Rrn6/11 2step_rev	GGTATATCTCCTTCTTAAAGTTAAACAAAATTATTTTATCCAACCCCGGATCCTT TTCTTC
CB-P098	Rrn6 seqfwd_1	CTTTAGAATTGAAAGTGTC
CB-P099	Rrn6 seqfwd_2	CATCATTGTCGACCATCC

2.1.4 Plasmids

Plasmids used for recombinant expression of from *E.coli* were generated by classical cloning (Table 7). Inserts were produced via single- or two-step PCR. Point mutations were introduces via Quick Change mutagenesis.

Table 7. Plasmids for expression in *E. coli*

ID	Type	Insert	cloning		
			From	Restriction sites	via
1686	pET-28b	Rrn3 (1-627)	genomic DNA	NheI, Hind III	Classical cloning
1688	pET-28b	Rrn3 (34-627)	genomic DNA	NheI, Hind III	Classical cloning
1689	pET-21b	Strep-Rrn3 (1-627)	genomic DNA	NheI, Hind III	Classical cloning
1690	pET-28b	Rrn3-Δloop	plasmid 1686	NheI, Hind III	Classical cloning
1691	pET-28b	Rrn3-S444/448D	plasmid 1686	NheI, Hind III	Quick Change
1692	pET-28b	Rrn3-S444/448A	plasmid 1686	NheI, Hind III	Quick Change
1693	pET-28b	Rrn3-D405A	plasmid 1686	NheI, Hind III	Quick Change
1694	pET-28b	Rrn3-R452G	plasmid 1686	NheI, Hind III	Quick Change
1695	pET-28b	Rrn3-E394A	plasmid 1686	NheI, Hind III	Quick Change
1696	pET-28b	Rrn3-S145D	plasmid 1686	NheI, Hind III	Quick Change
1697	pET-28b	Rrn3-S185D	plasmid 1686	NheI, Hind III	Quick Change
1698	pET-21b	Strep-Rrn3-S185D	genomic DNA	NheI, Hind III	Quick Change
1699	pET-28b	Rrn6	genomic DNA	NheI, Hind III	classical cloning
1700	pET-28b	Rrn7	genomic DNA	NdeI/NotI	Stefan Jennebach
1701	pET-21b	Rrn7	genomic DNA	NdeI/NotI	Stefan Jennebach
1702	pET-28b	Rrn11	genomic DNA	NdeI/NotI	classical cloning
1703	pET-28b	Rrn6/Rrrn11	genomic DNA	NheI/NotI	classical cloning
1704	pET-21b	Rrn6/Rrrn11	genomic DNA	NheI/NotI	classical cloning
1705	pET-21b	A43	genomic DNA	NdeI, NotI	Sebastian Geiger
1706	pET-21b	A43/14	genomic DNA	NdeI, NotI	Sebastian Geiger
1707	pET-21b	A43-14_S208D-S262/263D	plasmid 1706	NdeI, NotI	Quick Change
1708	pET-21b	A43-14QCA S208D-S262/263D-S285D	plasmid 1707	NdeI, NotI	Quick Change
1709	pET-21b	A43/14QCB S220D-S262/263D-S285D	plasmid 1710	NdeI, NotI	Quick Change
1710	pET-21b	A43/14 S262/263D-285D	plasmid 1706	NdeI, NotI	Quick Change

Plasmids used for *S. cerevisiae* complementation assays were generated by yeast *in vivo* recombination (Table 8).

Table 8. plasmids *S. cerevisiae*

ID	Type	Insert	cloning		
			From	Restriction sites	Via
1711	pRS316	5'UTR- <i>Rrn3</i> (1-627)-3'UTR	genomic DNA	NotI, Sall	yeast <i>in vivo</i> recombination
1712	pRS315	5'UTR- <i>Rrn3</i> (1-627)-3'UTR	genomic DNA	NotI, Sall	yeast <i>in vivo</i> recombination
1713	pRS315	5'UTR- <i>Rrn3-S444A</i> (1-627)-3'UTR	plasmid 1712	NotI, Sall	yeast <i>in vivo</i> recombination
1714	pRS315	5'UTR- <i>Rrn3-S444D</i> (1-627)-3'UTR	plasmid 1712	NotI, Sall	yeast <i>in vivo</i> recombination
1715	pRS315	5'UTR- <i>Rrn3-S448S</i> (1-627)-3'UTR	plasmid 1712	NotI, Sall	yeast <i>in vivo</i> recombination
1716	pRS315	5'UTR- <i>Rrn3-S448D</i> (1-627)-3'UTR	plasmid 1712	NotI, Sall	yeast <i>in vivo</i> recombination
1717	pRS315	5'UTR- <i>Rrn3-S444/448A</i> (1-627)-3'UTR	plasmid 1712	NotI, Sall	yeast <i>in vivo</i> recombination
1718	pRS315	5'UTR- <i>Rrn3-S444/448D</i> (1-627)-3'UTR	plasmid 1712	NotI, Sall	yeast <i>in vivo</i> recombination
1719	pRS315	5'UTR- <i>Rrn3-S101A</i> (1-627)-3'UTR	plasmid 1712	NotI, Sall	yeast <i>in vivo</i> recombination
1720	pRS315	5'UTR- <i>Rrn3-S101D</i> (1-627)-3'UTR	plasmid 1712	NotI, Sall	yeast <i>in vivo</i> recombination
1721	pRS315	5'UTR- <i>Rrn3-S102A</i> (1-627)-3'UTR	plasmid 1712	NotI, Sall	yeast <i>in vivo</i> recombination
1722	pRS315	5'UTR- <i>Rrn3-S102D</i> (1-627)-3'UTR	plasmid 1712	NotI, Sall	yeast <i>in vivo</i> recombination
1723	pRS315	5'UTR- <i>Rrn3-S109A</i> (1-627)-3'UTR	plasmid 1712	NotI, Sall	yeast <i>in vivo</i> recombination
1724	pRS315	5'UTR- <i>Rrn3-S109D</i> (1-627)-3'UTR	plasmid 1712	NotI, Sall	yeast <i>in vivo</i> recombination
1725	pRS315	5'UTR- <i>Rrn3-S110A</i> (1-627)-3'UTR	plasmid 1712	NotI, Sall	yeast <i>in vivo</i> recombination
1726	pRS315	5'UTR- <i>Rrn3-S110D</i> (1-627)-3'UTR	plasmid 1712	NotI, Sall	yeast <i>in vivo</i> recombination
1727	pRS315	5'UTR- <i>Rrn3-S145A</i> (1-627)-3'UTR	plasmid 1712	NotI, Sall	yeast <i>in vivo</i> recombination
1728	pRS315	5'UTR- <i>Rrn3-S145D</i> (1-627)-3'UTR	plasmid 1712	NotI, Sall	yeast <i>in vivo</i> recombination
1729	pRS315	5'UTR- <i>Rrn3-S146A</i> (1-627)-3'UTR	plasmid 1712	NotI, Sall	yeast <i>in vivo</i> recombination
1730	pRS315	5'UTR- <i>Rrn3-S146D</i> (1-627)-3'UTR	plasmid 1712	NotI, Sall	yeast <i>in vivo</i> recombination
1731	pRS315	5'UTR- <i>Rrn3-S185A</i> (1-627)-3'UTR	plasmid 1712	NotI, Sall	yeast <i>in vivo</i> recombination
1732	pRS315	5'UTR- <i>Rrn3-S185D</i> (1-627)-3'UTR	plasmid 1712	NotI, Sall	yeast <i>in vivo</i> recombination
1733	pRS315	5'UTR- <i>Rrn3-S186A</i> (1-627)-3'UTR	plasmid 1712	NotI, Sall	yeast <i>in vivo</i> recombination

ID	Type	Insert	cloning		
			From	Restriction sites	Via
1734	pRS315	5'UTR- <i>Rrn3-S186D</i> (1-627)-3'UTR	plasmid 1712	NotI, Sall	yeast <i>in vivo</i> recombination
1735	pRS315	5'UTR- <i>Rrn3-ΔL251^320</i> (1-627)-3'UTR	plasmid 1712	NotI, Sall	yeast <i>in vivo</i> recombination
1736	pRS315	5'UTR- <i>Rrn3-ΔL242^323</i> (1-627)-3'UTR	plasmid 1712	NotI, Sall	yeast <i>in vivo</i> recombination
1737	pRS315	5'UTR- <i>Rrn3-ΔN</i> (1-627)-3'UTR	plasmid 1712	NotI, Sall	yeast <i>in vivo</i> recombination
1738	pRS315	5'UTR- <i>Rrn3-ΔC617</i> (1-627)-3'UTR	plasmid 1712	NotI, Sall	yeast <i>in vivo</i> recombination
1739	pRS315	5'UTR- <i>Rrn3-S614D</i> (1-627)-3'UTR	plasmid 1712	NotI, Sall	yeast <i>in vivo</i> recombination
1740	pRS315	5'UTR- <i>Rrn3-TAP</i> (1-627)-3'UTR	plasmid 1712	NotI, Sall	yeast <i>in vivo</i> recombination
1741	pRS315	5'UTR- <i>Rrn3-S145D-TAP</i> (1-627)-3'UTR	plasmid 1740	NotI, Sall	yeast <i>in vivo</i> recombination
1742	pRS315	5'UTR- <i>Rrn3-S185D-TAP</i> (1-627)-3'UTR	plasmid 1740	NotI, Sall	yeast <i>in vivo</i> recombination

2.1.5 Chemicals

Table 9 Chemicals used for protein buffer solutions and crystallization

Chemical	Source	Application
β-Mercaptoethanol	Sigma-Aldrich	protein buffer
Dithiothreitol (DTT)	Promega	protein buffer
NaF	Roth	Phosphatase inhibitor
β-Phosphoglycerate	Sigma-Aldrich	Phosphatase inhibitor
Na-Pyrophosphate (H ₃ NaO ₇ P ₂)	Sigma-Aldrich	Phosphatase inhibitor
PEG 3350	Fluka	Crystallization and Yeast genomic Transformation
K-Na-tartrate	Fluka	Crystallization
Li-Acetate	Sigma-Aldrich	Yeast genomic Transformation

2.1.6 Media and additives

Cultivation media used in this study are listed in Table 10, additives are listed in Table 11.

Table 10. Media for *E. coli* and *S. cerevisiae* cultures

Media	Description	Applicaton
LB	1% (w/v) tryptone; 0.5% (w/v) yeast extract; 0.5% (w/v) NaCl	<i>E. coli</i> culture
TB	12 g Tryptone, 24 g Yeast extract, 4 ml Glycerol	<i>E. coli</i> culture
10 x Additives for TB	2.3% (w/v) KH ₂ PO ₄ , 12.54% (w/v) K ₂ HPO ₄	<i>E. coli</i> culture
autoinduction 5052	25% Glycerol, 2.5 % Glucose, 10% α-Lactose	<i>E. coli</i> culture
SOB	2% (w/v) tryptone; 0.5% (w/v) yeast extract; 8.55 mM NaCl; 2.5 mM KCl; 10 mM MgCl ₂	<i>E. coli</i> transformation
SOC	SOB + 20 mM glucose (before use)	<i>E. coli</i> transformation
YPD	2% (w/v) peptone; 2% (w/v) glucose; 1% (w/v) yeast extract	Yeast culture
Synthetic complete (SC) amino acid drop-out medium	0.69% (w/v) nitrogen base; 0.6% (w/v) CSM amino acid drop out mix; 2% (w/v) glucose; pH 5.6-6.0	Yeast culture
YPD plates	2% (w/v) peptone; 2% (w/v) glucose; 1% (w/v) yeast extract; 2% (w/v) agar	Yeast culture
SC amino acid drop-out plates	0.69% (w/v) nitrogen base; 0.6% (w/v) CSM amino acid drop out mix; 2% (w/v) glucose; pH 5.6-6.0; 2% (w/v) agar	Yeast culture
5-FOA Plates	SC (-ura) + 0.01% (w/v) uracil; 0.2% (w/v) 5-FOA; 2% (w/v) agar	Yeast culture
Pre-sporulation Plates	1% (w/v) KCH ₃ COO; 0.1% (w/v) yeast extract; 0.079% (w/v) CSM amino acid complete mix; 0.25% (w/v) glucose; pH 5.6-6.0; 2% (w/v) agar	Yeast culture
Sporulation plate	1% (w/v) KCH ₃ COO; 0.079% (w/v) CSM amino acid complete mix; pH 5.6-6.0; 2% (w/v) agar	Yeast culture

Table 11 Additives for *E. coli* and *S. cerevisiae* cultures

Additive	Description	Stock solution	Applied concentration
IPTG	<i>E. coli</i> induction	1 M in H ₂ O	0.5 mM
Ampicillin	Antibiotic	100 mg/ml in H ₂ O	100 µg/ml for <i>E. coli</i> culture
Kanamycin	Antibiotic	30 mg/ml in H ₂ O	30 µg/ml for <i>E. coli</i> culture
Chloramphenicol	Antibiotic	50 mg/ml in EtOH	50 µg/ml for <i>E. coli</i> culture
Tetracyclin	Antibiotic	12.5 mg/ml in 70% EtOH	50 µg/ml for <i>E. coli</i> culture
Geneticin (G418)	Antibiotic	200 mg/ml in H ₂ O	200 µg/ml for yeast culture
Rapamycin	Inhibitor of TOR kinase	2.5 mg/ml in DMSO	0.025 – 0.25 µg/ml for yeast culture
Cycloheximide	Inhibitor of protein biosynthesis	10 mg/ml in H ₂ O	0.1 – 0.5 µg/ml for yeast culture

2.1.7 Buffers and solutions

General Buffers used in this study are listed in Table 12. Buffers for protein purification are listed in Table 13-15.

Table 12 general buffers and solutions

Name	Description	Application
4x Stacking gel buffer	0.5 M Tris; 0.4% (w/v) SDS; pH 6.8 at 25°C	SDS-PAGE
4x Separation gel buffer	3 M Tris; 0.4% (w/v) SDS; pH 8.9 at 25°C	SDS-PAGE
Electrophoresis buffer	25 mM Tris; 0.1% (w/v) SDS; 250 mM glycine	SDS-PAGE
5x SDS sample buffer	250 mM Tris/HCl pH 7.0 at 25°C; 50% (v/v); glycerol; 0.5% (w/v) bromophenol blue; 7.5% (w/v) SDS; 12.5% (w/v) β-mercaptoethanol	SDS-PAGE
Gel staining solution	50% (v/v) Ethanol; 7% (v/v) acetic acid; 0.125% (w/v) Coomassie Brilliant Blue R-250	Coomassie staining
Gel destaining solution	5% (v/v) Ethanol; 7% (v/v) acetic acid	
2x transfer buffer	2.4% (w/v) glycine; 0.8% (w/v) Tris; 40% (v/v) ethanol	Wester blotting
pre-treatment solution	7.5% (v/v) β-mercaptoethanol, 1.85 M NaOH	Cell lysis for western blotting
Loading Buffer	1M Tris-HCl; pH 6.8, 8 % SDS, 10% Glycerol, 14.7 M β-mercaptoethanol, 0.5 M EDTA, 0.08 % Bromophenol Blue	4x SDS loading buffer
100x PI	0.028 mg/ml leupeptin; 0.137 mg/ml pepstatin A; 0.017 mg/ml PMSF; 0.33 mg/ml benzamidine; in 100% EtOH p.a.	Protease inhibitor mix
TFB1	30 mM KOAc; 50 mM MnCl ₂ ; 100 mM RbCl; 10 mM CaCl ₂ ; 15% (v/v) glycerol; pH 5.8 at 25°C	Preparation of chemically competent cells
TFB2	10 mM MOPS pH 7.0 at 25°C; 10 mM RbCl; 75 mM CaCl ₂ ; 15% (v/v) glycerol	Preparation of chemically competent cells
LitSorb	18.2% (w/v) D-Sorbitol in TELit, pH8.0	Preparation of competent yeast cells and transformation of yeast
TELit (pH 8.0)	155 mM LiOAc, 10 mM Tris/HCl (pH 8.0), 1mM EDTA	Preparation of competent yeast cells and transformation of yeast
LitPEG	40% (w/v) PEG 3350 in TELit, pH 8.0, filter sterlized	Preparation of competent yeast cells and transformation of yeast
TBE	8.9 mM Tris; 8.9 mM boric acid; 2 mM EDTA (pH 8.0,25°C)	Agarose gels
6x Loading buffer	10 mM Tris pH 7.6; 0.0015% (w/v) bromphenol blue; 0.0015% (w/v) xylene cyanol; 60% (v/v) glycerol; 100 mM EDTA; 1% SDS	Agarose gels
PBS	2 mM KH ₂ PO ₄ , 4 mM Na ₂ HPO ₄ , 140 mM NaCl, 3 mM KCl, pH 7.4 @ 25°C	General protein buffer

Name	Description	Application
50x d-desthiobiotin (DTB)	125 mM d-desthiobiotin, in 500 mM Tris pH 8.0	Strep-tag purification
avidine	50 μ mol/L Avidin 50% Glycerol 20 mM Tris pH 8.0, 150 mM NaCl, 10 mM β -ME	Strep-tag purification
Salmon Sperm DNA	2 mg/ml Salmon sperm DNA	Yeast genomic transformation
ChIP was buffer	10 mM Tris-HCl at pH 8.0, 0.25 M LiCl, 1 mM EDTA, 0.5 % NP-40, 0.5 % Na deoxycholate	ChIP assays
ChIP elution buffer	50 mM Tris-HCl at pH 7.5, 10 mM EDTA, 1 % SDS	ChIP assays
TE buffer	10 mM Tris-HCl at pH 7.4, 1 mM EDTA	General protein buffer

Table 13 Buffers for Rrn3 Purification

Buffer	Description
Ni-NTA Lysis buffer L	50 mM HEPES [pH 7.8], 0.2 M NaCl, 5 mM Imidazole, 10 % Glycerol, 3mM DTT, 1x Protease Inhibitor Mix
Ni-NTA washing buffer	50 mM HEPES [pH 7.8], 0.2 M NaCl, 20-50 mM Imidazole, 10 % Glycerol, 3mM DTT, 1x Protease Inhibitor Mix
Ni-NTA elution buffer	50 mM HEPES [pH 7.8], 0.2 M NaCl, 150 mM Imidazole, 10 % Glycerol, 3mM DTT, 1x Protease Inhibitor Mix
Strep lysis/washing buffer	50 mM HEPES [pH 7.8], 0.1 M NaCl, 5 mM MgCl ₂ , 10 % Glycerole, 10 mM β -ME, Protease Inhibitor Mix
Strep elution buffer	50 mM HEPES [pH 7.8], 0.1 M NaCl, 5 mM MgCl ₂ , 10 % Glycerole, 10 mM β -ME, Protease Inhibitor Mix , 1x DTB
Anion exchange buffer A	50 mM HEPES [pH 7.8], 10 % Glycerole, 5mM DTT.
Anion exchange buffer B	50 mM HEPES [pH 7.8], 10 % Glycerole, 2 M NaCl, 5mM DTT.
Gel filtration buffer C	50 mM HEPES [pH 7.8], 10 % Glycerole, 300 mM NaCl, 5mM DTT.

Table 14 Buffers for A43/14 Purification

Buffer	Description
Ni-NTA Lysis buffer L2	150 mM NaCl, 50 mM Tris (pH=7.5), 5 mM DTT, 1x Protease Inhibitor Mix
Ni-NTA washing buffer	150 mM NaCl, 50 mM Tris (pH=7.5), 5 mM DTT, 60 mM Imidazole, 1x Protease Inhibitor Mix
Ni-NTA elution buffer	150 mM NaCl, 50 mM Tris (pH=7.5), 5 mM DTT, 150 mM Imidazole, 1x Protease Inhibitor Mix
Anion exchange buffer A2	50 mM Tris (pH=7.5), 5 mM DTT
Anion exchange buffer B2	50 mM Tris (pH=7.5), 5 mM DTT
Gel filtration buffer C2	100 mM NaCl, 50 mM Tris (pH=7.5), 5 mM DTT

Table 15 Buffers and additives for Pol I purification

Buffer	Description	Additives
Lysis/ Freezing buffer	150 mM HEPES (pH 7,8) 60mM MgCl ₂ , 30 % Glycerol, 5 mM DTT, 1x PI	2 mM Na-Pyrophosphate (H ₃ NaO ₇ P ₂), 50 mM NaF, 5 mM β-Phosphoglycerate
Dilution buffer	100 mM Hepes (pH 7,8), 20mM MgCl ₂ , 400 mM (NH ₄) ₂ SO ₄	2 mM Na-Pyrophosphate (H ₃ NaO ₇ P ₂), 50 mM NaF, 5 mM β-Phosphoglycerate
Dialysis buffer (2x)	100 mM KoAc, 40 mM HEPES (pH 7,8), 2 mM MgCl ₂ , 10 % Glycerol, 10 mM β-Mercaptoethanol, 1xPI (benzamidine &PMSF)	0.4 mM Na-Pyrophosphate (H ₃ NaO ₇ P ₂), 5 mM NaF, 1 mM β-Phosphoglycerate
Res/W1 buffer	1.5 M KoAc, 20 mM HEPES (pH 7,8), 1 mM MgCl ₂ , 10 % Glycerol, 10 mM β-Mercaptoethanol, 1x PI	2 mM Na-Pyrophosphate (H ₃ NaO ₇ P ₂), 50 mM NaF, 5 mM β-Phosphoglycerate
W2 buffer	300 mM KoAc, 20 mM HEPES (pH 7,8), 1 mM MgCl ₂ , 10 % Glycerol, 10 mM β-Mercaptoethanol	2 mM Na-Pyrophosphate (H ₃ NaO ₇ P ₂), 50 mM NaF, 5 mM β-Phosphoglycerate
E100 buffer	300 mM KoAc, 20 mM HEPES (pH 7,8), 1 mM MgCl ₂ , 100 mM Imidazole, 10 % Glycerol, 10 mM β-Mercaptoethanol	2 mM Na-Pyrophosphate (H ₃ NaO ₇ P ₂), 50 mM NaF, 5 mM β-Phosphoglycerate
MonoQ buffer A3	20 mM HEPES (pH 7,8), 1 mM MgCl ₂ , 10 % Glycerol, 5 mM DTT	2 mM Na-Pyrophosphate (H ₃ NaO ₇ P ₂), 5 mM NaF, 5 mM β-Phosphoglycerate
MonoQ buffer B3	2 M KoAc, 20 mM HEPES (pH 7,8), 1 mM MgCl ₂ , 10 % Glycerol, 5 mM DTT	2 mM Na-Pyrophosphate (H ₃ NaO ₇ P ₂), 5 mM NaF, 5 mM β-Phosphoglycerate
Superose 6 buffer C3	60 mM (NH ₄) ₂ SO ₄ , 5 mM HEPES (pH 7,8), 1 mM MgCl ₂ , 0.1 μM ZnCl ₂ , 10 % Glycerol, 5 mM DTT	2 mM Na-Pyrophosphate (H ₃ NaO ₇ P ₂), 5 mM NaF, 5 mM β-Phosphoglycerate

2.2 General Methods

2.2.1 Preparation and transformation of competent *E. coli* cells

Chemically competent *E. coli* XL1-blue cells were prepared from a 400 ml LB culture. LB media, containing Tetracycline, was inoculated to an OD₆₀₀ of 0.05 with 4 ml over-night pre-culture, and grown to an OD₆₀₀ of 0.5. The culture was cooled down to 4 °C on ice and kept at that temperature for the following steps. Cells were centrifuged at 3200 g for 10 min, washed with 100 ml TFB1, and centrifuged again. The supernatant was discarded and the pellet resuspended in 8 ml TFB2. 50 µl Aliquots were shock-frozen in liquid nitrogen and stored at -80 °C. For transformation, 100 ng of a plasmid, or 7 µl of a ligation reaction were added to an aliquot of competent XL1-blue cells, incubated for 5-10 min on ice, followed by a 50 s heat shock at 42 °C. Subsequently cells were cooled on ice for 1 min, resuspended in 600 µl LB media, and incubated for 1 h at 37 °C under constant shaking at 750 rpm in a thermo mixer (Qiagen). Finally, cells were plated onto selective LB plates and incubated over night at 37 °C.

Electrocompetent *E. coli* XL1-blue cells were prepared from 1 l culture in SOB media. After inoculation of the media, containing Tetracycline, to an OD₆₀₀ of 0.05 with a 50 ml over-night pre-culture, cells were grown to a final OD₆₀₀ of 0.5. The culture was then cooled down to 4 °C on ice and kept at this temperature for all following steps. Cells were split in 250 ml fractions, centrifuged at 3200 g for 10 min, and washed with each 100 ml ice-cold sterile water, followed by a second centrifugation step, and resuspension of the cells in 2.5 ml ice-cold, sterile 10 % (v/v) glycerol. 50 µl aliquots were flash-frozen in liquid nitrogen and stored at -80 °C. For transformation 50 ng plasmid or 7 µl of a ligation reaction were added to an aliquot of competent cells, which were then transferred to a pre-cooled electroporation cuvette (Bio-Rad). After 5 min incubation on ice, cells were pulsed at 2.5 kV (Micro-Pulser, Bio-Rad), and then immediately resuspended in 700 µl pre-warmed SOC medium. Cells were incubated for at least 1 h at 37 °C under constant shaking at 750 rpm in a thermo mixer (Qiagen) and finally plated onto selective LB plates and incubated over night at 37 °C.

2.2.2 Preparation and transformation of competent *S. cerevisiae* cells

Chemical competent *S. cerevisiae* cells were prepared from 50 ml YPD cultures, which were inoculated with an over-night pre-culture to an OD₆₀₀ of 0.2 and grown to an OD₆₀₀ of 0.8-1.0. After the cells reached their final OD₆₀₀, they were centrifuged at 1800 g, washed with sterile water, centrifuged again, washed with 1ml Li-Acetate [100 mM], centrifuged and the pellet was finally resuspended in 500 µl Li-Acetate [100 mM]. 50 µl aliquots were prepared, centrifuged again and the supernatant was discarded. Competent cells were used directly for highest competence or stored at -20 °C for a few days. For transformation 240 µl PEG 3350 were added, followed by 50 µl salmon sperm DNA and 36 µl 1M Li-Acetate. 1000 ng digested vector and 600 ng Insert, or 500 ng plasmid were added, in a total volume of 34 µl. Samples were mixed vigorously by pipetting or vortexing and then incubated at 30 °C for 30 min, followed by a heat shock at 42 °C for 25 min. Finally cells were centrifuged for 15 s, resuspended in sterile water and plated on selective plates.

To prepare chemical competent *S. cerevisiae* cells for genomic recombination, 50 ml YPD cultures were grown as described above but to an OD₆₀₀ of 0.5-0.7. Cells were centrifuged at 1800 g, washed with sterile water, centrifuged again and resuspended in 5 ml LitSorb. After another centrifugation step the pellet was resuspended in 360 µl LitSorb. 40 µl pre-heated Salmon sperm DNA were added, and after mixing 50 µl aliquots were prepared and used directly. For transformation 10 µl of PCR product and 360 µl LitPEG were added to 50 µl of competent cells, followed by incubation at room temperature (RT) for 30 min. Then 47 µl DMSO were added and the cells were incubated at 42 °C for 15 min. Finally, cells were centrifuged at 1500 g for 3 min, the pellet was resuspended in 200 µl sterile water and plated on selective plates.

2.2.3 Cloning and mutagenesis

Primers for Polymerase Chain Reaction (PCR) were designed to have a melting temperature close to 55 °C, with primer pairs used in one reaction having the same melting temperature. Primers used for classical cloning had a 5'-overhang of several nucleotides before the restriction site to facilitate restriction cleavage. Complementary regions consisted of at least 18 bp. Primers for site-directed mutagenesis via Quick-Change, comprised at least 15 bp of complementary sequences harboring the mutation on

each side. PCR reactions were carried out using either Herculase II (Stratagene), Phusion Polymerase (Finnzymes) or Taq polymerase (Fermentas), depending on requirements. Reactions were carried out in 50 μ l sample volume, containing polymerase specific buffers, 10-50 ng of plasmid DNA or 100-200 ng genomic DNA, 0.2 mM dNTP-mix, 0.5 μ M of each, forward and reverse primer, 0.5 μ l Polymerase (2-5U) and optionally $MgCl_2$, if not included in the polymerase buffer. Quality of PCR products was usually controlled via agarose gel electrophoresis (1 % w/v), bands were visualized with SYBR-Safe DNA gel stain (1:10000, Invitrogen), and the desired bands were purified using a gel extraction kit (Qiagen). If no quality control was required, PCR products were directly purified using a PCR purification kit (Qiagen).

Purification tags were either introduced via encoding in the primer, or alternatively by in frame cloning into the vector. Vectors from the pET series, used for *E. coli* cloning, were obtained from Novagen. For *S. cerevisiae* cloning the pRS series from Euroscarf was used. PCR Products and vectors were digested using restriction endonucleases obtained from NEB or Fermentas. Digested vectors were dephosphorylated prior to ligation reactions using an Alkaline Phosphatase (NEB or Fermentas), which was then inactivated by incubation at 80 °C for 20 min, followed by purification via agarose gel electrophoresis. Concentrations of PCR products and linearized vectors were determined using a ND-1000 (NanoDrop) spectrophotometer, via the absorption at 260 nm. Different molar ratios of Vector to PCR product, usually 1:5 and 1:2, were used for ligation. Ligation reactions were carried out using a T4 DNA ligase (NEB or Fermentas) with the provided buffer in 20 μ l reaction volume. Ligation reactions were incubated for 3-4 h at RT, or over night at 16 °C. Transformation was performed as described in 2.2.1.

For cloning via homologous recombination, primer pairs were designed, harboring a 40 bp sequence, complementary to the borders of the multiple cloning site of the plasmid. PCR products were synthesized and purified as described above. The plasmid was digested with one or two different restriction enzymes, that cut only at the multiple cloning site and was purified as described above. Then competent yeast cells were transformed with digested plasmid and PCR product as described in section 2.2.2.

2.2.4 Protein expression in *E. coli*

Recombinant proteins were expressed in *E. coli* BL21 (DE3) RIL cells (Stratagene). Cells were transformed with plasmids carrying the desired protein as described in 2.2.1. For induction with IPTG, cells were grown in LB media including the required antibiotics at 37 °C to an OD₆₀₀ of 0.6, cooled down on ice to 18 °C, followed by addition of IPTG to a final concentration of 1 mM. Cultures were then further grown over night at 18 °C.

For autoinduction, cells were grown in TB media with antibiotics and the additive 5052 (Table 10). Cells were grown to an OD₆₀₀ of 0.5 at 37 °C, then cooled down to 24 °C and grown over night at this temperature. Cells were harvested by centrifugation at 3500 g at 4 °C for 20 min, washed with PBS and flash frozen in liquid nitrogen before they were stored at -80 °C.

2.2.5 purification of recombinant Rrn3

Proteins from *S. cerevisiae* were cloned and expressed as described in 2.2.3 and 2.2.4. Cell pellets were thawed and lysed by sonification. The lysate was centrifuged and the supernatant was loaded onto a 1 ml gravity flow Ni-NTA (QIAGEN) column equilibrated in Ni-NTA lysis buffer. The column was washed with 20 column volumes (CV) Ni-NTA wash buffer containing 20 mM imidazol, followed by washing steps with buffer A containing 30 mM and 50 mM imidazol. Protein was eluted with buffer A containing 150 mM imidazol.

Proteins carrying a *Strep*-Tag were bound to a 1 ml *Strep*-Tactin Separose column (IBA) equilibrated in buffer A and eluted with buffer A containing 2.5 mM d-Desthiobiotin. Elution fractions were analysed via SDS PAGE and fractions containing the desired protein in an appropriate purity were pooled. Proteins were further purified by anion exchange chromatography (Mono Q, GE Healthcare). The column was equilibrated in 90% buffer A and 10 % buffer B (100 mM NaCl) and proteins were eluted with a linear gradient of 20 CV from 100 mM to 1 M NaCl. After concentration, the sample was applied to a Superdex 200 size exclusion chromatography column (GE Healthcare) equilibrated with buffer C. Pooled peak fractions were concentrated to 10 mg/ml or higher.

2.2.6 Protein analysis

Determination of protein concentrations

Protein concentrations of crude protein solutions before purification were usually determined using the Bradford assay (Bradford, 1976). 1-10 μl of Protein solution were added to 1 ml of diluted (1:5 with ddH₂O) Bradford reagent solution (Bio-Rad), and the absorption at 595 nm was measured. Protein concentrations were then calculated from a reference curve that was previously prepared using bovine serum albumin as a standard (Fraktion V, Roth).

Protein concentrations after purification were determined by measuring the absorption at 280 nm using and ND-1000 (NanoDrop) spectrophotometer and calculated with the molar absorption coefficients calculated with ProtParam based on the Protein sequence (ExPASy, Bioinformatics resource portal).

SDS-Polyacrylamid gel electrophoresis

Proteins were usually analysed after electrophoretic separation via an SDS PAGE in a Bio-RAD gel system with acrylamide/bisacrylamide gels. For better resolution commercially available NuPAGE Novex Midi-Bis-Tris 4-12% gradient gels (Invitrogen) were used according to the manufacturer's instructions. Gels were stained with Coomassie solution for 15 min and destained over night in destaining solution (Table 12).

Limited proteolysis analyses

To determine stable and compactly folded domains of the protein for crystallization trials, a limited proteolysis was performed applying three different proteases, Trypsin, Chymotrypsin and Subtilisin. 120 μl protein solution (1 $\mu\text{g}/\mu\text{l}$) were incubated with each 1 μl of the first two proteases (1 $\mu\text{g}/\mu\text{l}$) and reactions were stopped by heat-inactivation after 1, 2, 10, 30 and 60 min. A 1 $\mu\text{g}/\mu\text{l}$ solution of Subtilisin was diluted 1:10, 1:100 and 1:1000 respectively, and 1 μl of each dilution was incubated with 20 μl of protein solution (1 $\mu\text{g}/\mu\text{l}$) on ice for 1 h and heat-inactivated afterwards. The samples were mixed with SDS sample buffer and degraded Protein fragments were separated via SDS-PAGE. Bands were excised from the gel and analysed via EDMAN sequencing (Niall, 1973).

Edman sequencing

Protein Bands excised from a coomassie stained SDS gel were transferred onto a PVDF membrane by passive adsorption. Therefore gel-bands were dried in a speed-vac centrifuge, rehydrated in 20 μ l swelling buffer at room temperature. A concentration gradient was set up by adding 100 μ l ddH₂O and a small piece of an ethanol-soaked PVDF membrane (Schleicher & Schuell) was added. After the solution turned blue, 10 μ l methanol were added as a catalyst and the mixture was incubated for 2-4 days until the transfer was complete. The membrane was washed 5 times in 10 % methanol and The protein was N-terminally sequenced from the dry membrane in a PROCISE 491 sequencer (Applied Biosystems).

2.3 Rrn3 Crystallization and characterization

2.3.1 Crystallization screening

For crystallization of Rrn3, pure protein was concentrated to 10 mg/ml. Initial crystallization screens in microplates with 200 nl sitting-drops were performed at the Crystallization Facility at the MPI of Biochemistry, Martinsried. Scale-up of initial crystallization conditions was done in 2 μ l hanging drops over 500 μ l reservoir solution, resulting in a final crystallization condition containing 14% PEG 3350 and 250 mM sodium-potassium-tartrate.

2.3.2 Crystal structure determination

Directly after harvesting crystals from the drop, they were cryo-protected by a stepwise transfer to reservoir solutions containing 5-20% PEG 200, and finally flash-frozen in liquid nitrogen. For structure determination crystals were soaked in a reservoir solution containing 10 mM Thiomersal for 2-12 min, depending on crystal shape and size and subsequently transferred to the solutions additionally containing the cryo-protectant, and finally flash frozen in liquid nitrogen. Diffraction data were obtained on a PILATUS 6M detector at the Swiss Light Source in Villigen, Switzerland and processed with XDS (Kabsch, 2010) (Table 16). With SHELXD (Schneider and Sheldrick, 2002) two mercury sites were detected. SHARP (Bricogne *et al*, 2003) was used for MAD phasing. Initial model building was performed with Buccaneer (Cowtan, 2006), and further building of the final structure was done with COOT (Emsley and Cowtan, 2004). Refinement was carried out using PHENIX (Terwilliger *et al*, 2008) and BUSTER (Blanc *et al*, 2004). The structures and diffraction data of Rrn3 have been deposited in the Protein Data Bank under accession code 3TJ1.

2.3.3 Small angle X-ray scattering

Rrn3 was purified as described in 2.2.5 and finally concentrated to 2 or 8 mg/ml in buffer C. The flow-through of the concentration step was used as buffer reference for the SAXS measurements. SAXS data were collected at beam line X33 at EMBL/DESY, Hamburg. BSA and lysozyme were measured as reference for molecular mass determination from I_0 , which was obtained from extrapolation of $s \rightarrow 0$ in Guinier-analysis with $s^*R_g < 1.3$ (Putnam

et al, 2007). Data analysis was done using the ATSAS package (Konarev *et al*, 2006). Theoretical scattering profiles from the known Rrn3 monomer or dimer structure were calculated and fitted to the measured profile with CRY SOL. *Ab initio* modeling from the experimental data was performed with DAMMIF and GASBOR without imposing symmetry or other restrictions. Models were aligned, filtered and averaged with SUPCOMB and DAMAVER (Volkov and Svergun, 2003). Envelope representations were calculated with SITUS (Wriggers and Chacon, 2001).

2.3.4 Static light scattering analysis

A size exclusion chromatography column (Superose 6 10/300 or Superdex 200 GE Healthcare) was connected to a triple detector TDA (Viscotek). The system was equilibrated and standardized with a BSA protein sample. Gel filtration runs were performed with Pol I-Rrn3 complex and, for direct comparison with Pol I alone on a Superose 6 column. Samples typically contained 100 µg Pol I. Rrn3 samples were tested for dimerization on a Superdex 200, using typically 200 µg Rrn3 in a sample. Wild-type Rrn3 (WT) was compared to mutants R452G, D405A and S444/448D and E398A. Data analysis was done with the OmniSEC software (Viscotek).

2.4 RNA Polymerase I-Rrn3 complex preparation and characterization

2.4.1 Purification of endogenous RNA Polymerase I

S. cerevisiae strain GPY2 (*ade2-101, trp1-Δ63, ura3-52, his3-Δ200, lys2-801, leu2::RPA43*), carrying a pAS22 plasmid coding for a HA- and hexahistidine tagged version of A43, was cultivated in a 200 l fermenter. Cells were harvested at an OD₆₀₀ of 5-9 by flow-through centrifugation, yielding a 2-2.5 kg cell pellet. 1 kg cells were resuspended in 500 ml freezing buffer, and flash-frozen in liquid nitrogen in batches of 225 ml, two of these batches were used for one Pol I purification. Fermentation and harvesting of cells was done by Stefan Benkert.

Cells were slowly thawed, then Ammonium Sulfate was added to a final concentration of 400 mM, together with Protease Inhibitors and DTT (5 mM). Phosphatase inhibitors were added as listed in table 15. For lysis, resuspended cells were filled into bead beaters (BioSpec Products) and 200 ml glass beads (0.5 mm, BioSpec Products) were added. To prevent foam formation the bead beater was filled up to the edge with dilution buffer and air bubbles were removed by stirring with a glass rod. Lysis was carried out in the cold room at 4 °C for 90 min in repetitive cycles of 30 s bead-beating followed by 90 s cooling. The bead beaters were additionally cooled with a mixture of ice and salt.

The lysate was then separated from the beads by filtration and centrifuged for 30 min at 75000 g (Sorvall SLA 1500), followed by ultra-centrifugation for 90 min at 30000 g (Beckmann SW28). The top fat layer was aspirated and the clear supernatant was separated from the pellet and dialysed over night at 4 °C against dialysis Buffer. The dialysed extract was centrifuged for 60 min at 18500 g (Beckmann Ti45). The supernatant was discarded and the resulting pellet was resuspended in Res/W1 buffer yielding a final volume of 50 ml. The sample was then split into two 25 ml batches and incubated on a turning wheel for 4 h at 4 °C with each 4 ml Ni-NTA resin (Qiagen), which was previously equilibrated in Res/W1 buffer. The resin was then loaded into two gravity-flow columns and washed with 5 CV Res/W1 buffer, followed by 5 CV W2 buffer, and finally eluted with 25 ml E1 buffer each. The eluate was pooled and subjected subsequently to an anion exchange chromatography (MonoQ 10/100, GE Healthcare). The column was equilibrated in 15 % MonoQ buffer B, and the sample was eluted in a multi-step gradient. Pol I fractions eluting at 1100 mM KoAc were pooled and diluted to a final concentration of

200 mM KoAc. Proteins were further purified via cation exchange chromatography (MonoS 5/50, GE Healthcare), using the MonoQ buffers A and B applying a gradient from 200 mM to 2 M KoAc. Pol I eluted at 500 mM KoAc, fractions were pooled, concentrated and further purified via Gel filtration chromatography (Superose 6 10/300, GE Healthcare).

2.4.2 Assembly of the RNA Polymerase I-Rrn3 complex

Pol I was purified as described in 2.4.1 with all buffers containing Phosphatase inhibitors (Table 15) and concentrated to 1 µg/µl. Rrn3 was purified as described in 2.2.5 and concentrated to 20 µg/µl. For assembly of the Pol I-Rrn3 complex, Pol I was incubated with a 9-fold molar excess of Rrn3 on ice over night, followed by size exclusion chromatography and concentration of the fractions containing the complex.

2.4.3 Native Mass-Spectrometry analysis

For native MS the sample buffer was exchanged to a solution containing 200 mM ammonium acetate using centrifugal filter units (Millipore) and sample concentration was adjusted to 2 µM. MS was carried out on a Q-ToF I instrument (Geiger *et al*, 2010; van den Heuvel *et al*, 2006). The cone voltage was 150 V and the needle voltage was 1.3 kV. The pressure in the source region was 10 mbar. Xenon was used as a collision gas with a pressure of 2×10^{-2} mbar (Lorenzen *et al*, 2007). Data were analyzed with MassLynx (Waters).

2.4.4 Protein crosslinking and Mass Spectrometry

Pol I was purified as described in 2.4.1 except that size exclusion chromatography (Superose 6 10/300, GE Healthcare) was performed in a buffer containing 20 mM HEPES at pH 7.8, 300 mM potassium acetate (KoAc), 1 mM MgCl₂, 10 % glycerol and 5 mM DTT. Pol I fractions were pooled and concentrated to 1 mg/ml and preparation of the Pol I-Rrn3 complex was done as described in 2.4.2. The complex was cross-linked using isotopically coded disuccinimidyl suberate (DSS-H12/D12, Creative Molecules Inc.). The purified Pol I-Rrn3 complex (100 µl containing 110 µg) was mixed with 25 mM DSS stock solution dissolved in dimethylformamide (DMF, Pierce Protein Research Products) to a final crosslinker concentration of 0.6 mM, 0.9 mM, 1.2 mM, 1.5 mM and 2 mM, respectively, to screen for the ideal crosslinking conditions. The result was analysed on an SDS-PAGE to

detect crosslinked proteins. The best crosslinker concentration, 1.2 mM, was sufficient to convert the free Rrn3 band and most of the individual Pol I subunits to a higher molecular weight band but still avoiding formation of oligomers of the complex. For the final reaction 110 µg Pol I was mixed with DSS to a concentration of 1.2 mM as described for the test-crosslinking reactions, and incubated for 30 min at 30 °C and 350 rpm. The reaction was stopped by addition of NH_4HCO_3 to a final concentration of 100 mM and incubation at 30 °C for 15 min. Cross-linked proteins were treated with two sample volumes of 8 M urea and reduced and alkylated using 5 mM Tris(2-carboxyethyl)phosphine (TCEP) and 10 mM iodoacetamide, respectively. The sample was digested with trypsin. MS analysis was performed as described (Leitner *et al*, 2010). The fragment ion spectra were finally assigned to crosslinked peptides using the software xQuest (Rinner *et al*, 2008).

2.4.5 Purification of recombinant A43/14

Plasmid pET21b (Novagen), carrying the genes for A14 and A43 with a Hexahistidine Tag encoded on the C-terminus of subunit A43, was used for expression of the Pol I subcomplex A14/43 in *E. coli*. Expression and lysis of cells was done as described in 2.2.4 and 2.2.5. After centrifugation the lysate was loaded onto a 2 ml Ni-NTA column pre-equilibrated in buffer L2. The column was washed with 5 CV buffer A2, then Proteins were eluted with buffer L2 containing 150 mM imidazol. Eluted fractions were diluted with buffer A2, to a final NaCl concentration of 100 mM. The sample was then subjected to an anion exchange chromatography (MonoQ 10/100 GE Healthcare). The column was pre-equilibrated with 10 % buffer B2, and proteins were eluted with a linear gradient from 100 mM to 1M NaCl. The heterodimer A14/43 eluted at 220 mM NaCl. After concentration, the sample was applied to a gel filtration chromatography (Superose 12 HR 10/300, GE Healthcare) equilibrated with buffer C2. Peak fractions were pooled and concentrated to 10 µg/µl.

2.4.6 Protein interaction analysis

Rrn3 carrying an N-terminal Strep-Tag was incubated with the A43/14 subcomplex, carrying a C-terminal Hexahistidine Tag on subunit A43, in different molar ratios. A43 was either the wild-type Protein or different S→D variants, mimicking a permanent

phosphorylation. A43 variants were produced by site directed mutagenesis as described in 2.2.3. Proteins were incubated on ice for 30 min and then loaded onto a Ni-NTA gravity-flow column, washed with L2 and then L2 containing 60 mM Imidazol, and eluted with L2 containing 150 mM Imidazol. Eluted fractions were concentrated or subjected to a TCA precipitation and analysed via SDS-PAGE.

2.4.7 Cryo-EM data collection and processing

A solution of purified Pol I-Rrn3 complex was diluted to ≤ 0.1 mg/ml using Pol I Superose 6 buffer and applied to glow-discharged pre-coated carbon holey grids (Quantifoil R3/3, 2nm carbon on top). For negative-stain, samples were treated with 2% uranyl acetate on the grid and subsequently dried at room temperature. Samples for Cryo EM were flash-frozen in liquid ethane using a semi-automated controlled environment system (Vitrobot, FEI Company) at 4° C, that keeps constant 95% humidity, and stored in liquid nitrogen until transfer to the microscope. Micrographs were recorded under low dose conditions of ~ 15 electrons/ \AA^2 on a FEI Tecnai Spirit microscope operating at 120 kV, equipped with a LaB6 filament and a Gatan side entry cryo-holder. Image collection was done at seven different under focus values in the range of 1.5-4 μm on a 2k x 2k FEI Eagle CCD camera with a pre-exposure of 100 ms at a magnification of 90.000x which resulted in a pixel size of 3.31 $\text{\AA}/\text{px}$ on the object scale. Initial particle selection and windowing was performed semi-automatically using the boxer program from the EMAN2 software package (Tang *et al*, 2007). Reference particles were picked manually on every micrograph to avoid discrepancies due to defocus and ice differences and the resulting automatically selected particles were verified visually. Windowed particles were aligned to 83 projections of the Pol II X-ray structure (1Y1W, Gaussian low-pass filtered to 35 \AA), which was modified by removing the OB and HRDC domains from subcomplex Rpb4/7 since they show high conformational flexibility and the HRDC domain is absent in the Pol I subcomplex A43/14. EMAN2 output files were reformatted to SPIDER stack files and further processing was carried out using the SPIDER software package (Frank *et al*, 1996). Backprojection of the particle images using the angles from reference-based alignment resulted in a first reconstruction, further used as reference for 20 rounds of angular refinement. Images were back-projected in real space using the refined angles. The final reconstruction from 11503 particles was Gaussian low-pass filtered to 25 \AA .

2.5 Yeast genetics and assays

2.5.1 Sporulation and Tetrad dissection

The diploid strain Y24975 (BY4743; Mat a/a; his3D1/his3D1; leu2D0/leu2D0; lys2D0/LYS2; MET15/met15D0; ura3D0/ura3D0; YKL125w::kanMX4/YKL125w) (Euroscarf) was first transformed with plasmid pRS316, containing the *URA3* gene and carrying a copy of wild-type *Rrn3* under a native promoter, as described in 2.2.2. For Sporulation cells were streaked out on pre-sporulation plates, and after incubation at 30 °C for 2 days, a few colonies grew on the plates and were restreaked onto sporulation plates, followed by another incubation for at least 3 days. For tetrad dissection, spores were treated with glucylase (Perkin Elmer) and then separated with a micromanipulator needle and deposited in distinct positions on a YPD plate. Clones were selected that carried a kanMX4 cassette replacing *Rrn3* in the haploid genome, by streaking out on plates containing G-418 (Geneticin). The resulting strains necessarily carry the pRS316 plasmid with a copy of *Rrn3*-WT under a native promoter. Nevertheless they were tested by streaking out clones that were positive for the kanMX4 cassette on –Ura selective plates, before further use for complementation assays.

2.5.2 long-term storage of yeast strains

The respective strain was cultivated in YPD media over night, then 750 µl were mixed in a 1.5 ml reaction tube with glycerol to a final concentration of 30 % glycerol and then stored at -80°C. For further use one glycerol-stock was thawed and streaked out on a YPD plate, or diluted in 25 ml YPD media and grown over night at 30 °C.

2.5.3 Mating type determination

To define the mating type of the resulting strains after tetrad dissection a colony-PCR reaction was performed using three primers (oligo 1: agtcacatcaagatcgtttatgg, oligo 2: cacggaatatgggacta-cttcg, oligo 3: actccacttcaagtaagagtttg) simultaneously. A specific pattern of resulting PCR products was analysed on an agarose gel and verified either mating type a or α .

2.5.4 Gene disruption and epitope tagging

To place genetically encoded purification Tags onto proteins of interest, *S. cerevisiae* cells were transformed as described in 2.2.2 with PCR products containing the desired tag, a selection marker and overlapping sequences, allowing for homologous recombination as described (Janke *et al*, 2004). Transformants that grew on selective plates were picked and streaked out again on YPD or selective plates, for further selection and to get more material, and were then tested for successful integration of the cassette by colony PCR and in some cases DNA sequencing of the resulting product. Successful expression of tagged proteins was proved via Western Blot with antibodies directed against the respective tag.

2.5.5 quantitative western blot analysis

To determine relative expression levels of TAP tagged Rrn3 variants or tagged Pol I subunits an alkaline lysis was performed and protein expression levels were analysed via western blot. A small amount of cells was collected from a plate with an inoculation loop, resuspended in 1 ml water, mixed with 150 µl alkaline lysis solution and incubated for 15 min on ice. Then 150 µl 55 % TCA were added, followed by incubation on ice for 10 min. Cells were centrifuged at 3500 g for 15 min at 4 °C, the supernatant was discarded and the pellet resuspended in 50 µl sample buffer, neutralized with ammonia and boiled for 5 min at 95 °C. 5 µl sample was then loaded onto an SDS gel. The gel was subsequently blotted onto a nitrocellulose membrane for 1 h at 100 V under constant cooling in the cold room (4 °C). The membrane was blocked for 1 h with PBS containing 2 % (w/v) milk powder. Then the membrane was cut into two pieces below the 70 kDa marker band. The upper part was incubated with an antibody against the TAP tag (PAP, Sigma), and the lower part with an antibody against tubulin (3H3087, Santa Cruz Biotechnology, rat). All antibodies were dissolved in 10 ml PBS containing 2 % (w/v) milk powder and incubated with the membrane for 1 h. After washing with PBS containing 0.1 % Tween, the lower part of the membrane was incubated with horseradish-peroxidase (HRP) coupled anti-rat antibody (Jackson ImmunoResearch) for one hour and washed again. Antibodies were detected by chemoluminescence (ECL Plus Western Blotting detection system, GE Healthcare). Detection was carried out with the LAS3000 detection system (Fuji) after incubation with the ECL Plus western blotting detection agent (GE Healthcare). Signals

were quantified in relation to the tubulin loading control using the ImageQuant TL 7.0 Image Analysis Software (GE Healthcare).

2.5.6 Complementation and phenotyping assays

A yeast shuffle strain was generated as described in 2.5.1. The strain was then transformed as described in 2.2.2 with plasmids carrying a *LEU2* marker and the wild-type gene or mutants of the gene of interest or, as a control, empty plasmid. Transformants, that grew on selective plates were streaked out on -LEU plates repeatedly to lose the pRS316 rescue plasmid carrying wt *Rrn3* as no selection for the URA3 marker is given anymore. Finally a small amount of cells was collected from the plate, washed in ddH₂O, set to an OD₆₀₀ of 1.0 in water, and spotted in serial dilution onto 5-FOA plates or YPD plates to test if the protein variants could complement the loss of the rescue plasmid.

Growth on 5-FOA plates is only possible after loss of the rescue plasmid carrying the wt *rrn3* gene and the URA3 marker, that encodes orotidine 5-phosphate decarboxylase (ODCase), which converts 5-FOA into the toxic compound 5-fluorouracil. Consequently, growth of the resulting strain is only observed if at least partial complementation by the protein variant expressed from the new rescue plasmid is possible. To further characterize the phenotype, a small amount of cells was collected from the 5-FOA plates, washed again, set to an OD₆₀₀ of 1.0 in water, and spotted in serial dilution onto YPD plates containing either 0.025 µg/ml Rapamycin, or 0.25 µg/ml Cycloheximide.

For growth curves, 50 ml YPD cultures were inoculated to an OD₆₀₀ of 0.1 with an overnight culture of a strain carrying either plasmid pRS315 expressing wt *Rrn3* or an *Rrn3* variant. Measurements of OD₆₀₀ were conducted every hour until an OD₆₀₀ of 0.8-1.0 was reached.

2.5.7 Chromatin Immunoprecipitation (ChIP) analysis

S. cerevisiae shuffle strain, derived from Y24975 (Euroscarf) and carrying wt or mutant *rrn3* on a rescue plasmid with or without TAP tag, as described in 2.5.6, was grown in 50 ml YPD medium and at 30 °C to mid-log phase (OD₆₀₀ ~ 0.8). Cells were treated with formaldehyde (1%, Sigma F1635) for 20 min at 20°C, and cross-linking was quenched with 5 ml of 3 M glycine for 10 min. Subsequent steps were performed at 4°C with pre-cooled

buffers containing protease inhibitors (1 mM Leupeptin, 2 mM Pepstatin A, 100 mM Phenylmethylsulfonyl fluoride, 280 mM Benzamidine). Cells were collected by centrifugation, washed twice with 1xTBS (20 mM Tris-HCl at pH 7.5, 150 mM NaCl), and twice with FA lysis buffer (50 mM HEPES-KOH pH 7.5, 150 mM NaCl, 1 mM EDTA, 1% Triton X-100, 0.1% sodium deoxycholate, 0.1% SDS). Pellets were flash-frozen in liquid nitrogen and stored at -80°C. Pellets were thawed, resuspended in 1 ml FA lysis buffer, and disrupted by bead beating (Retsch) in the presence of 1 ml silica-zirconia beads for 30 min at 4 °C. Chromatin was solubilized and fragmented via sonification with a Bioruptor™ UCD-200 (Diagenode Inc.). 700 µl sample was immuno-precipitated with 20 µl IgG Sepharose™ 6 Fast Flow beads (GE Healthcare) at 4 °C for 1 h. Immuno-precipitated chromatin was washed three times with FA lysis buffer, twice with FA lysis buffer containing 500 mM NaCl, twice with CHIP wash buffer and once with TE buffer. Immuno-precipitated chromatin was eluted for 10 min at 65 °C with CHIP elution buffer, digested with proteinase K (Sigma) at 37 °C for 2 h, and crosslinks were reversed at 65 °C overnight. DNA was purified with the QIAquick PCR Purification Kit (Qiagen). Input and immuno-precipitated samples were assayed by qPCR using primer pairs directed against different regions of the first repeat within the *RDN1* locus. PCR reactions contained 1 µl DNA template, 2 µl of 10 µM primer pairs and 12.5 µl iTaq SYBR Green Supermix (Bio-Rad). qPCR was performed on a Bio-Rad CFX96 Real-Time System (Bio-Rad Laboratories, Inc.) using a 3 min denaturing step at 95°C, followed by 49 cycles of 30 s at 95°C, 30 s at 61°C and 15 s at 72 °C. Threshold cycle (Ct) values were determined by application of the corresponding Bio-Rad CFX Manager software version 1.1 using the Ct determination mode “Regression”. Fold enrichment of any given region over a non-transcribed heterochromatic region on chromosome V was determined as described (Fan *et al*, 2008).

2.6 Bioinformatic tools

Protein and gene sequences were obtained from the NCBI (<http://www.ncbi.nlm.nih.gov/>), uniprot (<http://www.uniprot.org/>) or the *Saccharomyces cerevisiae* genome database (<http://www.yeastgenome.org/>). Bioinformatic analysis were performed mostly using the Bioinformatics Toolkit (Biegert et al, 2006). Multiple sequence alignments were done with ClustalW (Chenna et al, 2003) or MUSCLE (Edgar, 2004) and displayed with ESript (Gouet et al, 1999). Secondary structures were predicted with PredictProtein (Rost et al, 2004) or using the Bioinformatics Toolkit (Biegert et al, 2006). Molar absorption coefficients were calculated with ProtParam based on the Protein sequence (ExpASy, Bioinformatics resource portal) (Gasteiger et al, 2003). HHpred (Soding et al, 2005) was used for homology detection and structure prediction of Rrn7. Structures were modeled with Modeller (Eswar et al, 2008), from the online source (<http://toolkit.tuebingen.mpg.de/modeller>)

3 Results

3.1 Structural characterization of the RNA Polymerase I transcription initiation factor Rrn3

3.1.1 Rrn3 crystallization

Rrn3, the central transcription initiation factor of the RNA Polymerase I transcription system, is essential for efficient recruitment of the Polymerase to the pre-Initiation complex and subsequent transcription initiation. Rrn3 initially forms a stable complex with Pol I prior to recruitment of the whole complex to the promoter. To extend our knowledge on the function of this factor and to better understand the interplay of Rrn3 with Pol I we attempted to solve the structure of this central factor. Rrn3 was expressed recombinantly from *E. coli* and a purification protocol was established using auto-inductive TB medium for protein expression, that yielded 2-3 mg of pure protein from an 8 l culture (Methods 2.2.3-2.2.5). The purified protein was subjected to limited proteolysis and subsequent EDMAN sequencing (Methods 2.2.6), which revealed stable fragments lacking the N-terminal 33 or 47 aminoacids. Mass-spectrometry analysis of the protein combined with the results obtained from EDMAN sequencing and secondary structure predictions revealed a flexible loop between positions V242 and Q323 and a flexible C-terminal region, starting from position E545. Thus, a stable N-terminal and a stable C-terminal domain were predicted and constructs were designed and cloned accordingly. The wild-type protein (WT), a variant lacking the first 33 aminoacids (ΔN), a construct lacking the flexible N- and C-terminal regions ($\Delta N\Delta C$) and a construct lacking the middle loop (ΔL), as well as the N- and C-terminal domains (N-term, C-term), were expressed in *E. coli*. Only the wild-type protein and the ΔN variant were expressed properly and were soluble under the established conditions. After purification the protein was concentrated to 10 mg/ml in gelfiltration buffer and subjected to initial screens in sitting-drop 96 well crystallization plates either by an in-house crystallization-robot or at the crystallization facility at the MPI of Biochemistry, Martinsried. Several initial and promising hits were obtained from a range of different screens (examples are depicted in Figure 4). As the initial crystals of the wt protein seemed to be the same or better quality than for the ΔN construct, the full

length protein was used for scale-up of the crystal conditions to 2 μl hanging drops and optimization to get a crystal size and shape suitable for data collection. Scale-up led to large but very thin crystal plates (50 x 300 μm), which were mostly adhered and crooked and resulted in high mosaicity and bad quality diffraction data. This problem could be overcome by microseeding in the crystallization drops, further refinement of the crystallization condition and an improved protocol for cryo cooling protection (Figure 5). Diffraction data up to 2.8 \AA could be collected for a native crystal (Table 16).

As expression of the protein in minimal media was poor, selenomethionine derivatisation was not successful and therefore phasing of the crystals had to be accomplished through soaking with heavy metal derivatives. Several compounds were tested for derivatisation of crystals through co-crystallisation or soaking. Finally, a soak with 10 mM Thiomersal for a few minutes, fine-tuning of the incubation time in function of crystal size and shape, proved to be successful. Two mercury sites could be detected and the structure was determined by multiple wavelength anomalous diffraction (MAD) at 2.8 \AA resolution (Table 16).

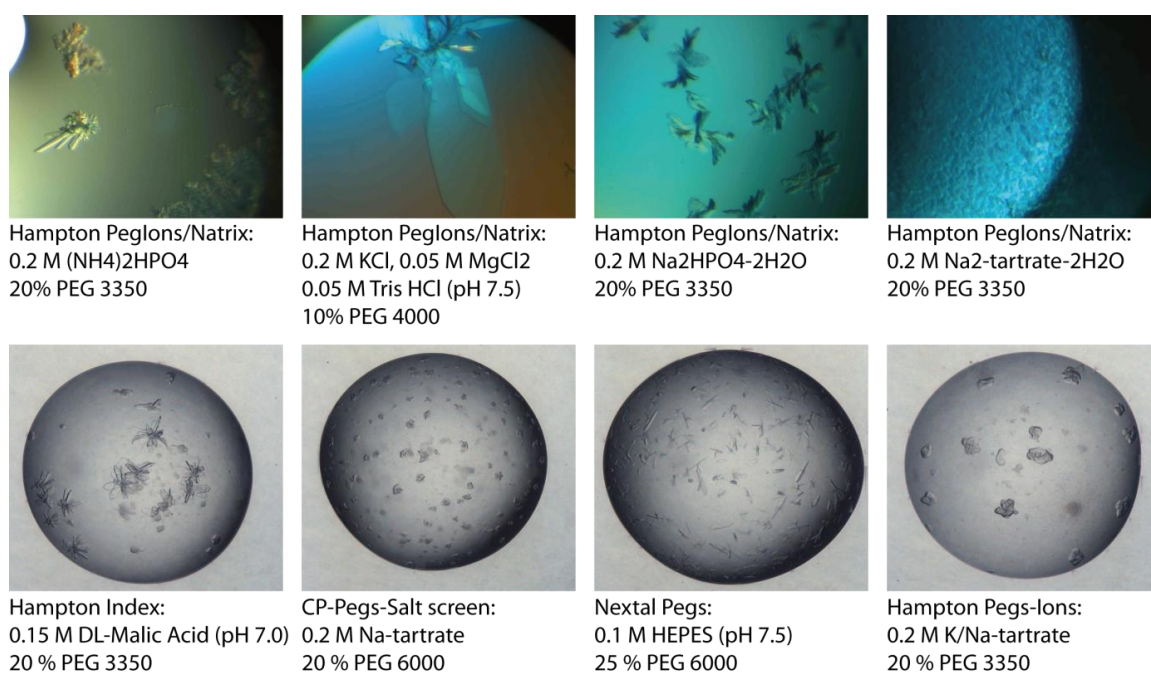


Figure 4. Initial Crystallization Hits

Upper lane: crystallization in-house robot, 96 well plate 200 μl sitting drops. Screen: Hampton Peg/Ions and Hampton Natrix. Lower lane: crystallization screen at MPI facility, 96 well plate, 100 μl sitting drops. Different screens. Con-ditions indicated below images.

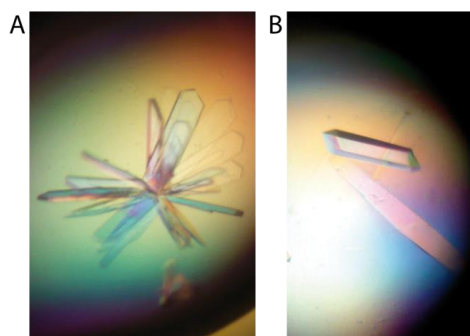


Figure 5. scale-up and optimization of crystals

(A) crystals after scale-up, crooked, thin plates. (B) crystals after optimization of conditions and seeding. Final crystallization condition: 0.25 M K/Na-Tartrate, 12 % PEG 3350.

Table 16 Data collection and refinement statistics for Rrn3

Crystal	Mercury derivative			Native
	Peak	Inflection	Remote	
<i>Data collection</i>				
Space group	P2 ₁ 2 ₁ 2 ₁			
Unit cell axes (Å)	94.8/107.8/160.7	94.9/108.2/160.6	94.8/107.9/161.1	96.8/101.8/162.0
Wavelength (Å)	1.0086	1.0094	1.0129	0.9814
Resolution (Å)	50–3.0 (3.08–3.0) ¹	50–3.0 (3.08–3.0)	50–3.0 (3.08–3.0)	50–2.85 (2.92–2.85)
Unique reflections	63,653 ² (4,723)	63,104 ² (4,650)	63,345 ² (4,706)	38,054 ³ (2,784)
Completeness (%)	100 (100)	99.7 (99.7)	99.7 (99.9)	99.9 (100)
Redundancy	3.48	3.46	3.48	9.1
Mosaicity (°)	0.29	0.25	0.26	0.28
R _{sym} (%)	8.8 (56.3)	7.9 (46.2)	8.1 (56.3)	11.0 (65.6)
<I/σI>	14.5 (3.45)	10.5 (2.6)	11.2 (2.32)	14.66 (3.83)
<i>Refinement</i>				
Number of residues				953
Number of nonhydrogen atoms				8,075
Number of solvent molecules				103
Average B-factor (Å ²)				62.5
RMSD bonds (Å)				0.01
RMSD angles (°)				1.13
R _{cryst} (%)				20.8
R _{free} (%)				24.2
Preferred ⁴ /Allowed/ Disallowed (%)				96.9/3.1/0.0

¹ Values in parentheses are for highest resolution shell throughout.

² Friedel pairs not merged

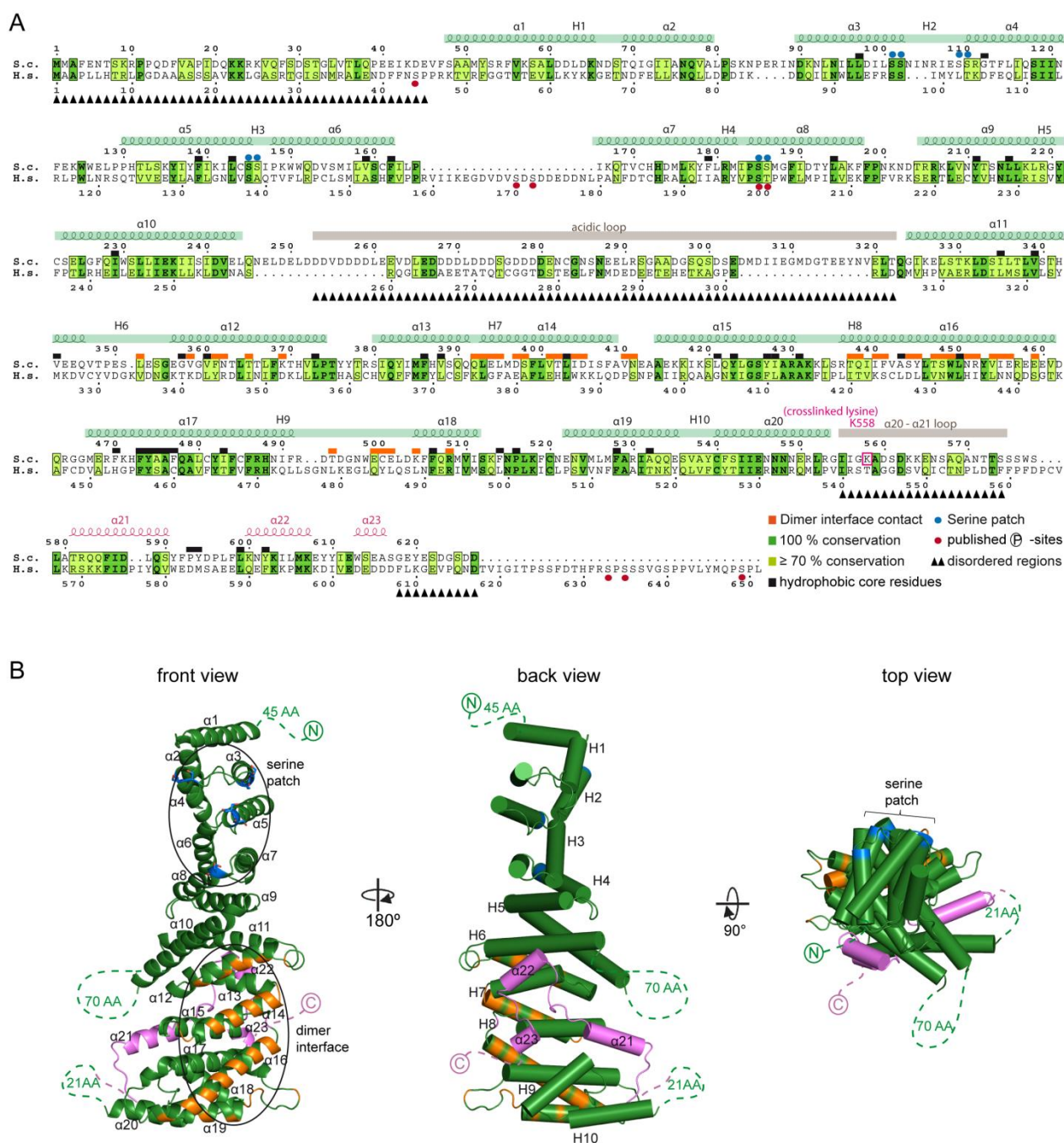
³ Friedel pairs merged

⁴ Ramachandran plot statistics from Molprobit

3.1.2 Rrn3 has a unique HEAT repeat structure

The structure of full-length Rrn3 encompasses ten HEAT repeats (H1-H10) formed by 20 pairs of anti-parallel α -helices arranged in a superhelical fold (Figure 6). Three additional C-terminal helices, separated by a flexible 25 aminoacid linker (called c-terminal loop in Figure 6) after H10, pack against repeats H6-H10. The term HEAT repeat is an acronym that originates from four cytoplasmic proteins (Huntingtin, elongation factor 3 (EF3), protein phosphatase 2A (PP2A), and the yeast PI3-kinase TOR1) all displaying a conserved rod-like superhelical fold, but fulfilling broadly distinct functions. HEAT repeat domains are known to be involved in protein-protein interactions, and are found in many transport proteins (Cingolani *et al*, 1999; Conti and Kuriyan, 2000), but were never described as part of a transcription factor. The superhelical Rrn3 fold is conserved throughout several different species, since hydrophobic core residues are conserved between yeast and human, as depicted in the alignment in Figure 6. The structure lacks only the 44 N-terminal residues, which had previously been identified as a flexible tail by limited proteolysis and EDMAN sequencing. Furthermore, an acidic loop (residues D253-T322), which was also previously predicted to be flexible, the c-terminal loop α 20- α 21 (residues I555-S574) connecting the HEAT repeat fold to the three C-terminal helices, and 11 C-terminal residues are not resolved in the structure (Figure 6).

Yeast *in vivo* complementation assays were performed as described in 2.5.6 to assay the impact of deletions of the parts that are not visible in the Rrn3 structure on viability of the resulting strain. The results proved that these mobile, less conserved regions are not required for essential Rrn3 functions *in vivo*, since deletion of the acidic loop (Δ L₂₅₁₋₃₂₀, Δ L₂₄₂₋₃₂₃) or the terminal tails (Δ C₆₁₇, Δ N (lacking the first 47 aminoacids)) did not result in a growth phenotype in yeast (Figure 7).



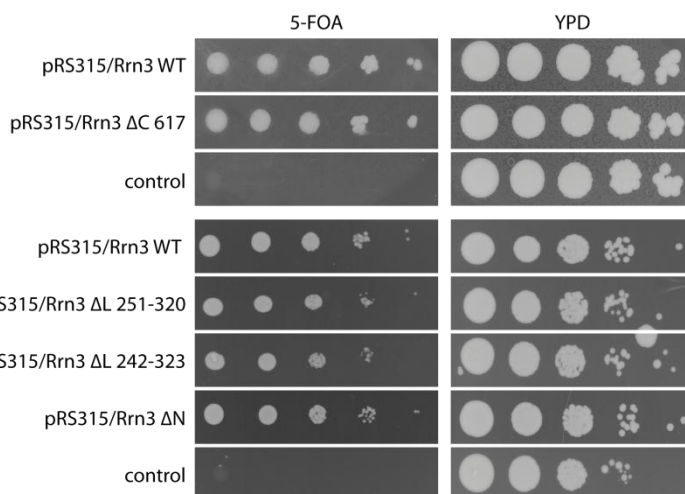


Figure 7. Yeast *in vivo* complementation assays.

Rrn3 variants were cloned into a pRS315 vector by homologous recombination, transformed into the *rrn3* shuffle strain and spotted in serial dilutions on 5-FOA-containing plates, to shuffle out the Rrn3-expressing URA3 plasmid and to test for viability of the resulting strain carrying the plasmid encoding mutant *rrn3*. Plates were incubated at 30 °C for 2-3 days. Results are compared to YPD Plates where normal growth is expected.

3.1.3 Rrn3 forms dimers in solution

During structure determination it became obvious that the asymmetric unit of the Rrn3-crystals contains a homodimer. Interface residues are depicted in orange in Figure 6. The 1353.7 Å interface of the homodimer comprises hydrophobic and few polar residues (Figure 8) and was predicted to be stable in solution (PISA, www.ebi.ac.uk). To test this, we analyzed Rrn3 samples with concentrations of 8 mg/ml and 2 mg/ml by small-angle X-ray scattering (SAXS) (Figure 8). SAXS analysis revealed a radius of gyration of 4.4 nm, which agrees with the calculated radius for the crystallographic dimer (4.2 nm), but not with the calculated monomer radius (3.1 nm). Taking into account that the crystal structure lacks the first 45 aminoacids, which would add to the radius of the crystallographic dimer, the fit with the SAXS calculation would be even more precise. The scattering curve also agrees with a theoretical curve calculated from the dimer structure (Figure 8A). Also, a SAXS-based *ab initio* model revealed a shape that resembles the dimer (Figure 8B). To test whether dimerization in solution occurs as in the crystals, we mutated different interface residues that caused strong ionic interactions or hydrogen bonds in the homodimer interface (Figure 6 and 8C). The Rrn3 variants D405A, R452G, and S444/S448D were purified and examined by size exclusion chromatography and static light scattering

(Viscotec, Figure 8D). This revealed molecular weights (MWs) between 74 and 85 kDa, compared to 140-150 kDa for the wild-type dimer (theoretical MW 145 kDa). Thus, Rrn3 forms a stable homodimer in solution that resembles the dimer in the crystals.

However, yeast *in vivo* complementation assays with the respective mutants did not show a phenotype, proving that a disruption of the dimer interface has no influence on vital Rrn3 function (Figure 8E).

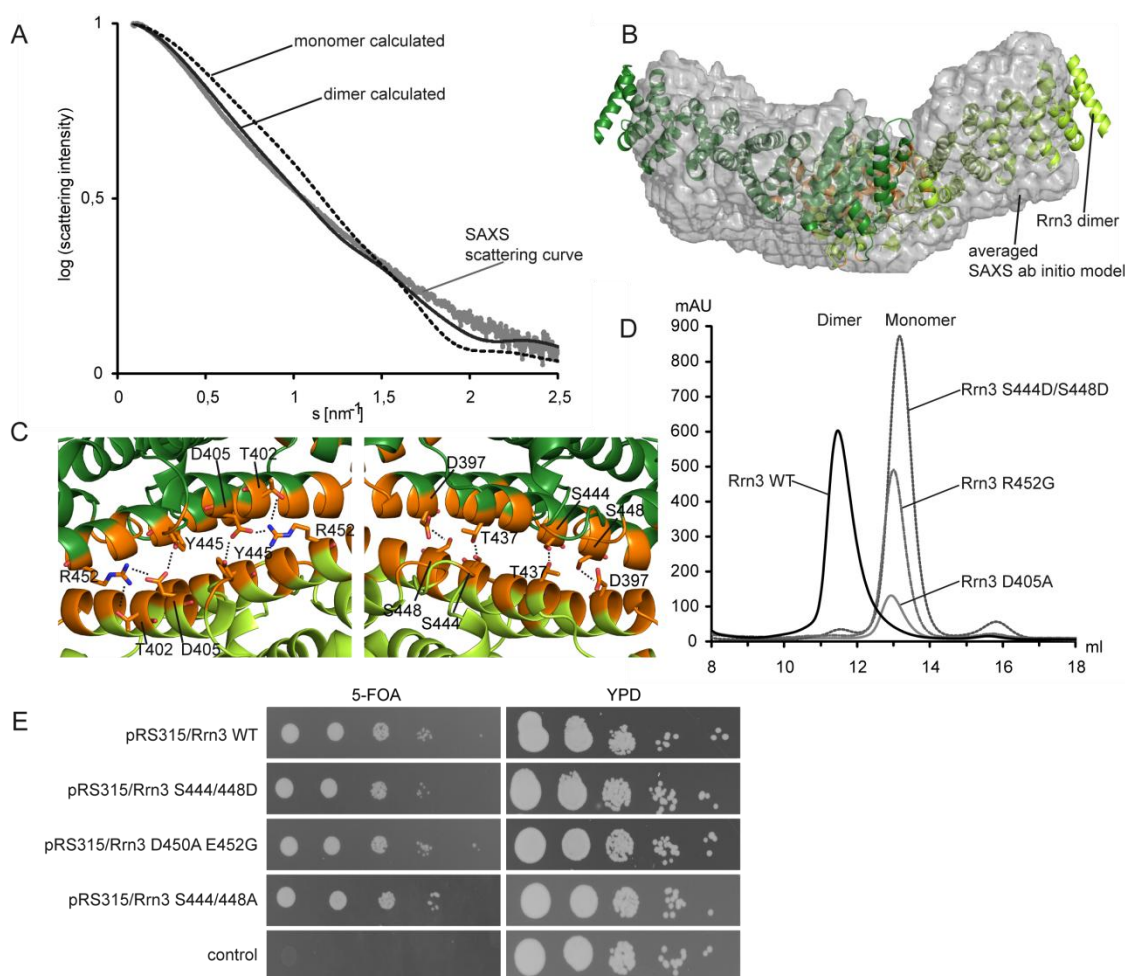


Figure 8. (A) SAXS scattering curve for Rrn3 (light grey) and calculated (Svergun *et al*, 1995) scattering curves for monomeric (black, dotted line) and dimeric Rrn3 (black line). (B) *Ab initio* SAXS envelope with docked Rrn3 homodimer structure. (C) Crystallographic dimer interface. The two views are related by a 180° rotation around a vertical axis. Interactions are indicated as dotted lines. Contact distances are within 2.8-3.5 Å. (D) Size exclusion chromatography shows that Rrn3 mutations S444/S448D, D405A, and R452G disrupt the dimer interface and lead to monomerization. The elution profile of wild-type Rrn3 is in black, profiles of mutants S444/448D, D405A and R452G are in grey. (E) Monomeric *rrn3* mutants were tested for complementation of a Δ Rrn3 strain and restored growth comparable to WT.

3.1.4 The Rrn3 structure exhibits characteristic surface properties

The Rrn3 surface reveals strongly conserved parts that may be protein binding surfaces as they exhibit a rather hydrophobic character (indicated with red circles in Figure 9A). Rrn3 is involved in many protein-protein interactions as it has been shown to interact with Pol I and core factor subunits Rrn6 and Rrn7, in order to recruit the polymerase to the rDNA promoter (Miller *et al*, 2001).

Surface charges are equally distributed all over the protein except one positively charged stretch, which could be involved in nucleic acids binding, although no proof for this could be found through preliminary EMSA experiments, suggesting that either a specific sequence is required for binding or that this stretch has a different function.

The dimerization interface observed in the crystal structure displays an overall rather hydrophobic character, with some slightly polar residues.

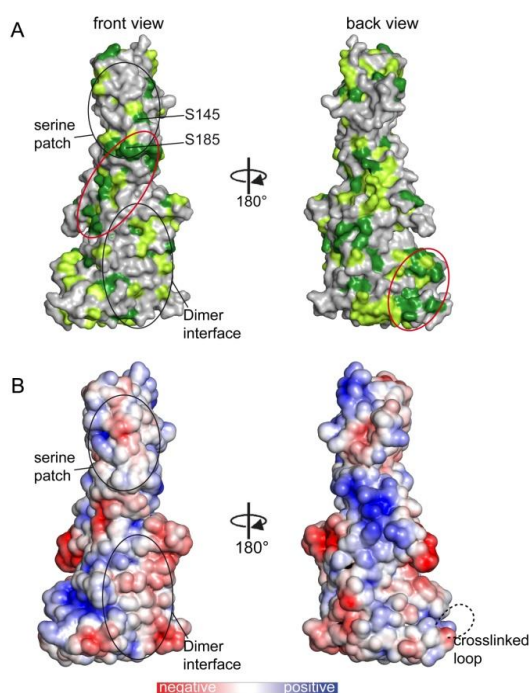


Figure 9. (A) Surface conservation. Identical and conserved residues are highlighted in dark and light green, respectively. Positions of residues S145 and S185 and the dimer interface are indicated.

(B) Surface charge distribution. Red, blue, and white areas indicate negative, positive, and neutral charge, respectively.

3.2 Structural and functional characterization of the RNA Polymerase I-Rrn3 complex

3.2.1 Rrn3 binds Pol I as a monomer

We next investigated whether Rrn3 binds to Pol I as a homodimer or whether the dimer is disrupted upon polymerase binding. Endogenous Pol I was purified with the use of a hexahistidine tag (2.4.1), and incubated with a nine-fold molar excess of recombinant Rrn3 carrying a Strep-Tag (2.2.5). The Pol I-Rrn3 complex was separated from excess Rrn3 by Ni-NTA affinity chromatography and subjected to native mass spectrometry (MS) (Heck, 2008). This revealed a molecular weight (MW) of 667 kDa (Figure 10), in agreement with a Pol I-Rrn3 monomer complex (663 kDa theoretical MW), but not with a Pol I-Rrn3 dimer complex (736 kDa).

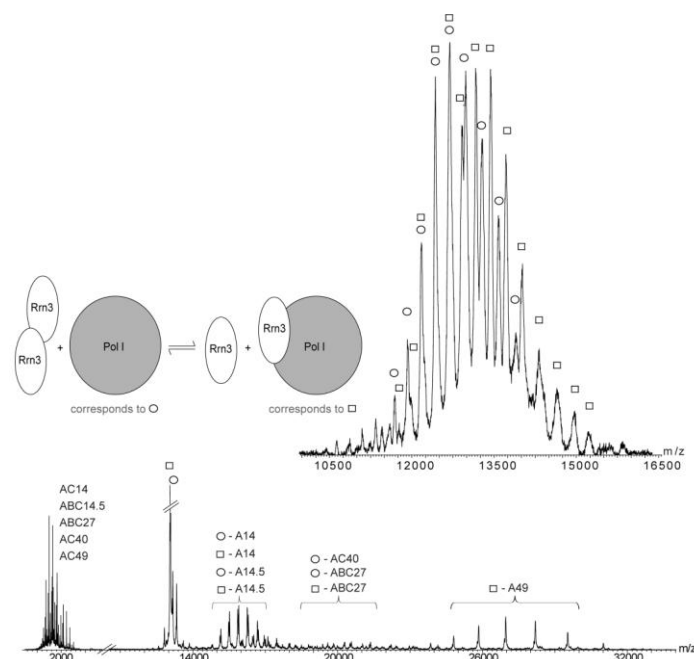


Figure 10. Native mass spectrometry reveals that Rrn3 binds Pol I as a monomer. Upper panel: Two different charge distributions were detected with masses of 593 and 667 kDa, which refer to Pol I alone (or a Pol I Δ A49/34.5-Rrn3 complex) and a Pol I-Rrn3 monomer complex, respectively.

Lower panel: Tandem Mass Spectrometry leads to elimination of subunit A49 from the 667 kDa complex, and to elimination of subunits A14, A14.5, and ABC27 from the 593 and the 667 kDa complexes. The 593 kDa complex additionally eliminates AC40. The remaining Pol I subcomplexes are observed at corresponding high mass/charge values.

As the A49/34.5 heterodimer is known to dissociate from Pol I (Huet *et al*, 1976) the complex with the molecular weight of 667 kDa could also be explained by a Pol I Δ (Pol I lacking A49/34.5) in complex with an Rrn3 dimer, as the molecular masses of the A49/34.5

heterodimer (73.5 kDa theoretical MW) and Rrn3 (73.5 kDa theoretical MW including Strep-Tag) are almost identical. Dissociation of the 667 kDa complex in the mass spectrometer liberated subunit A49, showing that the A49/34.5 heterodimer is present in this complex. This leads to the conclusion that monomeric Rrn3 is bound to Pol I.

Native MS revealed a second complex with a MW of 593 kDa, which can be explained by free Pol I (589 kDa theoretical MW) or by a Pol I-Rrn3 complex that lost the A49/34.5 heterodimer (589 kDa theoretical MW).

Further, to test the capability of Rrn3 to bind Polymerase as a monomer, the artificial monomer variants Rrn3 D405A and R452G were purified and incubated with Pol I to establish a complex as described in 2.4.2. Subsequent Gelfiltration separated the complex from excess Rrn3, and analysis of the two separated peaks revealed a stable complex of the Rrn3 variants with Pol I (Figure 11). These data demonstrate that Rrn3 binds Pol I as a monomer, consistent with the results of the yeast *in vivo* complementation assays that proved the viability of a yeast strain expressing an Rrn3 mutant that is incapable of dimer formation (Figure 8E).

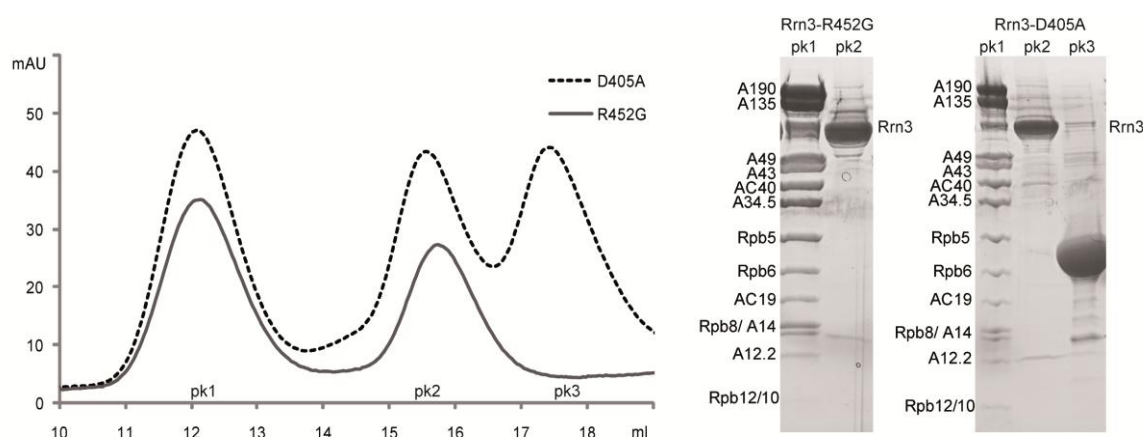


Figure 11. Rrn3 monomer still bind to Pol I. left: Gel Filtration profile. right, SDS PAGE analysis of Peak 1 (pk1), Peak 2 (pk2) and Peak 3 (pk3) after TCA Precipitation. Pk 3 contains an unknown impurity from the Rrn3 sample.

Moreover, we performed dissociation experiments of the large complex containing Rrn3 and compared these to dissociation experiments that were performed with Pol I alone. It came to our attention that the Pol I-Rrn3 complex shows a different dissociation pattern than free Pol I. While tandem mass spectrometry eliminates subunits A14 and A14.5 from both complexes, free Pol I also dissociates subunit AC40 at relatively low energy. These

results are consistent with previous dissociation experiments of Pol I (Geiger *et al*, 2010), and lead to a preliminary conclusion that Rrn3 binding to Pol I has a stabilizing effect on the Pol I subunit AC40, although, without further proof, this assumption remains speculative.

3.2.2 Rrn3 does not bind subunits A43/14 alone

It has been shown previously that Rrn3 interacts directly with Pol I subunits A43/14 and thereby forms a bridge between Pol I and the core factor, thus facilitating the recruitment of Pol I to the promoter (Peyroche *et al*, 2000). This interaction seems to be favored when Rrn3 is in an unphosphorylated state and Pol I is phosphorylated (Fath *et al*, 2001). This would lead to the conclusion that Rrn3 produced in *E. coli*, without posttranslational modifications should be able to bind A43 from an endogenous source, and probably also when A43 and Rrn3 are co-expressed in *E. coli*, as was shown previously (Peyroche *et al*, 2000). In our experiments no stable or stoichiometric binding could be observed between Rrn3 and A43 alone, or the A43/14 heterodimer, from recombinant expression (Figure 12). However, as five of the mapped Pol I phosphosites are located in subunit A43 (Gerber *et al*, 2008), we assayed the impact of A43 phosphomimetic point mutations on the Rrn3-A43 complex formation and stability. Strep-tagged Rrn3 was expressed and purified from *E. coli*, as well as A43 WT and variants S262/263D, 4P (S220D, S262/263D, S285D) and 5P (S208D, S220D, S262/263D, S285D).

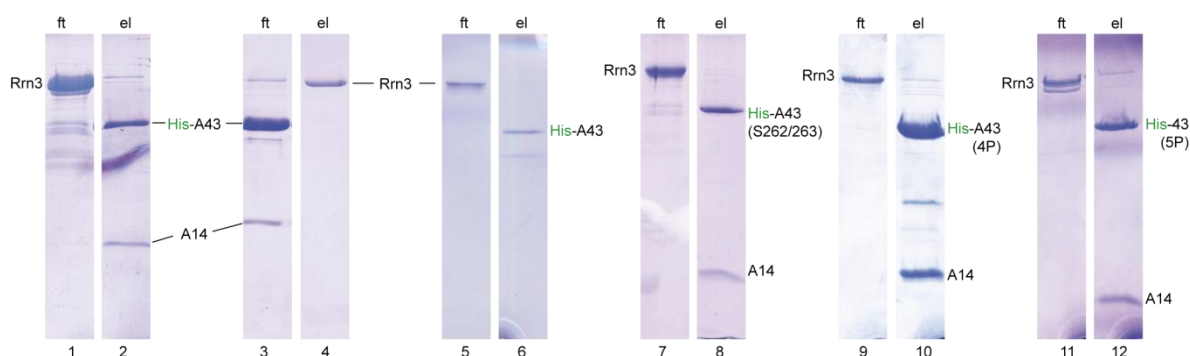


Figure 12. Pull-down binding assays. Rrn3 carrying a Strep-Tag was incubated with an excess of A43 or A43/14 heterodimer or with the respective variants as indicated, with A43 and variants carrying an C-terminal His₆-Tag. Proteins were bound to Ni-NTA beads, washed and eluted from a gravity flow column with 200 mM Imidazol. Except lane 3 and 4, where proteins were bound to Strep-beads, washed, and eluted with DTB. Flowthrough (ft) fractions containing unbound protein and Elution (el) fractions were analysed via an SDS page and stained with coomassie.

The A43 phosphomimetic variants were expressed and purified as a stable heterodimer with A14, but did not show an improved binding ability to Rrn3. These results suggest, that stable complex formation between Rrn3 and Pol I does either require a different pattern of posttranslational modifications, or an additional Pol I subunit as interaction partner.

As an interaction between the Pol I specific subunits A49/34.5 and Rrn3 has been postulated, with the heterodimer triggering the release of Rrn3 upon entering the elongation phase (Albert *et al*, 2011; Beckouet *et al*, 2008), we also examined a possible direct interaction of Rrn3 with A49. Co-purification experiments were performed as described for the A43/14 heterodimer, but no interaction could be found. This result was expected, and supports the idea of a repulsive interaction between A49/34.5 and Rrn3, triggering the release of Rrn3 from elongating Polymerase.

3.2.3 The Rrn3 structure exhibits a serine patch that is important for cell growth

Eight serine residues, arranged in four pairs, cluster on the surface of the Rrn3 structure, which are later referred to as the 'serine patch' (Figure 13A). Six of these residues are conserved between yeast and human (Figure 6A). Residues S185 and S186 correspond to human residues S199 and T200, which are phosphorylated *in vivo*, preventing Pol I association and thus shutting down Pol I transcription (Mayer *et al*, 2005; Mayer *et al*, 2004). Since the interaction of Pol I with TIF-IA depends on the phosphorylation status of TIF-IA (Bierhoff *et al*, 2008; Fath *et al*, 2001; Hoppe *et al*, 2009; Mayer *et al*, 2005; Mayer *et al*, 2004; Philimonenko *et al*, 2004; Schlosser *et al*, 2002; Zhao *et al*, 2003), we investigated whether the serine patch of Rrn3 is required for Pol I binding and whether phosphorylations in this patch have an effect on cell growth. We mutated the serines individually to alanine or aspartate, thereby disabling phosphorylation or mimicking a permanently phosphorylated state, respectively. Complementation assays in a $\Delta rrn3$ strain revealed that the Rrn3 mutation S145D causes severe slow growth on YPD plates under various conditions and in liquid culture (Figure 13 and 14A/B), whereas mutations of the other residues had no effect (Figure 13B). The phenotype was enhanced in the presence of rapamycin, an inhibitor of the TOR kinase pathway that regulates Pol I, and in the presence of cycloheximide, an inhibitor of protein biosynthesis (Figure 14A). This shows

the importance of the serine patch, and in particular S145, for cell growth, and suggests a conserved mechanism of Rrn3 phospho-regulation.

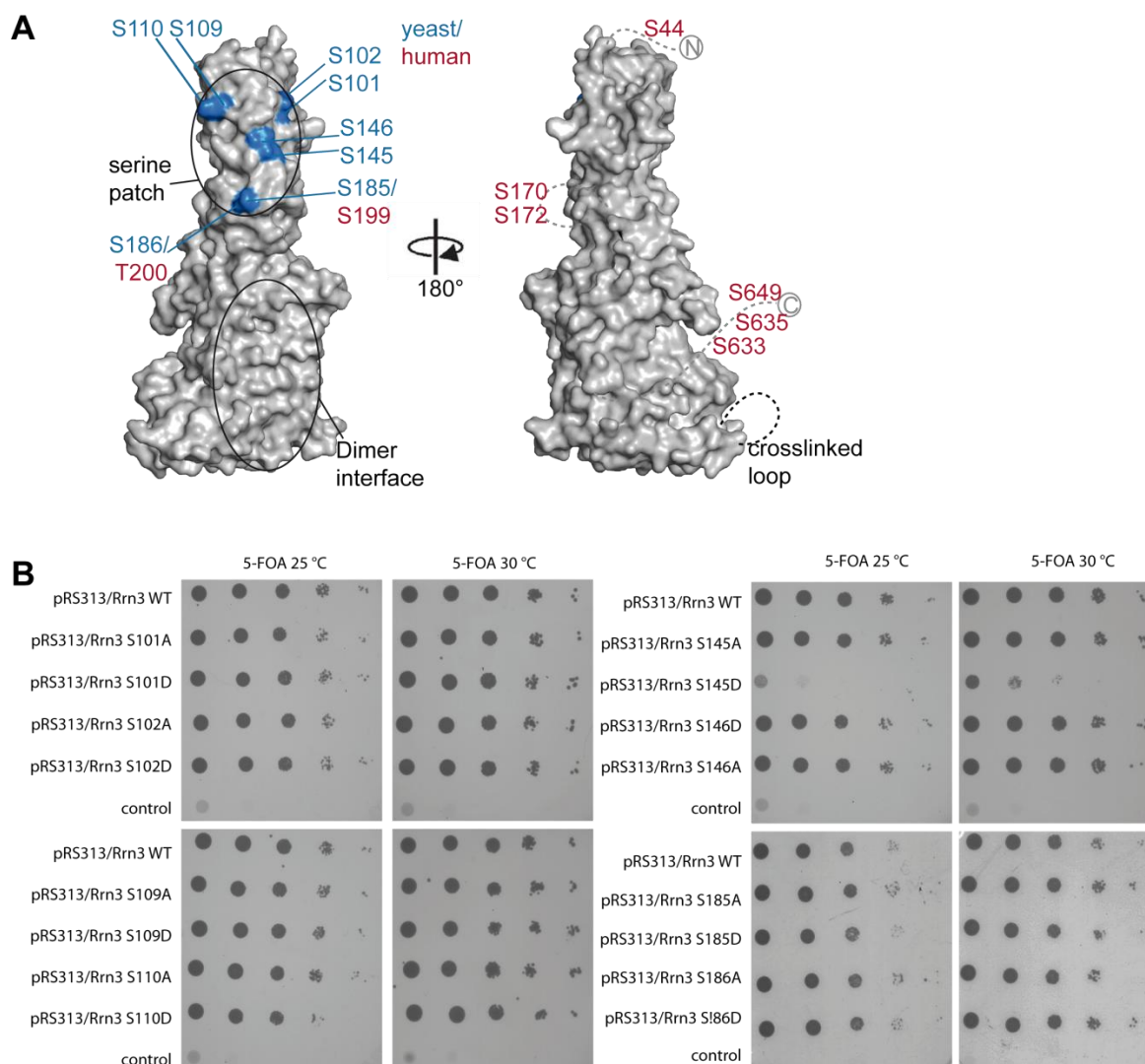


Figure 13. Surface serine patch. (A) serines in the patch are labeled in blue. The crosslinked loop and the dimer interface are indicated. The orientation on the right is the same as in the docking model, Figure xx. (B) *Rrn3* serine patch variants were cloned into a pRS315 vector by homologous recombination, transformed into the *rrn3* shuffle strain and spotted in serial dilutions onto 5-FOA-containing plates, to shuffle out the Rrn3-expressing URA3 plasmid. Plates were incubated at 30°C and 25°C to test the additional effect of temperature stress.

3.2.4 The serine patch is involved in Pol I binding *in vitro*

We expressed and purified the Rrn3 mutant S145D, which showed a growth defect in yeast (Figure 13B and 14A/B), and the mutant S185D, that corresponds to human S199D, which does not bind Pol I (Mayer *et al*, 2004). The purified Rrn3 mutants were tested for

their ability to form stable complexes with Pol I after size exclusion chromatography (Fig. 14C). Whereas wild-type Rrn3 bound Pol I in these assays, Rrn3 mutant S145D did not bind Pol I and the mutant S185D bound only weakly (Fig. 14C). Thus the serine patch of Rrn3 is involved in Pol I binding *in vitro* and phospho-mimetic mutations in this patch can impair Pol I binding.

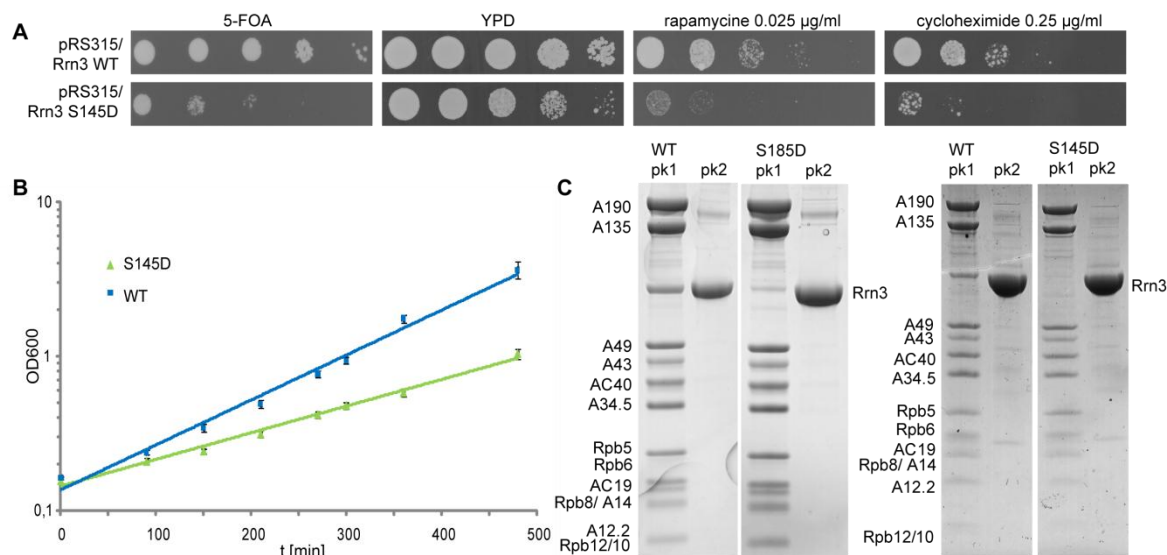


Figure 14. (A) Yeast complementation assays reveal a critical function of Rrn3 residue S145 for cell growth. Growth of *rrn3* mutants was further tested on plates containing 0.025 µg/ml rapamycin or 0.25 µg/ml cycloheximide.

(B) A yeast strain expressing the Rrn3 mutant S145D exhibits a slow-growth phenotype in liquid culture (green). Growth of the same strain under the same conditions but expressing wild-type Rrn3 from the same plasmid is shown in blue (WT).

(C) The serine patch is required for Pol I binding *in vitro*. Pol I was incubated with excess wild-type or mutant Rrn3 and subjected to size exclusion chromatography, which revealed two separated peaks (pk1, pk2) that were analyzed with Coomassie-stained SDS PAGE. In contrast to wild-type Rrn3 (WT), which forms a stable complex with Pol I in these assays, the Rrn3 mutants S185D and S145D bind Pol I weakly or not at all (pk1). The second peak corresponded to free excess Rrn3 proteins (pk2).

3.2.5 The Rrn3 serine patch is required for cell growth and promoter recruitment *in vivo*

To investigate Pol I recruitment to the rDNA gene locus *in vivo*, we performed chromatin immunoprecipitation (ChIP) experiments. We prepared yeast strains with a genomically expressed C-terminal tandem affinity purification (TAP) tag on Pol I subunit A190 and expressing Rrn3 wild-type or mutant S145D from a plasmid, and determined Pol I occupancy at rDNA genes by ChIP (Figure 15). Pol I occupancy at all tested regions of the rDNA locus was strongly decreased in the strain expressing Rrn3 mutant S145D (Figure 15B), although protein levels were unchanged (Figure 15D). This shows that

normal Pol I recruitment to rDNA *in vivo* requires an unphosphorylated S145 residue on Rrn3. We also tested whether the S145D mutation impairs Rrn3 recruitment to rDNA. We complemented the $\Delta rrn3$ strain with plasmids expressing TAP-tagged Rrn3 wild-type or mutant S145D. CHIP revealed that wild-type Rrn3 localizes to the rDNA promoter and the beginning of the transcribed region as shown before (Beckouet *et al*, 2008; Bier *et al*, 2004; Claypool *et al*, 2004; Philippi *et al*, 2010), whereas occupancy with mutant S145D was decreased 5- to 10-fold (Figure 15C). These results indicate that S145 phosphorylation impairs cooperative recruitment of Rrn3 and Pol I to the rDNA gene *in vivo*.

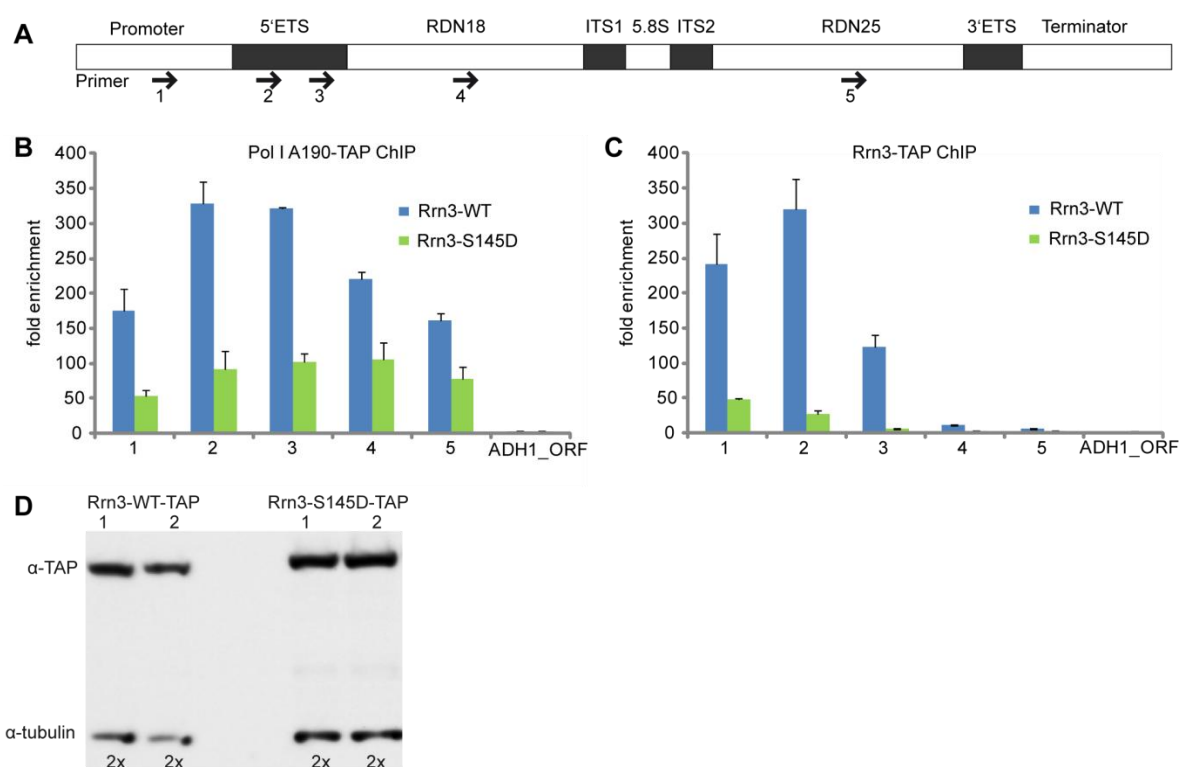


Figure 15. Rrn3 serine patch recruits Pol I to genes

(A) For CHIP analysis, primer pairs complementary to five regions of the rDNA locus were used (indicated by arrows). ETS, external transcribed spacer; ITS, internal transcribed spacer; RDN18, region encoding the 18S rRNA; RDN25, region encoding the 25S rRNA.

(B) CHIP analysis shows that the Rrn3 S145D mutation reduces Pol I occupancy at the rDNA locus. CHIP was carried out with haploid strain Y24975 ($\Delta rrn3$) expressing a plasmid encoding either Rrn3 wild-type (WT) or Rrn3 mutant S145D and carrying a C-terminal TAP tag on Pol I subunit A190. CHIP intensities over background are shown in a bar diagram. Errors were estimated from two biological replicate measurements. As a negative control, we used primers complementary to the open reading frame of the Pol II-transcribed gene *adh1* (ADH1_ORF).

(C) The Rrn3 S145D mutation reduces Rrn3 occupancy at the rDNA locus. CHIP was performed with a strain expressing the C-terminally TAP-tagged Rrn3 mutant S145D from plasmid pRS315.

(D) Rrn3 S145D mutation does not change cellular Rrn3 protein levels according to western blot analysis with TAP-tagged Rrn3 variants. The ratio of western blot signals for Rrn3 and tubulin was two-fold throughout, as calculated with ImageQuant TL 7.0 Image Analysis Software (GE Healthcare).

3.2.6 Rrn3 binds Pol I near subcomplex AC40/19

To elucidate the molecular basis for Pol I-Rrn3 binding, we subjected the Pol I-Rrn3 complex to chemical crosslinking and identified crosslinked lysines by MS (Leitner *et al*, 2010). This experiment reveals proximal lysine residues on adjacent proteins in stable multiprotein complexes and allows positioning of crystal structures to obtain topological models of large polymerase-factor complexes (Chen *et al*, 2010). Pol I-Rrn3 complex was purified as described in 2.4.2 and crosslinked with a final concentration of 1.2 mM disuccinimidyl suberate. The crosslinked complex was subjected to a trypsin digest and crosslinked lysines were identified by MS. The MS data were of high quality, as crosslinks between Pol I subunits were explained with the Pol I model (Kuhn *et al*, 2007) and the Pol II structure (Armache *et al*, 2005). Details of the crosslinks within Pol I are described in a separate study (Jennebach *et al*, 2011). The analysis revealed two high-confidence crosslinks between Rrn3 and Pol I, connecting Rrn3 residue K558 to Pol I residues K582 and K329 in subunits A190 and AC40, respectively (Figure 16B). The crosslinked Pol I residues were positioned on the 'back' of the homologous Pol II structure in the Rpb3/11 heterodimer, which corresponds to the AC40/19 heterodimer, and in Rpb1, which is the corresponding Pol II subunit to A190.

The interaction with subunit AC40 agrees with the effect that was seen in the native Masspec experiments (3.2.1), namely that subunit AC40 is somehow more stably bound in a Pol I-Rrn3 complex, than in free Pol I.

3.3 Model of a minimal RNA Polymerase I initiation Complex

3.3.1 Model of the Pol I-Rrn3 complex

To obtain a model for the Pol I-Rrn3 complex, we positioned the Rrn3 structure on the polymerase such that crosslinks were explained, and did not exceed a distance of 27.4 Å between C α atoms of crosslinked lysines. The crosslinked Rrn3 residue K558 is part of the short mobile loop α 20- α 21 that follows the ordered residue G554, which was allowed to be in a distance up to 30.9 Å from crosslinked Pol I lysines (the theoretical maximum C α distance of 27.4 Å plus 3.5 Å for mobile residues 555-558). Only one Rrn3 orientation positioned the serine patch towards Pol I, to explain the interaction data without producing protein clashes (Figure 16B).

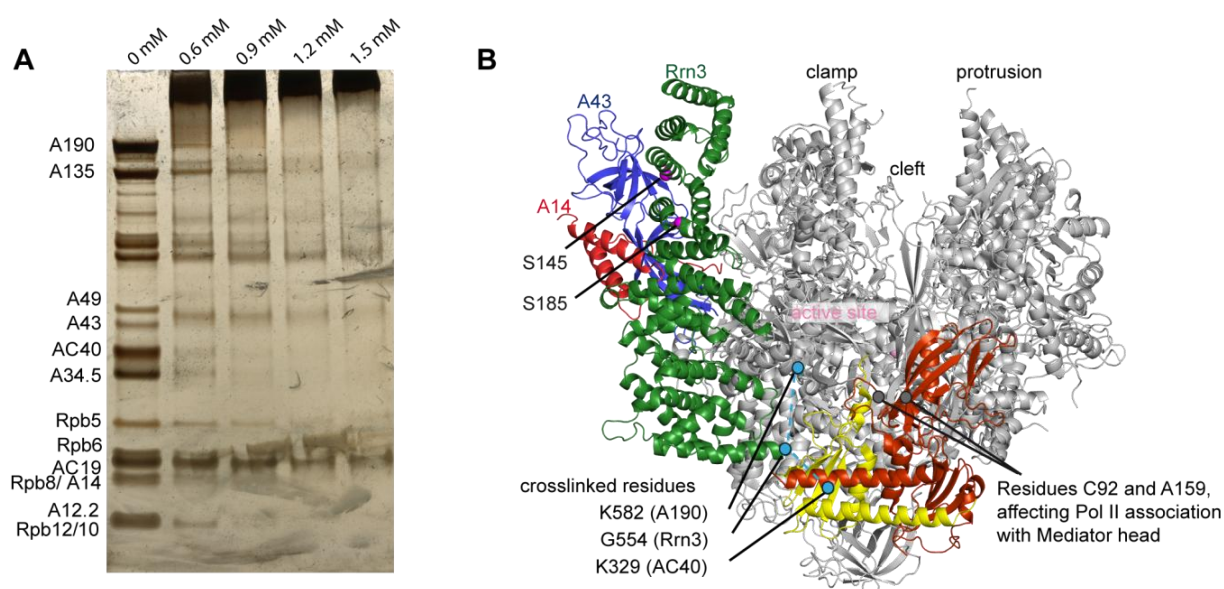


Figure 16. (A) crosslinking of the Pol I- Rrn3 complex. 10 μ g of crosslinked sample were analysed via SDS page and visualized with silver stain. concentrations of crosslinker are indicated above each lane. (B) Model of the Pol I-Rrn3 complex based on lysine-lysine crosslinking and protein interaction data. Back view of a 12-subunit Pol I model that is based on the Pol II core structure (silver) (Armache *et al*, 2005) and the structure of subcomplex A14/43 (red/blue) (Kuhn *et al*, 2007; Tsai and Sigler, 2000). The Pol II core heterodimer Rpb3/11 that is homologous to the Pol I heterodimer AC40/19 is highlighted in red/yellow. The positioned Rrn3 structure (green) contains a lysine residue (K558) that is part of a short mobile loop following the ordered residue G554 (cyan dot) and crosslinks to two Pol I residues (cyan dots connected with dashed lines). Crosslinked positions in the Pol I core are revealed in the homologous Pol II structure; K582 in A190 corresponds to M437 in Rpb1, and K329 in AC40 corresponds to L259 in Rpb3 (cyan dots). Positions C92 and A159 in Rpb3, influencing the interaction of Pol II with the Mediator head module (Soutourina *et al*, 2011) are indicated as grey spheres.

In the resulting model of the Pol I-Rrn3 complex, Rrn3 extends from the heterodimer AC40/19 alongside the RNA exit tunnel and dock domain up to A14/43, the counterpart of the Pol II subcomplex Rpb4/7. The model explains Rrn3 binding to the OB domain of subunit A43 (Peyroche *et al*, 2000), an early electron microscopic projection and colocalization of A43 and Rrn3 (Peyroche *et al*, 2000), the observation that Rrn3 can be fused to A43 *in vivo* maintaining the same growth rates as the wild-type strain (Laferte *et al*, 2006), and an apparently stabilizing effect of A14 on the Rrn3-Pol I interaction (Imazawa *et al*, 2005).

It further came to our attention that the crosslinks that locate the C-terminal part of Rrn3 on the Pol I surface structure, lie in proximity to two positions that affect binding of the mediator head module Med17 (Soutourina *et al*, 2011).

3.3.2 Rrn7 is the TFIIB-related factor in the RNA Polymerase I initiation apparatus

As crosslinking and mutational analysis helped to identify the location of Rrn3 to be close to the dock domain, we were encouraged to search for a homolog of the Pol II factor TFIIB in the Pol I initiation machinery, since TFIIB binds the Pol II dock domain (Chen and Hahn, 2003). A TFIIB homolog in the Pol I system could thus represent an Rrn3 interaction partner. We examined the three subunits of the Pol I core factor, Rrn6, Rrn7, and Rrn11, with the HHPred structure prediction server (Soding *et al*, 2005). This revealed a clear homology of the N-terminal region of Rrn7 (residues 1-316) with TFIIB (E-value 0.028, probability score 93.6). The structured domains of TFIIB, the N-terminal zinc ribbon and the two C-terminal cyclin folds (Kosa *et al*, 1997; Kostrewa *et al*, 2009; Tsai and Sigler, 2000) are present in Rrn7 (Figure 17) with a sufficient sequence homology to create a convincing model using MODELLER (Eswar *et al*, 2008) based on known TFIIB structures from different species (Kosa *et al*, 1997; Kostrewa *et al*, 2009; Liu *et al*, 2010; Tsai and Sigler, 2000). The predicted Rrn7 Zn-ribbon domain contains all four zinc-binding cysteine residues, with the C-terminal cysteine replaced by a functionally equivalent histidine, which are arranged in a tetrahedral conformation in the model, appropriate for coordination of a Zn ion. The C-terminal region of Rrn7 does not show homologies to known factors, similar to the TFIIB-related factor Brf1 in the Pol III system, which also contains a specific C-terminal region (Juo *et al*, 2003) (Figure 17B and 20).

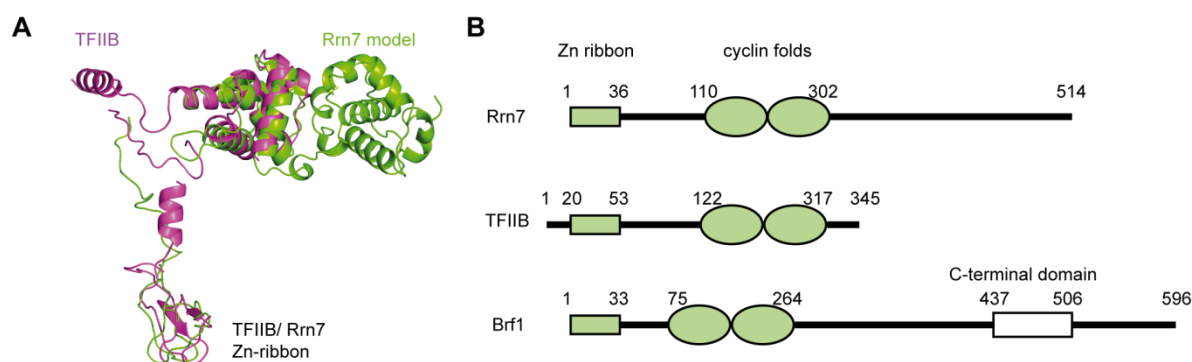


Figure 17. (A) homology model of Rrn7 in comparison with TFIIIB (Kostrewa *et al*, 2009). (B) Schematic representation of distinct structural domains in TFIIIB and the homologous factors Rrn7 and Brf1 in the Pol I and Pol III systems, respectively. All three proteins exhibit an N-terminal zinc ribbon followed by two conserved cyclin folds. In addition, Rrn7 and Brf1 contain a specific C-terminal region

3.3.3 Architecture of the Pol I initiation complex

The discovery of Rrn7 as the TFIIIB-related factor in the Pol I initiation apparatus allowed us to extend the current model to a minimal Pol I initiation complex (Figure 18). We included the above described model for Rrn7 on the basis of known TFIIIB structures, assuming that Rrn7, TBP, and promoter DNA are positioned similar to the previously described Pol II initiation complex model (Kostrewa *et al*, 2009). The resulting model revealed that the N-terminal zinc ribbon domain of Rrn7 that is bound to the polymerase dock domain could contact Rrn3 between heat repeats H4 and H5 (Figure 18), which would further provide an explanation for the known interaction between the human homologs of Rrn3/TIF-IA and Rrn7/TAF₁₆₈ (Miller *et al*, 2001). The model further suggests that the two other subunits of the core factor, Rrn6 and Rrn11, occupy positions between the Pol I clamp and subcomplexes A14/43 and dock domain. This location of the CF subunits explains known interactions of Rrn3 with Rrn6 in yeast (Peyroche *et al*, 2000) and TAF₁₁₀ in the human system (Miller *et al*, 2001) and moreover justifies an interaction between Rrn11 and TBP, as well as Rrn6-Rrn7 and Rrn11-Rrn7 as demonstrated previously (Lalo *et al*, 1996).

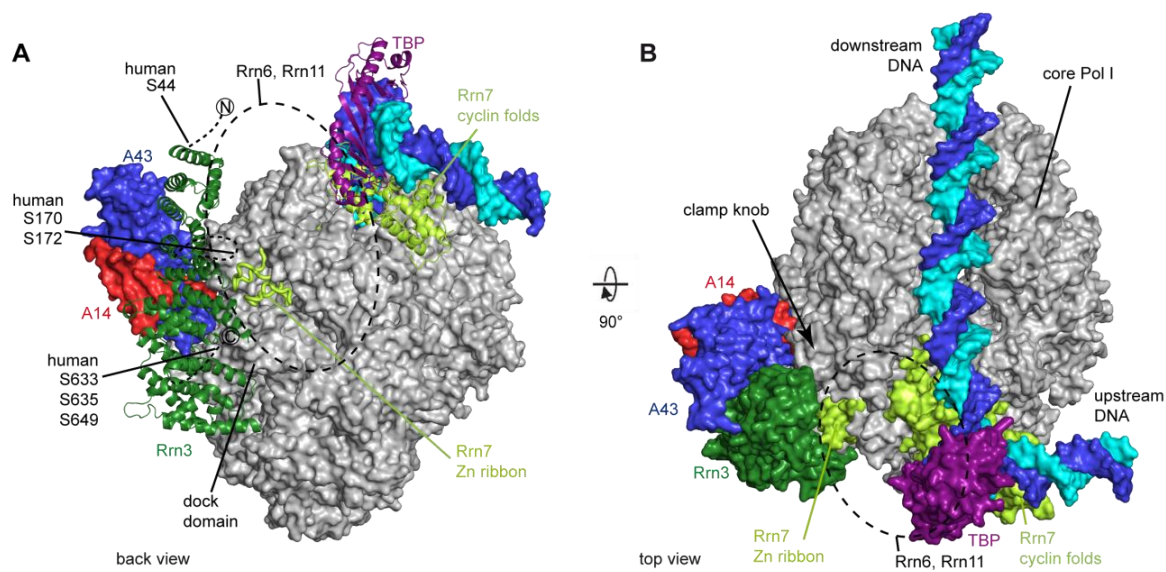


Figure 18. (A) Model of a minimal Pol I initiation complex. The Pol I-Rrn3 model in A was combined with the Pol II minimal initiation complex model containing TFIIB (light green, serving as a model for Rrn7), TBP (magenta), and closed promoter DNA (blue/cyan) (Kostrewa *et al*, 2009). Pol I and DNA are represented as molecular surfaces, whereas TBP, the Rrn7 model, and Rrn3 are shown as ribbons. The presumed location of the remaining core factor subunits Rrn6 and Rrn11 are indicated with a dashed circle. The view is from the back. Positions of phosphorylated serines outside the serine patch in human TIF-IA are indicated.

(B) Top view of the model in C containing all proteins in surface representation.

4 Discussion

The long-term goal of understanding how transcription initiation works and where evolution created differences and retained similarities requires examination of the three Polymerase systems and their transcription factors in molecular detail. By applying a combination of structural and functional methods, we elucidated the mechanism of Rrn3-regulated Pol I initiation and the effect of this interaction on cell growth in *S. cerevisiae*. The structure of Rrn3 revealed a unique HEAT repeat fold and a surface serine patch comprising four pairs of serines. Rrn3 forms a dimer in solution, but binds Pol I as a monomer with the binding interface extending along the back of Pol I from subcomplex AC40/19 to A14/43. In our docking model, the Rrn3 serine patch faces the Pol I subunit A43 and a phosphomimetic mutant in this patch impairs cell growth, Pol I binding *in vitro*, and Pol I recruitment to the rDNA promoter *in vivo*. This results in a reduced Pol I occupancy on the whole gene and a loss of Rrn3 from the promoter. Bioinformatic analysis identified Rrn7 as a putative functional homolog of TFIIB, leading to a model of a minimal Pol I-Rrn3 initiation complex.

The results obtained in this study recapitulate published data and converge on the molecular basis for Pol I initiation regulation by Rrn3. Our current model for this regulation suggests the following: during normal cell growth, the Rrn3 serine patch is not phosphorylated, enabling Rrn3 to bind Pol I, and resulting in stable Pol I recruitment to the rDNA promoter and efficient transcription initiation. During stress, phosphorylation of the serine patch impairs Rrn3 interaction with Pol I and thus Pol I recruitment to rDNA, resulting in a down-regulation of Pol I transcription, ribosome production, and cell growth. The phosphorylation of serine patch residues in human TIF-IA (Mayer *et al*, 2005; Mayer *et al*, 2004) argues for a conserved phospho-regulation mechanism of the Pol I-Rrn3 interaction and Pol I initiation. We tried to address this by phosphosite mapping of endogenous Rrn3 by MS, but this strategy proved to be unsuccessful despite extensive efforts using either exponentially growing cells or cells entering stationary phase. Purification of a phosphorylated state of Rrn3 turned out to be particularly difficult, since upon growth arrest in stationary phase, under any other stress condition such as rapamycin or cycloheximide treatment or upon aminoacid depletion Rrn3 levels are dramatically reduced (Philippi *et al*, 2010), which are the exact circumstances under which

we expect phosphorylation. With these very low cellular Rrn3 levels, it was impossible to get highly pure protein, which is necessary for phosphosite mapping via Masspec.

Phosphorylation of TIF-IA also occurs outside the conserved serine patch (Bierhoff *et al*, 2008; Hoppe *et al*, 2009; Philimonenko *et al*, 2004; Zhao *et al*, 2003) (Figure 13A and 18). Phosphorylation of residues S633 and S649 in the TIF-IA C-terminal tail activates transcription (Zhao *et al*, 2003), and S635 phosphorylation abolishes TIF-IA interaction with the human core factor (Hoppe *et al*, 2009). This is consistent with our model, which indicates that the TIF-IA C-terminal region that is not present in yeast Rrn3 could be near the predicted core factor location (Figure 18). Phosphorylation of the N-terminal serine S44 activates mammalian TIF-IA (Mayer *et al*, 2004), whereas in Rrn3 from *S. cerevisiae* a complete deletion of its 47 N-terminal residues had no effect in *in vivo* complementation assays. Phosphorylations at S170 and S172 are required for TIF-IA dissociation from elongating Pol I (Bierhoff *et al*, 2008), and may interfere with exiting RNA, which is predicted to displace the Rrn7 zinc ribbon (Figure 18).

Rrn3 dissociation also requires the A49/34.5 subcomplex (Albert *et al*, 2011; Beckouet *et al*, 2008), but it is unclear why. One hypothesis is, that the A49/34.5 heterodimer of one elongating Polymerase could contact Rrn3 bound to a succeeding polymerase and thereby facilitate its release (Albert *et al*, 2011). As the exact position of A49/34.5 still remains unclear, and no direct interaction between the heterodimer and Rrn3 has been found so far, we cannot support, nor disprove this hypothesis with our current knowledge.

In yeast, the Pol I-Rrn3 interaction is additionally regulated through phosphorylation of the Pol I subunit A43 that faces Rrn3, while Rrn3 is predominantly phosphorylated in its free form (Fath *et al*, 2001).

Taken together, current data converge on the view that both Rrn3 and TIF-IA are regulated by phosphorylation of a conserved surface serine patch, but further distinct phosphorylations in TIF-IA-specific regions and on Pol I additionally contribute to their function and regulation.

Rrn3 apparently also has a post-recruitment function, since Pol I can be recruited without Rrn3 at low levels, but requires Rrn3 for initiation (Aprikian *et al*, 2001; Schnapp and Grummt, 1991; Schnapp *et al*, 1993). We predict that Rrn3 binding causes a conformational change in Pol I that induces an initiation-competent state. Electron microscopy of free Pol I revealed a 'collapsed state' of the clamp (Kuhn *et al*, 2007) that

would prevent the DNA template strand from entering the active center cleft. Rrn3 binding may however hold the clamp in a position that allows template loading. Clamp positioning may additionally involve Pol I-specific surface features of the clamp and dock domains (Kuhn *et al*, 2007).

Our results also suggest that cells contain a reservoir of Rrn3 dimers that do not bind Pol I. The presence of serine residues S444 and S448 in the dimer interface further suggested that interface phosphorylation could release Rrn3 monomers that bind Pol I. However, the phospho-mimetic dimer-disrupting Rrn3 mutation S444/S448D had no phenotype in yeast (Figure 8), providing at present no evidence for regulated Rrn3 dimerization *in vivo*.

Finally, with the data obtained in this study we are able to extend the unifying evolutionary view of transcription initiation in eukaryotic cells.

Since regions in Pol I and Pol III subunits resemble parts of the Pol II initiation factors TFIIE and TFIIF (Geiger *et al*, 2010; Kassavetis *et al*, 2010; Lefevre *et al*, 2010; Vannini *et al*, 2010), and transcription initiation by archaeal Pol, Pol II, and Pol III additionally requires TBP and TFIIIB homologs (Colbert and Hahn, 1992; Kassavetis *et al*, 2005), it was always puzzling why the Pol I system lacks a factor related to TFIIIB. The previously undetected predicted homology of the core factor subunit Rrn7 with TFIIIB provides this missing link.

It now appears that the initiation complexes of both Pol I and Pol III resemble the core of the Pol II-TBP-TFIIIB/E/F complex.

While this work was about to be completed, two consistent studies were published showing a functional homology between Rrn7 or its human ortholog TAF1B with TFIIIB and Brf1. This was done by examining the effect of domain swaps between TFIIIB, Brf1 and Rrn7, and by a functional analysis of several mutants in the Pol I dock domain or the Rrn7 Zn-ribbon (Knutson and Hahn, 2011; Naidu *et al*, 2011), in full agreement with our results.

The similarity in transcription initiation complex topology may extend to coactivators. Electron microscopy and crosslinking in combination with mutational analysis indicates that the Mediator head subunit Med17 binds at the Rpb3/11 subcomplex of Pol II (Soutourina *et al*, 2011; Takagi *et al*, 2006), a position close to the location of the C-terminal part of Rrn3 on Pol I. Hence, regulatory cofactors differ in structure, but may still use the same molecular targets on conserved core initiation complexes.

5 Conclusions and Outlook

In this study, the high resolution structure of the central Pol I initiation factor Rrn3 was solved and revealed a new class of HEAT repeat proteins directly involved in Polymerase interaction. A structural biology hybrid approach combining SAXS, native-MS, X-ray and crosslinking-MS analysis, together with functional data of a mutagenesis study was applied. The obtained results firstly revealed a model for Rrn3 dimerization in solution and disruption of this dimer upon Pol I binding, secondly provided a model for Rrn3-Pol I interaction, thirdly indicated a possible regulation mechanism for the Pol I-Rrn3 interaction that is conserved between yeast and human, and finally led to a new model for a minimal Pol I initiation complex, including Rrn7 as the homolog of TFIIB in the Pol I transcription system.

It has been known for some time that Rrn3 binds to the Pol I subunits A43/14, but the docking model provided here now offers new insight into the Pol I-Rrn3 interaction, which involves a much broader interface than previously expected. However, new questions arise from these findings. As discussed before, Rrn3 might interact with the Pol I clamp to ensure an “open” state that allows entering of the DNA template strand and thereby facilitates efficient transcription initiation. Further, the position of Rrn3 on the Pol I surface close to the RNA exit channel theoretically allows contact of Rrn3 with the newly synthesized rRNA, and a positively charged stretch on the Rrn3 surface further supports this idea. However, preliminary electrophoretic mobility shift assays did not reveal an interaction of Rrn3 with a random dsDNA, ssDNA, or RNA template. Still, these experiments could be further optimized, and the possibility of an interaction of Rrn3 with a specific rRNA template and release of Rrn3 from the elongating Pol I in complex with the nascent rRNA would be an interesting question to address.

Our current model, comprising Pol I, Rrn3, TBP and Rrn7 with DNA, provides an ideal basis for further investigations concerning the additional factors that are required for Pol I initiation. To date very little is known about the core factor subunits Rrn6 and Rrn11 that are interaction partners of Rrn7 and TBP.

Extensive trials have been made in the past to purify several rationally designed Rrn7 constructs from a recombinant *E. coli* expression system. All trials were fruitless, most likely due to a lack of stability of the protein alone, without its binding partners.

Consequently, the core factor subunits should be purified as a complex of a least two subunits, as very strong interactions between the subunits have been proved (Keener *et al*, 1998; Lalo *et al*, 1996; Lin *et al*, 1996). A possible stabilizing effect of TBP on the core factor is also conceivable, as it specifically interacts individually with Rrn6, Rrn7 and Rrn11 (Lalo *et al*, 1996; Steffan *et al*, 1996).

In order to follow up on this study and to establish a more comprehensive view of the Pol I initiation complex, a structural and functional investigation of the core factor is clearly the next step to be made. Examination of the additional subunits Rrn6 and Rrn11 and their interaction with the initiation-competent Pol I, and comparison of the results to characterized Pol II transcription factors and coactivators will further help to understand connections and differences between the three Polymerase systems, and to understand their evolutionary relationship.

6 Appendix (unpublished results)

6.1 EM studies on the Pol I-Rrn3 complex

Before we succeeded to map the location of Rrn3 on the surface of Pol I through mutational analysis in combination with crosslinking, an attempt was started to locate Rrn3 on the surface of a Pol I EM map. Therefore Pol I- Rrn3 complexes were prepared as described in 2.4.2 and Cryo-EM data was collected and processed from these samples as described in 2.4.7.

During refinement only slight differences to the reference EM density calculated from a modified Pol II structure could be observed. Assuming that the homologous Pol I subunits would assemble similar to the Pol II subunits, the additional Pol I subunits A49/34.5 and the bound factor Rrn3 should be clearly visible as additional densities on the surface. In Figure 19 the initial particle selection and the Rrn3-Pol I docking model fitted into the resulting EM density is depicted.

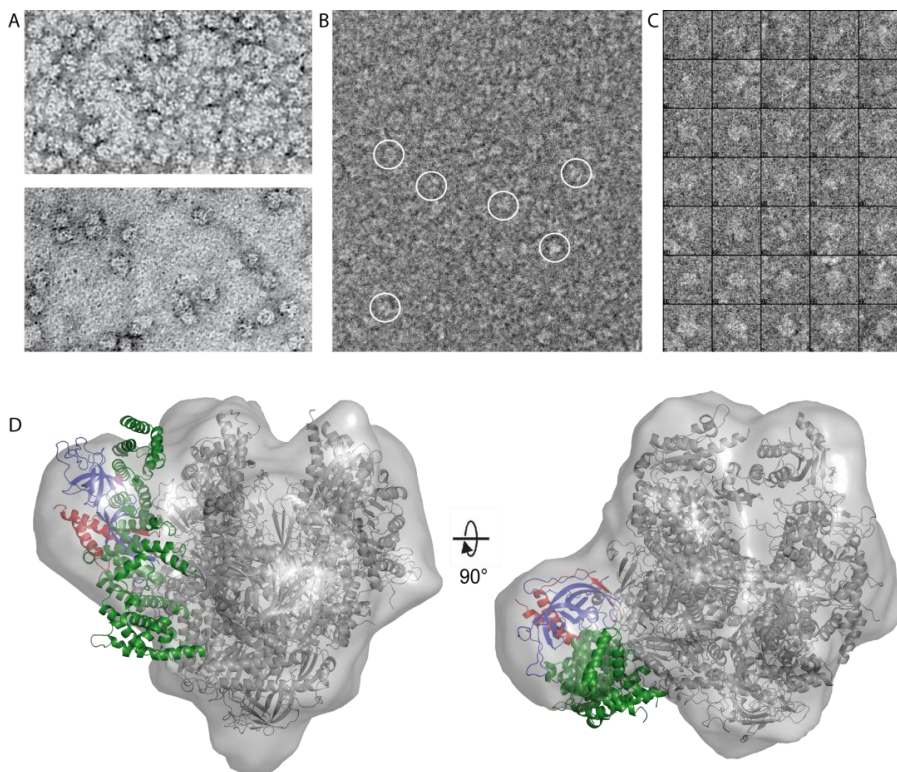


Figure 19. Cryo EM of Pol I-Rrn3 complex. (A) EM micrographs in negative stain of Pol I-Rrn3 complex in two different concentrations to evaluate the sample quality for cryo-EM. (B) EM micrograph of Pol I-Rrn3 in vitrified ice, white circles indicate particles. (C) single particle images selected with EMAN2. (D) Cryo-EM reconstruction of Pol I-Rrn3. The 10 subunit Pol II core homology model, the A43/14 crystal structure and the docked Rrn3 crystal structure shown as ribbon model were fitted into the map.

The EM reconstruction that was obtained in this preliminary experiment using 11503 particles could not support the presence of the additional Pol I subunits A49/34.5, neither is an extra density visible that would clearly represent a bound Rrn3, at the position it was located by crosslinking and mutational analysis. Besides possible problems concerning data collection and data processing certain biochemical properties could have led to this observation. Since it is known, that the A49/34.5 heterodimer can dissociate from Pol I (Geiger *et al*, 2010; Huet *et al*, 1976) and is therefore represented in a substoichiometric manner in the endogenous enzyme, we might have used a heterogeneous sample for data collection, which will lead to loss of information, without further specific sorting of the particles. The same problem might have occurred for the Rrn3 complexation. As there is only little known about the stability of the Pol I-Rrn3 complex *in vitro* it is to presume, that Rrn3 at least partially dissociated from the complex and the sample is additionally heterogeneous in this respect. From a sample with these high variabilities, it is hard to draw clear conclusions, and further improvements in sample preparation and data processing are indispensable, also when aiming at an EM reconstruction of a complete Pol I PIC.

6.2 Pol I Phosphopeptide mapping

The prerequisites for a stable interaction between Rrn3 and Pol I *in vivo* have been extensively studied in the mammalian system, and several pathways seem to regulate this interaction through specific phosphorylations of Rrn3/ TIF-IA. In the yeast system it has been shown that Rrn3 is predominantly phosphorylated in its free form but Pol I phosphorylations are necessary to form a stable Pol I-Rrn3 complex (Fath *et al*, 2001).

Several Phosphosites have been mapped on the Pol I surface (Table 17) (Gerber *et al*, 2008).

Table 17 mapped Pol I phosphosites (Gerber *et al*, 2008)

Subunit	Sequence	phosphosite
A190	ADSFMDVLVVPTR	S354
	DSFFTR	S685
	GSNVNVSQIMCLLGQQALEGR	S936 or S941
A43	FSFGNR	S208
	SLGHWVDSNGEPIDGK	S220
	VVSVDGTLISDADEEGNGYNSSR	S262 or S263
	IVFDDEVSIENK	S285
A34.5	DYVSDSDSDEVISNEFSIPDGFKK	S10/S12/S14
ABC23	ALQISMNAPVFDLEGETDPLR	S102
AC19	HIQEEEEQDVMGTGDEEQEEEPDREK	T33
	LLTQATSEDTGTSASFQIVEEDHTLGNALR	T51 or T54 or S55

To facilitate assembly of stable Pol I-Rrn3 complexes from recombinantly produced Rrn3 and endogenous Pol I, we purified Pol I with Phosphatase inhibitors, as described in 2.4.1. In order to get an idea which phosphosites were preserved through this procedure, we performed phosphopeptide mapping via Masspec, using Pol I samples purified with or without phosphatase inhibitors, respectively (Table 18 and 19).

Table 18. Pol I phosphosites, purification with phosphatase inhibitors

Subunit	Sequence	Phosphosite
A14	KETSIGVSATGGK	120;121 ^{1,4}
A43	IVFDDEVSIENK	262;263; ²
	VVSVDGTLISDADEEGNGYNSSR	285 ²
A49	RSVSEIEIESVQDQPSVAVGSFFK	8 ^{1,4}
AC19	HIQEEEEQDVMGTGDEEQEEEPDREK	33 ²
A190	KLDGSNEASANDEESFDVGRNPTRPK	287 ^{2,4}

Table 19. Pol I phosphosites, purification without phosphatase inhibitors

Subunit	Sequence	Phosphosite
A14	KETSIGVSATGGK	121 ^{1,4}
A49	RSVSEIEIESVQDQPSVAVGSFFK	8 ^{1,4}
AC19	TATEVTPQEPK	15 ^{3,4}
Rpb12	SREGFQIPTNLDAAAAGTSQAR	2 ^{3,4}
A135	IFIDDSQIWEDGQGK	1156 ^{3,4}

¹ Phosphosites identical in both samples, with and without phosphatase inhibitors

² Phosphosites only identified in the sample purified with phosphatase inhibitors

³ Phosphosites only identified in the sample purified without phosphatase inhibitors

⁴ New Phosphosites that have not been published previously

These experiments revealed a few new phosphosites that are distributed over the Polymerase surface in subunits A14, A49, AC19, Rpb12, A135 and A190. Pol I purified without Phosphatase inhibitors is not completely dephosphorylated, in contrary, some phosphosites were detected in this sample, which are not present in the sample that was treated with phosphatase inhibitors. However, concerning the Rrn3 interaction, one could draw the conclusion, that phosphorylations of subunit A43 at positions 262, 263 and 285, which are only observed in the sample treated with phosphatase inhibitors during purification, might affect Rrn3 binding.

6.4 Core Factor purification

The Pol I core factor (CF) comprises subunits Rrn6, Rrn7 and Rrn11, essential for Pol I transcription *in vivo*, which form a stable 200 kDa protein complex. Rrn7 was identified as the homolog of TFIIB, and a structural model could be obtained. For Rrn11 structural predictions using HHpred did not yet give a clear hint, whereas 400 aminoacids (residues 169-569) of Rrn6 could be predicted to form a β -propeller or a WD40 repeat domain, a structural feature known to coordinate multi-protein complex assemblies.

Several attempts were made to express the single subunits in *E. coli* without a proper expression yields, or yielding aggregated proteins. Here a new approach was made by expressing all three subunits in parallel in *E. coli* assuming that the proteins need their binding partners for proper folding and stability. Therefore, Rrn6 and Rrn11 were cloned into one plasmid, separated by an additional ribosomal binding site and a TATA sequence. The sequences were cloned in either pET28, carrying a Kanamycin resistance cassette, and resulting in an N-terminal His₆-Tag on Rrn6 and a C-terminal His₆-Tag on Rrn11, or in pET21, carrying an Ampicillin resistance cassette and expressing Rrn6 without a Tag and Rrn11 with a C-terminal His₆-Tag. Rrn7 was cloned into either pET28 or pET21 resulting accordingly in either an N-terminal or a C-terminal His₆-Tag. Transformation of an *E. coli* expression strain was then performed with two plasmids carrying two different antibiotic resistance cassettes, expressing Rrn7 and Rrn6/Rrn11, respectively.

Using this expression method a better yield could be obtained and the core factor seems to bind as a stoichiometric complex to the Ni-NTA affinity column, even when Rrn6 does not carry a His₆-Tag, proving that we are able to express and purify a stable trimeric complex recombinantly.

However, there are still substantial problems as the complex is not pure after the affinity purification step, and one major *E. coli* protein impurity, identified as ArnA, could not yet be removed through subsequent chromatography steps (Figure 21).

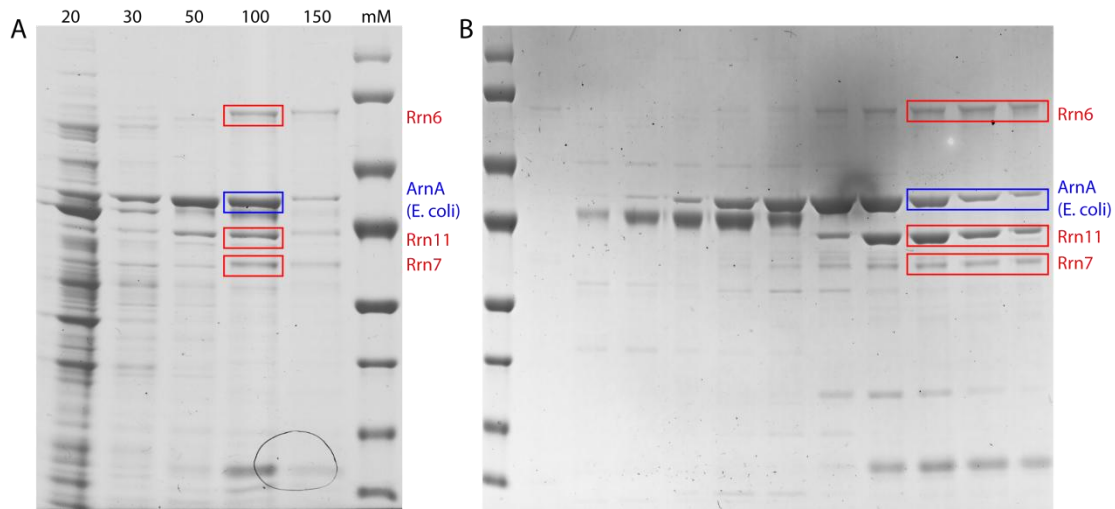


Figure 21. Core Factor purification

(A) Ni-NTA elution profile after expression of Rrn6/Rrn11 from pET21 and Rrn7 from pET28. Centrifuged cell lysate was loaded onto a gravity flow column as described in 2.2.5 and eluted with increasing concentrations of imidazole as indicated above each lane. (B) Mono Q elution profile. Elution fractions from the affinity purification step, containing the desired proteins, were subjected to an ion exchange chromatography. Proteins eluted from 150 mM to 400 mM NaCl. After both purification steps proteins were identified via masspec. Results are indicated as blue and red labels.

7 Abbreviations

bp	base pairs
BSA	bovine serum albumin
CHX	Cycloheximide
CV	column volumes
Da	dalton
DMSO	dimethyl sulfoxide
DTT	1,4-dithio-D,L-threitol
<i>E. coli</i>	<i>Escherichia coli</i>
EM	electron microscopy
ETS	external transcribed spacer
5-FOA	5-Fluoroorotic acid
GTF	general transcription factor
HEPES	N-2-hydroxyethylpiperazine-N'-2-ethane sulfonic acid
IGS	intergenic spacer
IPTG	Isopropyl- β -D-thiogalactopyranoside
IM-MS	ion mobility mass spectrometry
ITS	internal transcribed spacer
kDa	kilo dalton
LB	Luria-Bertani (media)
MCS	multiple cloning site
MES	(2-(N-morpholino)ethanesulfonic acid)
MOPS	4-morpholinepropanesulfonic acid
MW	molecular weight
NaCl	sodium chloride
Ni-NTA	nickel nitrilotriacetic acid
OD_x	optical density at a wavelength of X nm
ORF	open reading frame
PAGE	polyacrylamide gel electrophoresis
PBS	phosphate buffered saline

PDB	Protein Data Bank
PEG	Polyethylene glycol
pH	(<i>potentia hydrogenii</i>) measure of acidity
PIC	pre-initiation complex
Pol	RNA polymerase
rpm	rounds per minute
rapa	Rapamycin
rRNA	ribosomal RNA
SAXS	Small angle X-ray scattering
<i>S. cerevisiae</i>	<i>Saccharomyces cerevisiae</i>
<i>S. pombe</i>	<i>Schizosaccharomyces pombe</i>
SDS	sodium dodecylsulfate
SL1	Selectivity factor 1
SLS	static light scattering
SLS	Swiss light source
SOB	Super Optimal Broth (media)
SOC	Super Optimal broth with Catabolite repression (media)
TAF	TBP-associated factor
TB	Terrific Broth (media)
TCEP	tris(2-carboxyethyl)phosphine hydrochloride
TIF	transcription initiation factor
TF	transcription factor
TOR	Target of Rapamycin
Tris	tris-(hydroxymethyl)-aminomethane
UAF	upstream activating factor
UBF	upstream binding factor
wt	wild type

8 References

Albert B, Leger-Silvestre I, Normand C, Ostermaier MK, Perez-Fernandez J, Panov KI *et al* (2011). RNA polymerase I-specific subunits promote polymerase clustering to enhance the rRNA gene transcription cycle. *J Cell Biol* 192(2): 277-293.

Aprikian P, Moorefield B, Reeder RH (2001). New model for the yeast RNA polymerase I transcription cycle. *Mol Cell Biol* 21(15): 4847-4855.

Armache KJ, Mitterweger S, Meinhart A, Cramer P (2005). Structures of complete RNA polymerase II and its subcomplex, Rpb4/7. *J Biol Chem* 280(8): 7131-7134.

Baek HJ, Kang YK, Roeder RG (2006). Human Mediator enhances basal transcription by facilitating recruitment of transcription factor IIB during preinitiation complex assembly. *J Biol Chem* 281(22): 15172-15181.

Baumli S, Hoepfner S, Cramer P (2005). A conserved mediator hinge revealed in the structure of the MED7.MED21 (Med7.Srb7) heterodimer. *J Biol Chem* 280(18): 18171-18178.

Beckouet F, Labarre-Mariotte S, Albert B, Imazawa Y, Werner M, Gadad O *et al* (2008). Two RNA polymerase I subunits control the binding and release of Rrn3 during transcription. *Mol Cell Biol* 28(5): 1596-1605.

Biegert A, Mayer C, Remmert M, Soding J, Lupas AN (2006). The MPI Bioinformatics Toolkit for protein sequence analysis. *Nucleic Acids Res* 34(Web Server issue): W335-339.

Bier M, Fath S, Tschochner H (2004). The composition of the RNA polymerase I transcription machinery switches from initiation to elongation mode. *FEBS Lett* 564(1-2): 41-46.

Bierhoff H, Dunder M, Michels AA, Grummt I (2008). Phosphorylation by casein kinase 2 facilitates rRNA gene transcription by promoting dissociation of TIF-IA from elongating RNA polymerase I. *Mol Cell Biol* 28(16): 4988-4998.

Blanc E, Roversi P, Vonrhein C, Flensburg C, Lea SM, Bricogne G (2004). Refinement of severely incomplete structures with maximum likelihood in BUSTER-TNT. *Acta Crystallogr D Biol Crystallogr* 60(Pt 12 Pt 1): 2210-2221.

Bodem J, Dobrev G, Hoffmann-Rohrer U, Iben S, Zentgraf H, Delius H *et al* (2000). TIF-IA, the factor mediating growth-dependent control of ribosomal RNA synthesis, is the mammalian homolog of yeast Rrn3p. *EMBO Rep* 1(2): 171-175.

Bordi L, Cioci F, Camilloni G (2001). In vivo binding and hierarchy of assembly of the yeast RNA polymerase I transcription factors. *Mol Biol Cell* 12(3): 753-760.

- Boukhgalter B, Liu M, Guo A, Tripp M, Tran K, Huynh C *et al* (2002). Characterization of a fission yeast subunit of an RNA polymerase I essential transcription initiation factor, SpRrn7h/TAF(I)68, that bridges yeast and mammals: association with SpRrn11h and the core ribosomal RNA gene promoter. *Gene* 291(1-2): 187-201.
- Bradford MM (1976). A rapid and sensitive method for the quantitation of microgram quantities of protein utilizing the principle of protein-dye binding. *Anal Biochem* 72: 248-254.
- Bricogne G, Vonrhein C, Flensburg C, Schiltz M, Paciorek W (2003). Generation, representation and flow of phase information in structure determination: recent developments in and around SHARP 2.0. *Acta Crystallogr D Biol Crystallogr* 59(Pt 11): 2023-2030.
- Burley SK, Roeder RG (1996). Biochemistry and structural biology of transcription factor IID (TFIID). *Annu Rev Biochem* 65: 769-799.
- Cavanaugh AH, Hirschler-Laszkiwicz I, Hu Q, Dundr M, Smink T, Misteli T *et al* (2002). Rrn3 phosphorylation is a regulatory checkpoint for ribosome biogenesis. *J Biol Chem* 277(30): 27423-27432.
- Chen HT, Hahn S (2003). Binding of TFIIB to RNA polymerase II: Mapping the binding site for the TFIIB zinc ribbon domain within the preinitiation complex. *Mol Cell* 12(2): 437-447.
- Chen HT, Warfield L, Hahn S (2007). The positions of TFIIF and TFIIE in the RNA polymerase II transcription preinitiation complex. *Nat Struct Mol Biol* 14(8): 696-703.
- Chen ZA, Jawhari A, Fischer L, Buchen C, Tahir S, Kamenski T *et al* (2010). Architecture of the RNA polymerase II-TFIIF complex revealed by cross-linking and mass spectrometry. *EMBO J* 29(4): 717-726.
- Chenna R, Sugawara H, Koike T, Lopez R, Gibson TJ, Higgins DG *et al* (2003). Multiple sequence alignment with the Clustal series of programs. *Nucleic Acids Res* 31(13): 3497-3500.
- Cingolani G, Petosa C, Weis K, Muller CW (1999). Structure of importin-beta bound to the IBB domain of importin-alpha. *Nature* 399(6733): 221-229.
- Claypool JA, French SL, Johzuka K, Eliason K, Vu L, Dodd JA *et al* (2004). Tor pathway regulates Rrn3p-dependent recruitment of yeast RNA polymerase I to the promoter but does not participate in alteration of the number of active genes. *Mol Biol Cell* 15(2): 946-956.
- Colbert T, Hahn S (1992). A yeast TFIIB-related factor involved in RNA polymerase III transcription. *Genes Dev* 6(10): 1940-1949.

- Comai L, Tanese N, Tjian R (1992). The TATA-binding protein and associated factors are integral components of the RNA polymerase I transcription factor, SL1. *Cell* 68(5): 965-976.
- Conti E, Kuriyan J (2000). Crystallographic analysis of the specific yet versatile recognition of distinct nuclear localization signals by karyopherin alpha. *Structure* 8(3): 329-338.
- Coulombe B, Burton ZF (1999). DNA bending and wrapping around RNA polymerase: a "revolutionary" model describing transcriptional mechanisms. *Microbiol Mol Biol Rev* 63(2): 457-478.
- Cowtan K (2006). The Buccaneer software for automated model building. 1. Tracing protein chains. *Acta Crystallogr D Biol Crystallogr* 62(Pt 9): 1002-1011.
- Cramer P, Bushnell DA, Kornberg RD (2001). Structural basis of transcription: RNA polymerase II at 2.8 angstrom resolution. *Science* 292(5523): 1863-1876.
- Dammann R, Lucchini R, Koller T, Sogo JM (1995). Transcription in the yeast rRNA gene locus: distribution of the active gene copies and chromatin structure of their flanking regulatory sequences. *Mol Cell Biol* 15(10): 5294-5303.
- De Carlo S, Carles C, Riva M, Schultz P (2003). Cryo-negative staining reveals conformational flexibility within yeast RNA polymerase I. *J Mol Biol* 329(5): 891-902.
- Denissov S, Lessard F, Mayer C, Stefanovsky V, van Driel M, Grummt I *et al* (2011). A model for the topology of active ribosomal RNA genes. *EMBO Rep* 12(3): 231-237.
- Drygin D, Rice WG, Grummt I (2010). The RNA polymerase I transcription machinery: an emerging target for the treatment of cancer. *Annu Rev Pharmacol Toxicol* 50: 131-156.
- Edgar RC (2004). MUSCLE: multiple sequence alignment with high accuracy and high throughput. *Nucleic Acids Res* 32(5): 1792-1797.
- Eichner J, Chen HT, Warfield L, Hahn S (2010). Position of the general transcription factor TFIIF within the RNA polymerase II transcription preinitiation complex. *EMBO J* 29(4): 706-716.
- Emsley P, Cowtan K (2004). Coot: model-building tools for molecular graphics. *Acta Crystallogr D Biol Crystallogr* 60(Pt 12 Pt 1): 2126-2132.
- Eswar N, Eramian D, Webb B, Shen MY, Sali A (2008). Protein structure modeling with MODELLER. *Methods Mol Biol* 426: 145-159.
- Fan X, Lamarre-Vincent N, Wang Q, Struhl K (2008). Extensive chromatin fragmentation improves enrichment of protein binding sites in chromatin immunoprecipitation experiments. *Nucleic Acids Res* 36(19): e125.

- Fath S, Milkereit P, Peyroche G, Riva M, Carles C, Tschochner H (2001). Differential roles of phosphorylation in the formation of transcriptional active RNA polymerase I. *Proc Natl Acad Sci U S A* 98(25): 14334-14339.
- Fernandez-Tornero C, Bottcher B, Rashid UJ, Steuerwald U, Florchinger B, Devos DP *et al* (2010). Conformational flexibility of RNA polymerase III during transcriptional elongation. *EMBO J* 29(22): 3762-3772.
- Ferreira-Cerca S, Poll G, Kuhn H, Neueder A, Jakob S, Tschochner H *et al* (2007). Analysis of the in vivo assembly pathway of eukaryotic 40S ribosomal proteins. *Mol Cell* 28(3): 446-457.
- Flores O, Lu H, Killeen M, Greenblatt J, Burton ZF, Reinberg D (1991). The small subunit of transcription factor IIF recruits RNA polymerase II into the preinitiation complex. *Proc Natl Acad Sci U S A* 88(22): 9999-10003.
- Frank J, Radermacher M, Penczek P, Zhu J, Li Y, Ladjadj M *et al* (1996). SPIDER and WEB: processing and visualization of images in 3D electron microscopy and related fields. *J Struct Biol* 116(1): 190-199.
- Gaiser F, Tan S, Richmond TJ (2000). Novel dimerization fold of RAP30/RAP74 in human TFIIIF at 1.7 Å resolution. *J Mol Biol* 302(5): 1119-1127.
- Gasteiger E, Gattiker A, Hoogland C, Ivanyi I, Appel RD, Bairoch A (2003). ExPASy: The proteomics server for in-depth protein knowledge and analysis. *Nucleic Acids Res* 31(13): 3784-3788.
- Geiger SR, Kuhn CD, Leidig C, Renkawitz J, Cramer P (2008). Crystallization of RNA polymerase I subcomplex A14/A43 by iterative prediction, probing and removal of flexible regions. *Acta Crystallogr Sect F Struct Biol Cryst Commun* 64(Pt 5): 413-418.
- Geiger SR, Lorenzen K, Schrieck A, Hanecker P, Kostrewa D, Heck AJ *et al* (2010). RNA polymerase I contains a TFIIIF-related DNA-binding subcomplex. *Mol Cell* 39(4): 583-594.
- Gerber J, Reiter A, Steinbauer R, Jakob S, Kuhn CD, Cramer P *et al* (2008). Site specific phosphorylation of yeast RNA polymerase I. *Nucleic Acids Res* 36(3): 793-802.
- Gorski JJ, Pathak S, Panov K, Kasciukovic T, Panova T, Russell J *et al* (2007). A novel TBP-associated factor of SL1 functions in RNA polymerase I transcription. *EMBO J* 26(6): 1560-1568.
- Gouet P, Courcelle E, Stuart DI, Metz F (1999). ESPript: analysis of multiple sequence alignments in PostScript. *Bioinformatics* 15(4): 305-308.
- Granneman S, Baserga SJ (2004). Ribosome biogenesis: of knobs and RNA processing. *Exp Cell Res* 296(1): 43-50.

Groft CM, Uljon SN, Wang R, Werner MH (1998). Structural homology between the Rap30 DNA-binding domain and linker histone H5: implications for preinitiation complex assembly. *Proc Natl Acad Sci U S A* 95(16): 9117-9122.

Grummt I, Voit R (2010). Linking rDNA transcription to the cellular energy supply. *Cell Cycle* 9(2): 225-226.

Guettg C, Lienemann P, Sirri V, Grummt I, Hernandez-Verdun D, Hottiger MO *et al* (2010). The NoRC complex mediates the heterochromatin formation and stability of silent rRNA genes and centromeric repeats. *EMBO J* 29(13): 2135-2146.

Hahn S. (2004). *Nat Struct Mol Biol*, Vol. 11, pp 394-403.

Hamada M, Huang Y, Lowe TM, Maraia RJ (2001). Widespread use of TATA elements in the core promoters for RNA polymerases III, II, and I in fission yeast. *Mol Cell Biol* 21(20): 6870-6881.

Heck AJ (2008). Native mass spectrometry: a bridge between interactomics and structural biology. *Nat Methods* 5(11): 927-933.

Heix J, Vente A, Voit R, Budde A, Michaelidis TM, Grummt I (1998). Mitotic silencing of human rRNA synthesis: inactivation of the promoter selectivity factor SL1 by cdc2/cyclin B-mediated phosphorylation. *EMBO J* 17(24): 7373-7381.

Hoppe S, Bierhoff H, Cado I, Weber A, Tiebe M, Grummt I *et al* (2009). AMP-activated protein kinase adapts rRNA synthesis to cellular energy supply. *Proc Natl Acad Sci U S A* 106(42): 17781-17786.

Huet J, Dezelee S, Iborra F, Buhler JM, Sentenac A, Fromageot P (1976). Further characterization of yeast RNA polymerases. Effect of subunits removal. *Biochimie* 58(1-2): 71-80.

Iben S, Tschochner H, Bier M, Hoogstraten D, Hozak P, Egly JM *et al* (2002). TFIIF plays an essential role in RNA polymerase I transcription. *Cell* 109(3): 297-306.

Imasaki T, Calero G, Cai G, Tsai KL, Yamada K, Cardelli F *et al* (2011). Architecture of the Mediator head module. *Nature* 475(7355): 240-243.

Imazawa Y, Hisatake K, Mitsuzawa H, Matsumoto M, Tsukui T, Nakagawa K *et al* (2005). The fission yeast protein Ker1p is an ortholog of RNA polymerase I subunit A14 in *Saccharomyces cerevisiae* and is required for stable association of Rrn3p and RPA21 in RNA polymerase I. *J Biol Chem* 280(12): 11467-11474.

Imazawa Y, Hisatake K, Nakagawa K, Muramatsu M, Nogi Y (2002). The fission yeast RPA21 subunit of RNA polymerase I: an evolutionarily conserved subunit interacting with ribosomal DNA (rDNA) transcription factor Rrn3p for recruitment to rDNA promoter. *Genes Genet Syst* 77(3): 147-157.

- Janke C, Magiera MM, Rathfelder N, Taxis C, Reber S, Maekawa H *et al* (2004). A versatile toolbox for PCR-based tagging of yeast genes: new fluorescent proteins, more markers and promoter substitution cassettes. *Yeast* 21(11): 947-962.
- Jantzen HM, Chow AM, King DS, Tjian R (1992). Multiple domains of the RNA polymerase I activator hUBF interact with the TATA-binding protein complex hSL1 to mediate transcription. *Genes Dev* 6(10): 1950-1963.
- Jasiak AJ, Armache KJ, Martens B, Jansen RP, Cramer P (2006). Structural biology of RNA polymerase III: subcomplex C17/25 X-ray structure and 11 subunit enzyme model. *Mol Cell* 23(1): 71-81.
- Juo ZS, Kassavetis GA, Wang J, Geiduschek EP, Sigler PB (2003). Crystal structure of a transcription factor IIIB core interface ternary complex. *Nature* 422(6931): 534-539.
- Kabsch W (2010). Xds. *Acta Crystallogr D Biol Crystallogr* 66(Pt 2): 125-132.
- Kamada K, De Angelis J, Roeder RG, Burley SK (2001). Crystal structure of the C-terminal domain of the RAP74 subunit of human transcription factor IIF. *Proc Natl Acad Sci U S A* 98(6): 3115-3120.
- Kang JS, Kim SH, Hwang MS, Han SJ, Lee YC, Kim YJ (2001). The structural and functional organization of the yeast mediator complex. *J Biol Chem* 276(45): 42003-42010.
- Kassavetis GA, Prakash P, Shim E (2010). The C53/C37 subcomplex of RNA polymerase III lies near the active site and participates in promoter opening. *J Biol Chem* 285(4): 2695-2706.
- Kassavetis GA, Soragni E, Driscoll R, Geiduschek EP (2005). Reconfiguring the connectivity of a multiprotein complex: fusions of yeast TATA-binding protein with Brf1, and the function of transcription factor IIIB. *Proc Natl Acad Sci U S A* 102(43): 15406-15411.
- Keener J, Josaitis CA, Dodd JA, Nomura M (1998). Reconstitution of yeast RNA polymerase I transcription in vitro from purified components. TATA-binding protein is not required for basal transcription. *J Biol Chem* 273(50): 33795-33802.
- Kettenberger H, Armache KJ, Cramer P (2003). Architecture of the RNA polymerase II-TFIIS complex and implications for mRNA cleavage. *Cell* 114(3): 347-357.
- Keys DA, Lee BS, Dodd JA, Nguyen TT, Vu L, Fantino E *et al* (1996). Multiprotein transcription factor UAF interacts with the upstream element of the yeast RNA polymerase I promoter and forms a stable preinitiation complex. *Genes Dev* 10(7): 887-903.

- Kihm AJ, Hershey JC, Haystead TA, Madsen CS, Owens GK (1998). Phosphorylation of the rRNA transcription factor upstream binding factor promotes its association with TATA binding protein. *Proc Natl Acad Sci U S A* 95(25): 14816-14820.
- Kim TK, Ebright RH, Reinberg D (2000). Mechanism of ATP-dependent promoter melting by transcription factor IIH. *Science* 288(5470): 1418-1422.
- Kim YJ, Bjorklund S, Li Y, Sayre MH, Kornberg RD (1994). A multiprotein mediator of transcriptional activation and its interaction with the C-terminal repeat domain of RNA polymerase II. *Cell* 77(4): 599-608.
- Kiss T (2001). Small nucleolar RNA-guided post-transcriptional modification of cellular RNAs. *EMBO J* 20(14): 3617-3622.
- Klein J, Grummt I (1999). Cell cycle-dependent regulation of RNA polymerase I transcription: the nucleolar transcription factor UBF is inactive in mitosis and early G1. *Proc Natl Acad Sci U S A* 96(11): 6096-6101.
- Knutson BA, Hahn S (2011). Yeast Rrn7 and human TAF1B are TFIIB-related RNA polymerase I general transcription factors. *Science* 333(6049): 1637-1640.
- Konarev PV, Petoukhov MV, Volkov VV, Svergun DI (2006). ATSAS 2.1, a program package for small-angle scattering data analysis. *Journal of Applied Crystallography* 39: 277-286.
- Kos M, Tollervey D (2010). Yeast pre-rRNA processing and modification occur cotranscriptionally. *Mol Cell* 37(6): 809-820.
- Kosa PF, Ghosh G, DeDecker BS, Sigler PB (1997). The 2.1-A crystal structure of an archaeal preinitiation complex: TATA-box-binding protein/transcription factor (II)B core/TATA-box. *Proc Natl Acad Sci U S A* 94(12): 6042-6047.
- Koschubs T, Lorenzen K, Baumli S, Sandstrom S, Heck AJ, Cramer P (2010). Preparation and topology of the Mediator middle module. *Nucleic Acids Res* 38(10): 3186-3195.
- Koschubs T, Seizl M, Lariviere L, Kurth F, Baumli S, Martin DE *et al* (2009). Identification, structure, and functional requirement of the Mediator submodule Med7N/31. *EMBO J* 28(1): 69-80.
- Kostrewa D, Zeller ME, Armache KJ, Seizl M, Leike K, Thomm M *et al* (2009). RNA polymerase II-TFIIB structure and mechanism of transcription initiation. *Nature* 462(7271): 323-330.
- Kuhn CD, Geiger SR, Baumli S, Gartmann M, Gerber J, Jennebach S *et al* (2007). Functional architecture of RNA polymerase I. *Cell* 131(7): 1260-1272.

- Kwon H, Green MR (1994). The RNA polymerase I transcription factor, upstream binding factor, interacts directly with the TATA box-binding protein. *J Biol Chem* 269(48): 30140-30146.
- Laferte A, Favry E, Sentenac A, Riva M, Carles C, Chedin S (2006). The transcriptional activity of RNA polymerase I is a key determinant for the level of all ribosome components. *Genes Dev* 20(15): 2030-2040.
- Lalo D, Steffan JS, Dodd JA, Nomura M (1996). RRN11 encodes the third subunit of the complex containing Rrn6p and Rrn7p that is essential for the initiation of rDNA transcription by yeast RNA polymerase I. *J Biol Chem* 271(35): 21062-21067.
- Landrieux E, Alic N, Ducrot C, Acker J, Riva M, Carles C (2006). A subcomplex of RNA polymerase III subunits involved in transcription termination and reinitiation. *EMBO J* 25(1): 118-128.
- Lariviere L, Geiger S, Hoepfner S, Rother S, Strasser K, Cramer P (2006). Structure and TBP binding of the Mediator head subcomplex Med8-Med18-Med20. *Nat Struct Mol Biol* 13(10): 895-901.
- Lariviere L, Seizl M, van Wageningen S, Rother S, van de Pasch L, Feldmann H *et al* (2008). Structure-system correlation identifies a gene regulatory Mediator submodule. *Genes Dev* 22(7): 872-877.
- Larkin MA, Blackshields G, Brown NP, Chenna R, McGettigan PA, McWilliam H *et al* (2007). Clustal W and Clustal X version 2.0. *Bioinformatics* 23(21): 2947-2948.
- Lee TI, Young RA (2000). Transcription of eukaryotic protein-coding genes. *Annu Rev Genet* 34: 77-137.
- Lefevre S, Dumay-Odelot H, El-Ayoubi L, Budd A, Legrand P, Pinaud N *et al* (2010). Structure-function analysis of hRPC62 provides insights into RNA polymerase III transcription initiation. *Nat Struct Mol Biol* 18(4): 516.
- Lefevre S, Dumay-Odelot H, El-Ayoubi L, Budd A, Legrand P, Pinaud N *et al* (2011). Structure-function analysis of hRPC62 provides insights into RNA polymerase III transcription initiation. *Nat Struct Mol Biol* 18(3): 352-358.
- Leitner A, Walzthoeni T, Kahraman A, Herzog F, Rinner O, Beck M *et al* (2010). Probing native protein structures by chemical cross-linking, mass spectrometry, and bioinformatics. *Mol Cell Proteomics* 9(8): 1634-1649.
- Lin CW, Moorefield B, Payne J, Aprikian P, Mitomo K, Reeder RH (1996). A novel 66-kilodalton protein complexes with Rrn6, Rrn7, and TATA-binding protein to promote polymerase I transcription initiation in *Saccharomyces cerevisiae*. *Mol Cell Biol* 16(11): 6436-6443.

- Liu X, Bushnell DA, Wang D, Calero G, Kornberg RD (2010). Structure of an RNA polymerase II-TFIIB complex and the transcription initiation mechanism. *Science* 327(5962): 206-209.
- Lorenzen K, Vannini A, Cramer P, Heck AJ (2007). Structural biology of RNA polymerase III: mass spectrometry elucidates subcomplex architecture. *Structure* 15(10): 1237-1245.
- Mayer C, Bierhoff H, Grummt I (2005). The nucleolus as a stress sensor: JNK2 inactivates the transcription factor TIF-IA and down-regulates rRNA synthesis. *Genes Dev* 19(8): 933-941.
- Mayer C, Zhao J, Yuan X, Grummt I (2004). mTOR-dependent activation of the transcription factor TIF-IA links rRNA synthesis to nutrient availability. *Genes Dev* 18(4): 423-434.
- Meinhart A, Blobel J, Cramer P (2003). An extended winged helix domain in general transcription factor E/TFIIA. *J Biol Chem* 278(48): 48267-48274.
- Milkereit P, Tschochner H (1998). A specialized form of RNA polymerase I, essential for initiation and growth-dependent regulation of rRNA synthesis, is disrupted during transcription. *EMBO J* 17(13): 3692-3703.
- Miller G, Panov KI, Friedrich JK, Trinkle-Mulcahy L, Lamond AI, Zomerdijk JC (2001). hRRN3 is essential in the SL1-mediated recruitment of RNA Polymerase I to rRNA gene promoters. *EMBO J* 20(6): 1373-1382.
- Miller OL, Jr., Beatty BR (1969). Visualization of nucleolar genes. *Science* 164(882): 955-957.
- Moorefield B, Greene EA, Reeder RH (2000). RNA polymerase I transcription factor Rrn3 is functionally conserved between yeast and human. *Proc Natl Acad Sci U S A* 97(9): 4724-4729.
- Moss T, Langlois F, Gagnon-Kugler T, Stefanovsky V (2007). A housekeeper with power of attorney: the rRNA genes in ribosome biogenesis. *Cell Mol Life Sci* 64(1): 29-49.
- Naidu S, Friedrich JK, Russell J, Zomerdijk JC (2011). TAF1B is a TFIIB-like component of the basal transcription machinery for RNA polymerase I. *Science* 333(6049): 1640-1642.
- Niall HD (1973). Automated Edman degradation: the protein sequenator. *Methods Enzymol* 27: 942-1010.
- Nikolov DB, Chen H, Halay ED, Usheva AA, Hisatake K, Lee DK *et al* (1995). Crystal structure of a TFIIB-TBP-TATA-element ternary complex. *Nature* 377(6545): 119-128.

- Okuda M, Watanabe Y, Okamura H, Hanaoka F, Ohkuma Y, Nishimura Y (2000). Structure of the central core domain of TFIIIEbeta with a novel double-stranded DNA-binding surface. *EMBO J* 19(6): 1346-1356.
- Panova TB, Panov KI, Russell J, Zomerdijk JC (2006). Casein kinase 2 associates with initiation-competent RNA polymerase I and has multiple roles in ribosomal DNA transcription. *Mol Cell Biol* 26(16): 5957-5968.
- Paule MR, White RJ (2000). Survey and summary: transcription by RNA polymerases I and III. *Nucleic Acids Res* 28(6): 1283-1298.
- Peyroche G, Milkereit P, Bischler N, Tschochner H, Schultz P, Sentenac A *et al* (2000). The recruitment of RNA polymerase I on rDNA is mediated by the interaction of the A43 subunit with Rrn3. *EMBO J* 19(20): 5473-5482.
- Philimonenko VV, Zhao J, Iben S, Dingova H, Kysela K, Kahle M *et al* (2004). Nuclear actin and myosin I are required for RNA polymerase I transcription. *Nat Cell Biol* 6(12): 1165-1172.
- Philippi A, Steinbauer R, Reiter A, Fath S, Leger-Silvestre I, Milkereit P *et al* (2010). TOR-dependent reduction in the expression level of Rrn3p lowers the activity of the yeast RNA Pol I machinery, but does not account for the strong inhibition of rRNA production. *Nucleic Acids Res* 38(16): 5315-5326.
- Poole AM, Jeffares DC, Penny D (1998). The path from the RNA world. *J Mol Evol* 46(1): 1-17.
- Putnam CD, Hammel M, Hura GL, Tainer JA (2007). X-ray solution scattering (SAXS) combined with crystallography and computation: defining accurate macromolecular structures, conformations and assemblies in solution. *Q Rev Biophys* 40(3): 191-285.
- Rinner O, Seebacher J, Walzthoeni T, Mueller LN, Beck M, Schmidt A *et al* (2008). Identification of cross-linked peptides from large sequence databases. *Nat Methods* 5(4): 315-318.
- Rost B, Yachdav G, Liu J (2004). The PredictProtein server. *Nucleic Acids Res* 32(Web Server issue): W321-326.
- Russell J, Zomerdijk JCBM (2005). RNA-polymerase-I-directed rDNA transcription, life and works. *Trends in Biochemical Sciences* 30(2): 87-96.
- Santoro R, Grummt I (2005). Epigenetic mechanism of rRNA gene silencing: temporal order of NoRC-mediated histone modification, chromatin remodeling, and DNA methylation. *Mol Cell Biol* 25(7): 2539-2546.

- Santoro R, Li J, Grummt I (2002). The nucleolar remodeling complex NoRC mediates heterochromatin formation and silencing of ribosomal gene transcription. *Nat Genet* 32(3): 393-396.
- Schlosser A, Bodem J, Bossemeyer D, Grummt I, Lehmann WD (2002). Identification of protein phosphorylation sites by combination of elastase digestion, immobilized metal affinity chromatography, and quadrupole-time of flight tandem mass spectrometry. *Proteomics* 2(7): 911-918.
- Schnapp A, Grummt I (1991). Transcription complex formation at the mouse rDNA promoter involves the stepwise association of four transcription factors and RNA polymerase I. *J Biol Chem* 266(36): 24588-24595.
- Schnapp A, Schnapp G, Erny B, Grummt I (1993). Function of the growth-regulated transcription initiation factor TIF-IA in initiation complex formation at the murine ribosomal gene promoter. *Mol Cell Biol* 13(11): 6723-6732.
- Schneider TR, Sheldrick GM (2002). Substructure solution with SHELXD. *Acta Crystallogr D Biol Crystallogr* 58(Pt 10 Pt 2): 1772-1779.
- Seizl M, Lariviere L, Pfaffeneder T, Wenzek L, Cramer P (2011). Mediator head subcomplex Med11/22 contains a common helix bundle building block with a specific function in transcription initiation complex stabilization. *Nucleic Acids Res* 39(14): 6291-6304.
- Soding J, Biegert A, Lupas AN (2005). The HHpred interactive server for protein homology detection and structure prediction. *Nucleic Acids Res* 33(Web Server issue): W244-248.
- Soutourina J, Wydau S, Ambroise Y, Boschiero C, Werner M (2011). Direct interaction of RNA polymerase II and mediator required for transcription in vivo. *Science* 331(6023): 1451-1454.
- Steffan JS, Keys DA, Dodd JA, Nomura M (1996). The role of TBP in rDNA transcription by RNA polymerase I in *Saccharomyces cerevisiae*: TBP is required for upstream activation factor-dependent recruitment of core factor. *Genes Dev* 10(20): 2551-2563.
- Svergun D, Barberato C, Koch MHJ (1995). CRY SOL - A program to evaluate x-ray solution scattering of biological macromolecules from atomic coordinates. *Journal of Applied Crystallography* 28: 768-773.
- Takagi Y, Calero G, Komori H, Brown JA, Ehrensberger AH, Hudmon A *et al* (2006). Head module control of mediator interactions. *Mol Cell* 23(3): 355-364.
- Tang G, Peng L, Baldwin PR, Mann DS, Jiang W, Rees I *et al* (2007). EMAN2: an extensible image processing suite for electron microscopy. *J Struct Biol* 157(1): 38-46.

- Teichmann M, Wang Z, Roeder RG (2000). A stable complex of a novel transcription factor IIB- related factor, human TFIIIB50, and associated proteins mediate selective transcription by RNA polymerase III of genes with upstream promoter elements. *Proc Natl Acad Sci U S A* 97(26): 14200-14205.
- Terwilliger TC, Grosse-Kunstleve RW, Afonine PV, Moriarty NW, Zwart PH, Hung LW *et al* (2008). Iterative model building, structure refinement and density modification with the PHENIX AutoBuild wizard. *Acta Crystallogr D Biol Crystallogr* 64(Pt 1): 61-69.
- Thomas MC, Chiang CM (2006). The general transcription machinery and general cofactors. *Crit Rev Biochem Mol Biol* 41(3): 105-178.
- Towpik J, Graczyk D, Gajda A, Lefebvre O, Boguta M (2008). Derepression of RNA polymerase III transcription by phosphorylation and nuclear export of its negative regulator, Maf1. *J Biol Chem* 283(25): 17168-17174.
- Tsai FT, Sigler PB (2000). Structural basis of preinitiation complex assembly on human pol II promoters. *EMBO J* 19(1): 25-36.
- Tsang CK, Bertram PG, Ai W, Drenan R, Zheng XF (2003). Chromatin-mediated regulation of nucleolar structure and RNA Pol I localization by TOR. *EMBO J* 22(22): 6045-6056.
- Tschochner H, Hurt E (2003). Pre-ribosomes on the road from the nucleolus to the cytoplasm. *Trends Cell Biol* 13(5): 255-263.
- Tuan JC, Zhai W, Comai L (1999). Recruitment of TATA-binding protein-TAFI complex SL1 to the human ribosomal DNA promoter is mediated by the carboxy-terminal activation domain of upstream binding factor (UBF) and is regulated by UBF phosphorylation. *Mol Cell Biol* 19(4): 2872-2879.
- van den Heuvel RH, van Duijn E, Mazon H, Synowsky SA, Lorenzen K, Versluis C *et al* (2006). Improving the performance of a quadrupole time-of-flight instrument for macromolecular mass spectrometry. *Anal Chem* 78(21): 7473-7483.
- Vannini A, Ringel R, Kusser AG, Berninghausen O, Kassavetis GA, Cramer P (2010). Molecular basis of RNA polymerase III transcription repression by Maf1. *Cell* 143(1): 59-70.
- Venema J, Tollervey D (1999). Ribosome synthesis in *Saccharomyces cerevisiae*. *Annu Rev Genet* 33: 261-311.
- Voit R, Schnapp A, Kuhn A, Rosenbauer H, Hirschmann P, Stunnenberg HG *et al* (1992). The nucleolar transcription factor mUBF is phosphorylated by casein kinase II in the C-terminal hyperacidic tail which is essential for transactivation. *EMBO J* 11(6): 2211-2218.
- Volkov VV, Svergun DI (2003). Uniqueness of ab initio shape determination in small-angle scattering. *Journal of Applied Crystallography* 36: 860-864.

- Wang Z, Roeder RG (1995). Structure and function of a human transcription factor TFIIB subunit that is evolutionarily conserved and contains both TFIIB- and high-mobility-group protein 2-related domains. *Proc Natl Acad Sci U S A* 92(15): 7026-7030.
- Wang Z, Roeder RG (1997). Three human RNA polymerase III-specific subunits form a subcomplex with a selective function in specific transcription initiation. *Genes Dev* 11(10): 1315-1326.
- Warner JR (1999). The economics of ribosome biosynthesis in yeast. *Trends Biochem Sci* 24(11): 437-440.
- White RJ (2005). RNA polymerases I and III, growth control and cancer. *Nat Rev Mol Cell Biol* 6(1): 69-78.
- Wriggers W, Chacon P (2001). Using Situs for the registration of protein structures with low-resolution bead models from X-ray solution scattering. *Journal of Applied Crystallography* 34: 773-776.
- Wu CC, Lin YC, Chen HT (2011). The TFIIF-like Rpc37/53 Dimer Lies at the Center of a Protein Network to Connect TFIIC, Bdp1, and the RNA Polymerase III Active Center. *Mol Cell Biol*.
- Yamamoto RT, Nogi Y, Dodd JA, Nomura M (1996). RRN3 gene of *Saccharomyces cerevisiae* encodes an essential RNA polymerase I transcription factor which interacts with the polymerase independently of DNA template. *EMBO J* 15(15): 3964-3973.
- Yamashita S, Hisatake K, Kokubo T, Doi K, Roeder RG, Horikoshi M *et al* (1993). Transcription factor TFIIB sites important for interaction with promoter-bound TFIID. *Science* 261(5120): 463-466.
- Yan Q, Moreland RJ, Conaway JW, Conaway RC (1999). Dual roles for transcription factor IIF in promoter escape by RNA polymerase II. *J Biol Chem* 274(50): 35668-35675.
- Zhao J, Yuan X, Frodin M, Grummt I (2003). ERK-dependent phosphorylation of the transcription initiation factor TIF-IA is required for RNA polymerase I transcription and cell growth. *Mol Cell* 11(2): 405-413.

Curriculum Vitae

Personal data

Place of birth: Lörrach, Germany

Date of birth: 07.02.1983

Nationality: German

Research

Doctoral Thesis 10/2007-12/2011

Gene Center Munich, Germany

Prof. P. Cramer

Structural and functional studies of RNA polymerase I transcription initiation factor Rrn3

Education

Albert-Ludwigs-University, Freiburg, Germany 10/2006-08/2007

Diploma Thesis

Prof. T. Friedrich

Investigation of a conformational change of fluorescent labelled NADH:Ubiquinone Oxidoreductase from *E. coli* via FRET

Albert-Ludwigs-University, Freiburg, Germany 10/2001-08/2007

Studies of Chemistry

Department of Chemistry, University of Manchester, UK 10/2004-02/2005

Research Project

Studies on the asymmetric induction of an aza-Diels-Alder reaction that involved an attached Evans auxiliary.

Publication

Blattner C, Jennebach S, Herzog F, Mayer A, Cheung AC, Witte G *et al* (2011). Molecular basis of Rrn3-regulated RNA polymerase I initiation and cell growth. *Genes Dev* 25(19): 2093-2105.